NTIS #PB95-144382

SSC-379

IMPROVED SHIP HULL STRUCTURAL DETAILS RELATIVE TO FATIGUE

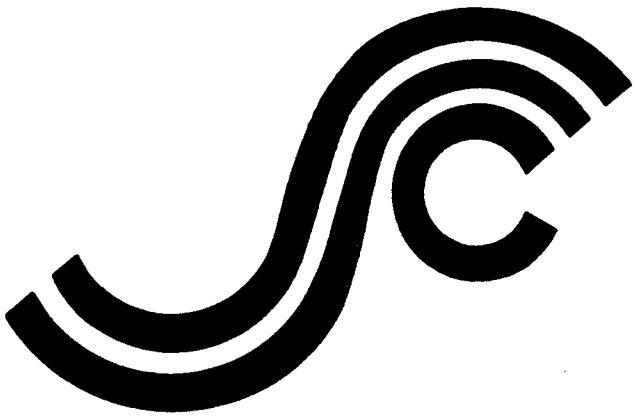

SHIP STRUCTURE COMMITTEE

1994

SHIP STRUCTURE COMMITTEE

The SHIP STRUCTURE COMMITTEE is constituted to prosecute a research program to improve the hull structures of ships and other marine structures by an extension of knowledge pertaining to design, materials, and methods of construction.

RADM J. C. Card, USCG (Chairman)
Chief, Office of Marine Safety, Security and Environmental Protection
U. S. Coast Guard

Mr. Thomas H. Peirce
Marine Research and Development Coordinator
Transportation Development Center
Transport Canada

Mr. H. T. Haller
Associate Administrator for Ship-building and Ship Operations
Maritime Administration

Dr. Donald Liu
Senior Vice President
American Bureau of Shipping

Mr. Edward Comstock
Director, Naval Architecture Group (SEA O3H)
Naval Sea Systems Command

Mr. Thomas W. Allen
Engineering Officer (N7)
Military Sealift Command

Mr. Warren Nethercote
Head, Hydronautics Section
Defence Research Establishment-Atlantic

EXECUTIVE DIRECTOR

CDR Stephen E. Sharpe, USCG
U. S. Coast Guard

CONTRACTING OFFICER TECHNICAL REPRESENTATIVE

Mr. William J. Siekierka
Naval Sea Systems Command

SHIP STRUCTURE SUBCOMMITTEE

The SHIP STRUCTURE SUBCOMMITTEE acts for the Ship Structure Committee on technical matters by providing technical coordination for determinating the goals and objectives of the program and by evaluating and interpreting the results in terms of structural design, construction, and operation.

MILITARY SEALIFT COMMAND

Mr. Robert E. Van Jones (Chairman)
Mr. Rickard A. Anderson
Mr. Michael W. Touma
Mr. Jeffrey E. Beach

MARITIME ADMINISTRATION

Mr. Frederick Seibold
Mr. Norman O. Hammer
Mr. Chao H. Lin
Dr. Walter M. Maclean

U. S. COAST GUARD

CAPT G. D. Marsh
CAPT W. E. Colburn, Jr.
Mr. Rubin Scheinberg
Mr. H. Paul Cojeen

AMERICAN BUREAU OF SHIPPING

Mr. Stephen G. Arntson
Mr. John F. Conlon
Mr. Phillip G. Rynn
Mr. William Hanzelek

NAVAL SEA SYSTEMS COMMAND

Mr. W. Thomas Packard
Mr. Charles L. Null
Mr. Edward Kadala
Mr. Allen H. Engle

TRANSPORT CANADA

Mr. John Grinstead
Mr. Ian Bayly
Mr. David L. Stocks
Mr. Peter Timonin

DEFENCE RESEARCH ESTABLISHMENT ATLANTIC

Dr. Neil Pegg
LCDR D. O'Reilly
Dr. Roger Hollingshead
Mr. John Porter

SHIP STRUCTURE SUBCOMMITTEE LIAISON MEMBERS

U. S. COAST GUARD ACADEMY

LCDR Bruce R. Mustain

U. S. MERCHANT MARINE ACADEMY

Dr. C. B. Kim

U. S. NAVAL ACADEMY

Dr. Ramswar Bhattacharyya

CANADA CENTRE FOR MINERALS AND ENERGY TECHNOLOGIES

Dr. William R. Tyson

SOCIETY OF NAVAL ARCHITECTS AND MARINE ENGINEERS

Dr. William Sandberg

U. S. TECHNICAL ADIVSORY GROUP TO THE INTERNATIONAL STANDARDS ORGANIZATION

CAPT Charles Piersall

NATIONAL ACADEMY OF SCIENCES - MARINE BOARD

Dr. Robert Sielski

NATIONAL ACADEMY OF SCIENCES - COMMITTEE ON MARINE STRUCTURES

Mr. Peter M. Palermo

WELDING RESEARCH COUNCIL

Dr. Martin Prager

AMERICAN IRON AND STEEL INSTITUTE

Mr. Alexander D. Wilson

OFFICE OF NAVAL RESEARCH

Dr. Yapa D. S. Rajapaske

STUDENT MEMBER

Mr. Trevor Butler
Memorial University of Newfoundland

Member Agencies:

American Bureau of Shipping
Defence Research Establishment Atlantic
Maritime Administration
Military Sealift Command
Naval Sea Systems Command
Transport Canada
United States Coast Guard

Ship Structure Committee

An Interagency Advisory Committee

Address Correspondence to:

Executive Director
Ship Structure Committee
U.S. Coast Guard (G-MI/SSC)
2100 Second Street, S.W.
Washington, D.C. 20593-0001
Ph:(202) 267-0003
Fax:(202) 267-4677

SSC-379
SR-1346

December 22, 1994

IMPROVED SHIP HULL DETAILS RELATIVE TO FATIGUE

As margins for operating ships get tighter and the costs for failures rise exponentially the need to prevent fractures at the design stage becomes increasingly more critical. This report provides one more tool for the designer to use. It presents a fatigue design methodology that applies existing fatigue data to welded ship details. A variation of the nominal stress approach is used for weld terminations in attached bracket details. This helps in selecting the weld configurations that improve fatigue life and assesses the impact of geometric stress concentration factors and combined loadings that are typical of welded ship structural details. Case studies are shown to demonstrate the methodology. A glossary of terms used is provided and recommendations are presented for future research.

J. C. CARD
Rear Admiral, U.S. Coast Guard
Chairman, Ship Structure Committee

(THIS PAGE INTENTIONALLY LEFT BLANK)

Technical Report Documentation Page

1. Report No.	2. Government Accession No.	3. Recipient's Catalog No.
SSC-379	PB95-144382	

4. Title and Subtitle	5. Report Date
Improved Ship Hull Structural Details Relative to Fatigue	September 6, 1994
	6. Performing Organization Code
	8. Performing Organization Report No.
7. Author(s) Karl A. Stambaugh, Dr. Frederick Lawrence and Stimati Dimitriakis	SR-1346
9. Performing Organization Name and Address	10. Work Unit No. (TRAIS)
Consulting Naval Architects 794 Creek View Road Severna Park, MD 21146	11. Contract or Grant No. DTCG23-92-C-E01028
	13. Type of Report and Period Covered
12. Sponsoring Agency Name and Address Ship Structure Committee U.S. Coast Guard (G-M) 2100 Second Street, SW Washington, DC 20593	Final Report
	14. Sponsoring Agency Code G-M

15. Supplementary Notes

Sponsored by the Ship Structure Committee and its member agencies.

16. Abstract

This report presents a fatigue design strategy for welded ship structural details. The fatigue design strategy is based on cumulative damage theory using nominal stress. The approach is modified to account for the complex geometry of welded ship structural details. Fatigue notch factors and stress concentration factors are derived from experimental data and finite element analysis. Guidance is provided showing detail designers how to improve the fatigue life of details using this approach.

17. Key Words	18. Distribution Statement
Fatigue Ship Structure Structural Details S-N Curves	Distribution unlimited. Available from: National Technical Information Service U.S. Department of Commerce Springfield, VA 22151

19. Security Classif. (of this report)	20. Security Classif. (of this page)	21. No. of Pages	22. Price
Unclassified	Unclassified	150	$27.00 Paper $12.50 Microf.

Form DOT F 1700.7 (8-72) Reproduction of completed page authorized

United States Department of Commerce
Technology Administration
National Institute of Standards and Technology
Metric Program, Gaithersburg, MD 20899

METRIC CONVERSION CARD

Approximate Conversions to Metric Measures

Symbol	*When You Know*	*Multiply by*	*To Find*	*Symbol*
	LENGTH			
in	inches	2.5	centimeters	cm
ft	feet	30	centimeters	cm
yd	yards	0.9	meters	m
mi	miles	1.6	kilometers	km
	AREA			
in^2	square inches	6.5	square centimeters	cm^2
ft^2	square feet	0.09	square meters	m^2
yd^2	square yards	0.8	square meters	m^2
mi^2	square miles	2.6	square kilometers	km^2
	acres	0.4	hectares	ha
	MASS (weight)			
oz	ounces	28	grams	g
lb	pounds	0.45	kilograms	kg
	short tons (2000 lb)	0.9	metric ton	t
	VOLUME			
tsp	teaspoons	5	milliliters	mL
Tbsp	tablespoons	15	milliliters	mL
in^3	cubic inches	16	milliliters	mL
fl oz	fluid ounces	30	milliliters	mL
c	cups	0.24	liters	L
pt	pints	0.47	liters	L
qt	quarts	0.95	liters	L
gal	gallons	3.8	liters	L
ft^3	cubic feet	0.03	cubic meters	m^3
yd^3	cubic yards	0.76	cubic meters	m^3
	TEMPERATURE (exact)			
°F	degrees Fahrenheit	subtract 32, multiply by 5/9	degrees Celsius	°C

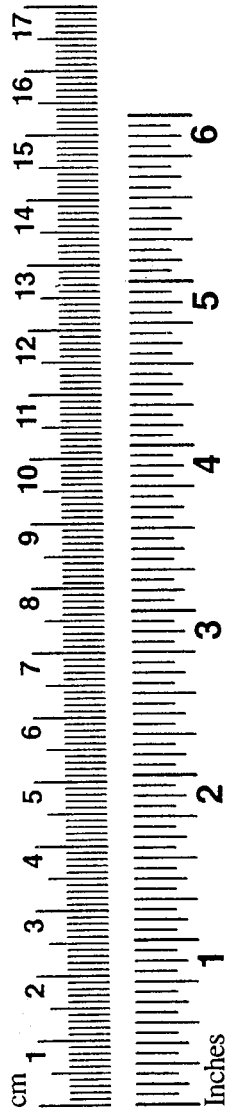

Approximate Conversions from Metric Measures

Symbol	*When You Know*	*Multiply by*	*To Find*	*Symbol*
	LENGTH			
mm	millimeters	0.04	inches	in
cm	centimeters	0.4	inches	in
m	meters	3.3	feet	ft
m	meters	1.1	yards	yd
km	kilometers	0.6	miles	mi
	AREA			
cm^2	square centimeters	0.16	square inches	in^2
m^2	square meters	1.2	square yards	yd^2
km^2	square kilometers	0.4	square miles	mi^2
ha	hectares (10,000 m^2)	2.5	acres	
	MASS (weight)			
g	grams	0.035	ounces	oz
kg	kilograms	2.2	pounds	lb
t	metric ton (1,000 kg)	1.1	short tons	
	VOLUME			
mL	milliliters	0.03	fluid ounces	fl oz
mL	milliliters	0.06	cubic inches	in^3
L	liters	2.1	pints	pt
L	liters	1.06	quarts	qt
L	liters	0.26	gallons	gal
m^3	cubic meters	35	cubic feet	ft^3
m^3	cubic meters	1.3	cubic yards	yd^3
	TEMPERATURE (exact)			
°C	degrees Celsius	multiply by 9/5, add 32	degrees Fahrenheit	°F

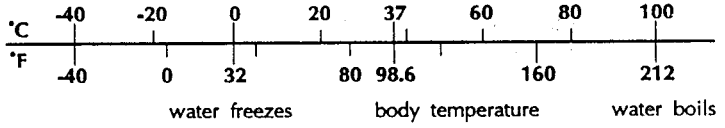

TABLE OF CONTENTS

FIGURES

TABLES

LIST OF SYMBOLS

a	=	Bracket leg length
b	=	Fatigue strength exponent
BM	=	Base Metal
C	=	Constant relating to the mean S-N curve
D	=	Depth of structural member
HAZ	=	Heat affected zone
K_f	=	Fatigue notch factor
K_{fweld}	=	Fatigue notch factor for weldment
$K_{f\,max}^{A}$	=	Value of K_f for axial component of applied stress
$K_{f\,max}^{B}$	=	Value of K_f for bending component of applied stress
$K_{f\,max}^{eff}$	=	Value of K_f representing combined effects of axial and bending stresses
K_{scf}	=	Geometric Stress Concentration Factor
K_t	=	Elastic stress concentration factor
m	=	Inverse slope of mean S-N regression line, also used as exponent controlling the thickness effect
N	=	Number of cycles corresponding to a particular fatigue strength; total number of nominal stress range cycles also known as fatigue life
n_i	=	Number of stress cycles in stress block i
N_i	=	Number of cycles of failure at a constant stress range
N_I	=	Life devoted to crack initiation and early growth
N_p	=	Life devoted to fatigue crack propagation
N_T	=	Total fatigue life
R	=	Ratio of minimum to maximum applied stress
s	=	Standard deviation
SD	=	Log standard deviation of fatigue strength at 10^6 cycles
ΔS_{pp}	=	Fatigue strength of a plain plate specimen at a given life (N_t)

LIST OF SYMBOLS
(continued)

ΔS_{weld}	=	Experimental fatigue strength range of a welded plate specimen at a given life (N_f)
ΔS_R	=	Stress range
S_{ref}	=	Design stress for the reference thickness
S_a^A	=	Axial component of applied stress
S_a^B	=	Bending component of applied stress
S_a^T	=	Applied mean stress
S_u	=	Ultimate strength
S_y	=	Yield strength
t	=	Plate thickness
WM	=	Weld metal
V_S	=	Variation due to uncertainty in equivalent stress range; includes effects of error in stress analysis
x	=	Ratio of applied bending to applied total stresses
α	=	Geometry factor
β	=	Number of stress blocks
ΔS_R	=	Design stress range
η	=	Limit damage ratio
σ'_f	=	Fatigue strength coefficient
σ_r	=	Local (notch root) residual stress
σ_B	=	Bending stress
τ	=	Shear Stress
σ_f	=	Fatigue design stress
σ_n	=	Nominal stress
θ	=	Weld flank angle
ΔS^A_{weld}	=	Experimental fatigue strength under pure axial loading
ΔS^B_{weld}	=	Experimental fatigue strength under pure bending loading

(THIS PAGE INTENTIONALLY LEFT BLANK)

1.0 INTRODUCTION

Cyclic loading causes fatigue cracking in a ship's welded structural details. If these details are not designed to resist fatigue cracking, the ship's profitability may be affected by repair costs and its economic life shortened. Fatigue cracks, for instance, may lead to fractures in ship's primary hull structure, an event resulting in catastrophic failure. Therefore, designers should use structural details that minimize fatigue damage and ensure structural integrity for the ship's intended service life.

One technique for predicting and assessing fatigue cracking uses empirical data derived from laboratory tests of representative structural details. After details undergo fatigue tests, test data are analyzed in terms of stress applied to each detail and the number of cycles required to reach failure. The test results are commonly referred to as S-N data and are presented in S-N curves.

The fatigue design curves presented by Munse (1) and re-analyzed by Stambaugh and Lawrence (2) are for various structural geometries that are difficult to apply to ship structural details. This report presents a fatigue design strategy to apply fatigue data to welded ship structural details. The fatigue design strategy is based on the nominal stress approach for basic welded structural configurations. A variation of the nominal stress approach is used for weld terminations in attached bracket details. After having separated the global geometric stress concentration factors from the welded details, it is possible to select weld configurations that improve fatigue life and assess the impact of geometric stress concentration factors and combined loadings typical of welded ship structural details.

The case studies used to characterize the stress in typical ship structural details are presented in Appendix A. The approach used to develop the fatigue design strategy is presented in Appendix B. A methodology for evaluating the effect of weld parameters (e.g., geometry and residual stress) is presented in Appendix C. A glossary of terms is presented in Appendix D.

(THIS PAGE INTENTIONALLY LEFT BLANK)

2.0 FATIGUE IN SHIP STRUCTURAL DETAILS

Throughout its service life, a ship experiences environmental loading which causes cyclic stress variations in structural members. Those variations can cause fatigue cracking in welded structural details if the details are inadequately designed. A fatigue assessment, supported when appropriate by fatigue analysis, should ensure that structural members do not lead to catastrophic failure. Fatigue-critical locations have been identified in a survey of standard structural details by Jordan et al. in SSC-272 (3) and SSC 294 (4). Stambaugh (5) presents fatigue-critical locations for special details that may lead to fracture. The fatigue life of a structural detail is determined by the number of cycles required to initiate a fatigue crack and propagate it from subcritical to critical size. Description of the fatigue cracking in ships has been documented by Jordan (1) and Stambaugh (3). One example of a side shell longitudinal and transverse cutout connection is shown in Figure 2-1 (6). This example is one of many that illustrate the complexity of fatigue cracking in welded ship structural details. In the example, lateral load from internal cargo and wave impact produces local loads on the side shell longitudinals. High stress concentrations are produced at the toe of welds in attached stiffeners and tripping brackets. This, combined with the use of high strength steel, (HTS) produces higher nominal stresses in the longitudinal stiffener (with little corresponding increase on fatigue strength) reduces fatigue life to five or ten years at best. Fatigue analysis should be considered for these locations and wherever special or new details are introduced in the ship's primary structure.

2.1 STRUCTURAL LOADING AND STRESS

Hull loads from waves and other sources must be transformed to stress distributions in the structural detail. Because it depends on the type of ship and operational environment, predicting and analyzing fatigue stresses is complex. The designer must estimate the magnitude of the stresses and determine their impact on fatigue response.

In a ship's steel structure, stress cycles are generally caused by the seaway and by dynamic effects such as bottom slamming and hull girder whipping. Changes in cargo distribution and local loads induce bending moments. Together, all of these loads produce bending stress and shear stress in the ship's hull girder. Local stresses caused by changes in hydrostatic pressure and local loading from cargo or ballast are also superimposed on the hull girder stress. If pertinent to a particular ship, other loading from dynamic effects, stresses from thermal differences in the girder, and residual stresses should be considered in the fatigue analysis.

Global loads are distributed through plates, girders, and panel stiffeners, all of which are connected by welded structural details that may concentrate stress.

A LONGITUDINAL STIFFENER CRACKED
B FLAT BAR STIFFENER CRACKED
C SHELL PLATE TO WEB WELD CRACKED
C1 CRACK EXTENDING INTO SHELL PLATE
D WEB FRAME CRACKED
E BRACKET CRACKED
F LUG CRACKED (TYPICAL DETAIL)

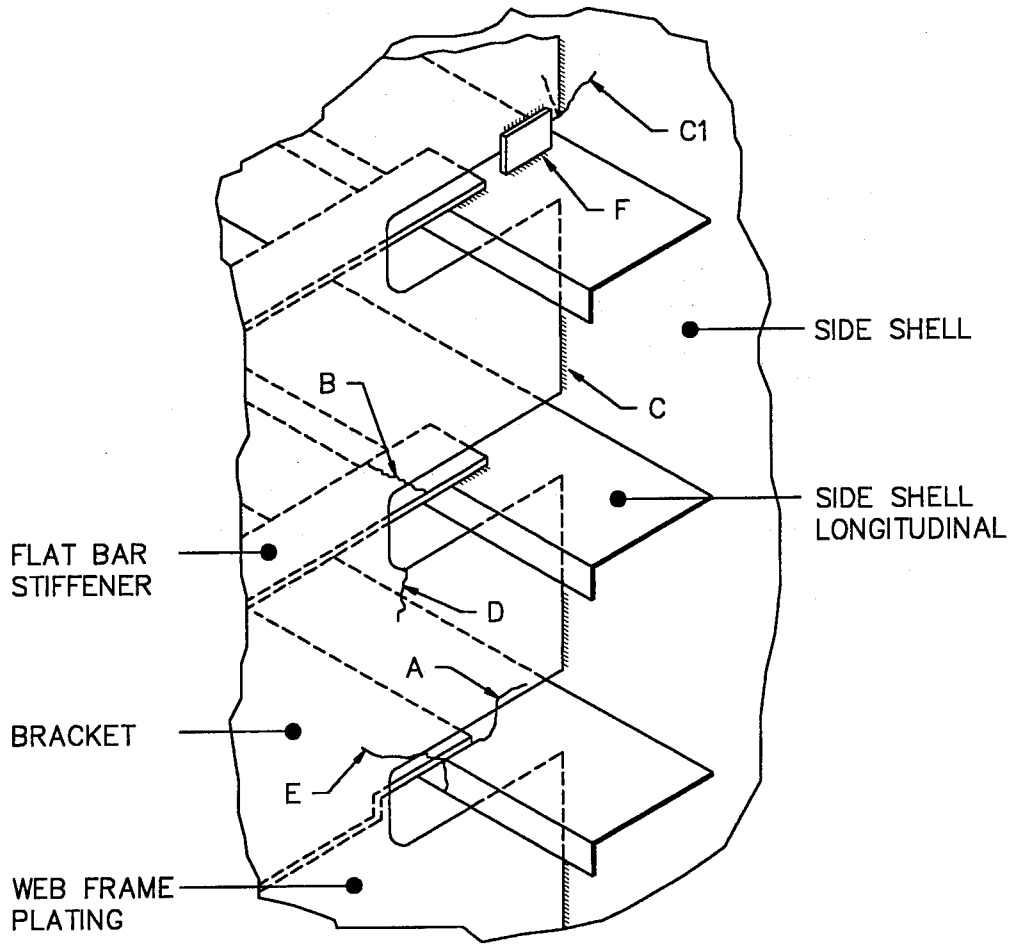

TYPICAL SIDE SHELL STRUCTURAL DEFECTS

Figure 2-1 Typical example of fatigue cracking in ship structural details

2.2 PREDICTING FATIGUE RESPONSE

Loading and resultant stresses are complex and random in nature. Therefore, a probabilistic approach is often used to characterize the long-term stress response distribution. The distribution is first developed by combining probabilities for each load and corresponding stress state. Then, the stress response transfer function is predicted for the individual load cases; and, finally, the distribution of joint probabilities are combined based on the probability of occurrence of each sea state.

Techniques for predicting long-term load and stress distribution and their development have been investigated extensively by Munse (1), White (7), Wirsching (8), and others but with little agreement as to the type of distribution that accounts for random load effects. The designer, therefore, must choose the dominant loads and combine them as they are expected to combine during the ship's service life. The long-term stress distribution is used in the cumulative damage analysis along with the S-N data applicable to the structural detail in question.

The cumulative damage approach is a method used to predict and assess fatigue life. As developed by Miner (14), this approach requires knowledge of structural loading and the structure's capacity expressed as stress range and number of cycles to failure. Developed from test data typically illustrated as (S-N curves), this method is based on the hypothesis that fatigue damage accumulates linearly and that damage due to any given cycle is independent of neighboring cycles. By this hypothesis, the total fatigue life under a variety of stress ranges is the weighted sum of the individual lives at constant S, as given by the S-N curves, with each being weighted according to the fractional exposure to that level of stress range. To apply this hypothesis, the long-term distribution of stress range is replaced by a stress histogram, consisting of a convenient number of constant amplitude stress range blocks, S_i, and a number of stress cycles, n_i. The constraint against fatigue fracture is then expressed in terms of a nondimensional damage ratio, η:

$$\sum_{i=1}^{\beta} \frac{n_i}{N_i} \leq \eta_L$$

where
- β = number of stress blocks
- n_i = number of stress cycles in stress block i
- N_i = number of cycles of failure at a constant stress range. S_i
- η_L = limit damage ratio

The limit damage ratio η_L depends on maintainability, that is, the possibility for inspection and repair, and the fatigue characteristics of the particular detail. These factors also have probabilistic uncertainty associated with them.

Fatigue design, using the linear cumulative damage approach, ensures the safety or performance of a system for a given period of time and/or under a "specified" loading condition. But the absolute safety of the system cannot be guaranteed because of the number of uncertainties involved. In structural design, these uncertainties can be due to the random nature of loads, simplifying assumptions in the strength analysis, material properties, etc.

3.0 FATIGUE DESIGN STRATEGY

A fatigue design strategy is presented to facilitate correlation between existing fatigue data and welded ship structural details. The fatigue design strategy is based on fatigue data presented by Munse (1) and re-analyzed by Stambaugh and Lawrence (2) for various structural geometries. Fatigue response data are presented to use with geometric stress concentration factors and combined loadings typical of ship structural details as developed in Appendix A and B. The fatigue design strategy is based on the nominal stress approach with modifications for induced stress concentration factors (e.g., brackets, toes and weld terminations) with various geometries. After having separated the global geometric stress concentration factors from the welded details, it is possible to select weld configurations that improve fatigue life and assess the impact of geometric stress concentration factors. A methodology for evaluating the effect of weld parameters (e.g., geometry and residual stress) is presented in Appendix C.

3.1 FATIGUE DESIGN STRESS

Fatigue design stress (σ_f) is defined as the stress range (double amplitude) in the location of the weld in the absence of the weld. The overall geometry of the weld need not be considered unless there are discontinuities from overfill, undercutting, or gross variations in the weld geometry. The relevant stress range must include any local bending and stress concentrations caused by the geometry of the detail as described next.

For bracketed details, combined stress from various load sources (shown in Figure 3-1) can be obtained from Finite Element Analysis (FEA). The maximum principal stress (9) should be used for combined stress fields. For deep beams and girders, bending stress is essentially an axial stress at the location of interest. This is in contrast to plate bending and associated gradients that have an effect on the fatigue life. Where out of plane stresses are high, the maximum principal stress may occur at the upper weld toe in the attachment. Thus, knowing where the maximum principal stress occurs is important and can be identified from FEA.

An illustration of global geometry and local weld toe geometry is shown in Figure 3-1. Stress associated with the physical geometry in structural details can be estimated by FEA. The stress gradients are very steep in the vicinity of the weld toe. Because of the high gradients, the maximum stress computed or measured will be sensitive to the mesh size. Because of this mesh sensitivity the fatigue design stress developed using FEA must be defined. The fatigue design stress is the principal stress on the order of one plate thicknesses from the weld toe as illustrated in Figure 3-2. Parametric approximations of stress concentration factors can be used to screen details; however, FEA should be used for fatigue critical locations. The application of the finite element technique to ship structural details is described by Liu and Bakker (10).

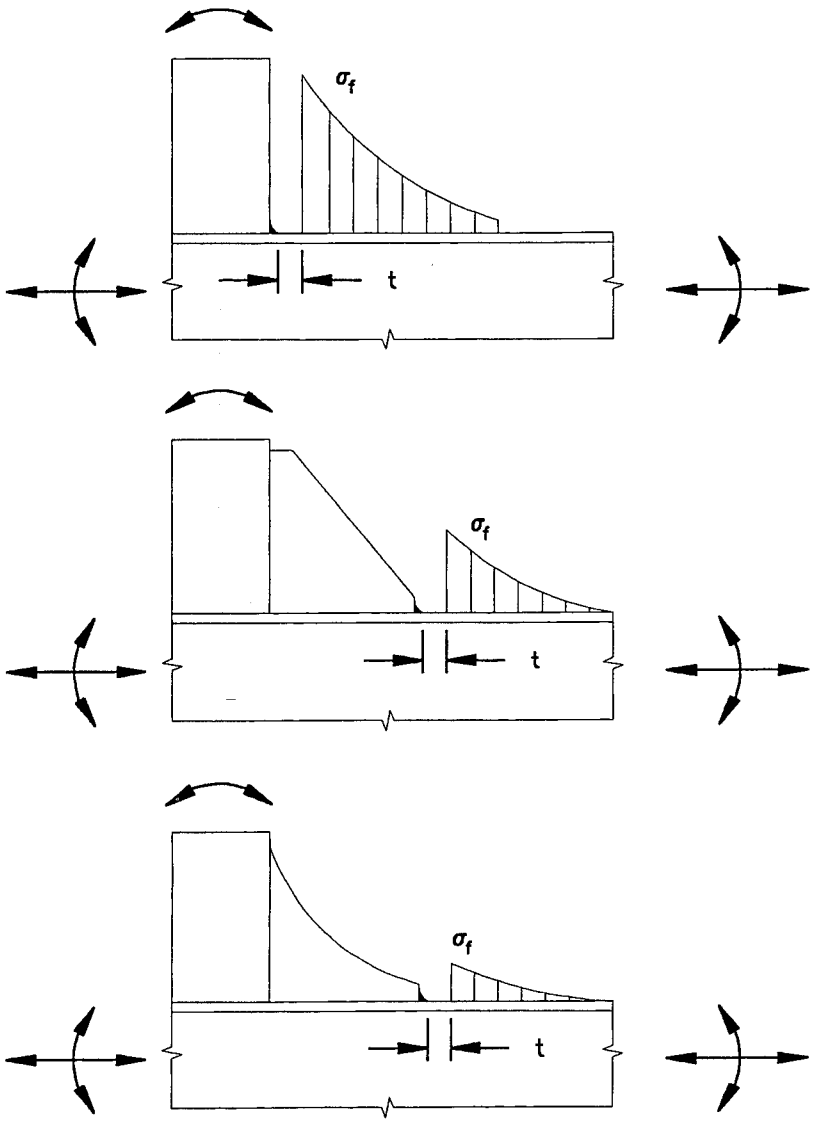

$$\sigma_f = \sigma_{principal} \quad \text{FROM FEA}$$

$$\sigma_f = \sigma_n \bullet K_{scf} \quad \text{FROM BEAM ANALYSIS}$$

Figure 3-1 Definition of fatigue design stress for bracket details

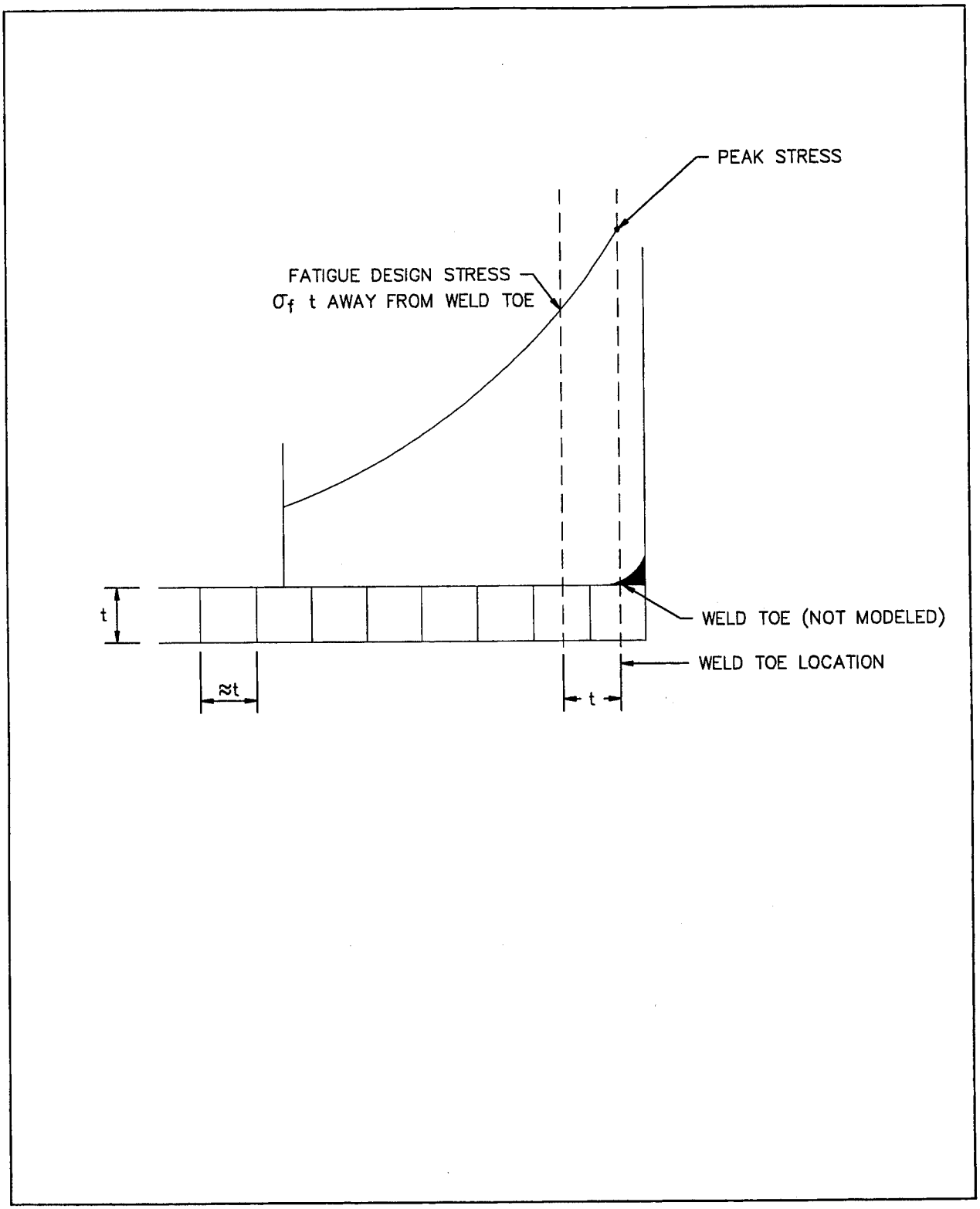

Figure 3-2 Estimating fatigue design stress from FEA

3.2 FATIGUE NOTCH FACTORS

Fatigue Notch Factors (K_f) associated with basic weld details provide a valuable tool in assessing the fatigue life of welded ship structural details because they can be used in quantitative evaluations and comparisons. Clearly, this is beneficial for application to various geometries of welded ship structural details. Baseline fatigue notch factors are developed that represent butt welds or fillet welds. In this case the effect of the local stress concentration at the weld toe is included in K_f. Therefore, the fatigue notch factor includes effects associated with weld geometry.

3.2.1 Definition of Fatigue Notch Factors

The basic weld configurations presented in Table 3-1 are correlated to a basic ship structural detail design curve using a fatigue notch factor K_f.

The fatigue notch factor K_f for each detail was estimated from the University of Illinois Urbana-Champagne (UIUC) fatigue data bank (2),(11) information in the following manner. At a given fatigue life, the fatigue notch factor K_f is defined as:

$$K_f = \frac{\Delta S_{smooth\ specimen}}{\Delta S_{weldment}} \tag{2}$$

The ratio of mean fatigue strength at 10^6 cycles of smooth specimen to that of plain plate is 1.43. Therefore, the K_f can be written as:

$$K_f = 1.43\ \frac{\Delta S_{plain\ plate}}{\Delta S_{weldment}} \tag{3}$$

$$K_f = 1.43\ \frac{\Delta S_{plain\ plate}}{\Delta S_{weldment}}\ \ at\ 10^6\ cycles and\ for\ R{=}0 \tag{4}$$

The development of fatigue notch factors is presented in Appendix B.

Table 3-1
Basic Weld Configurations and Fatigue Notch Factors

Weld Detail	Description	K_f		Fatigue Design Stress σ_f
		Axial	Bending	
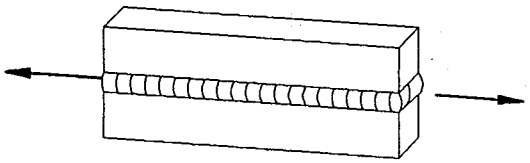	Longitudinally loaded butt weld	2.07	2.07	$\sigma_f = \sigma_n$ K_f is the same in deep sections for axial and bending .
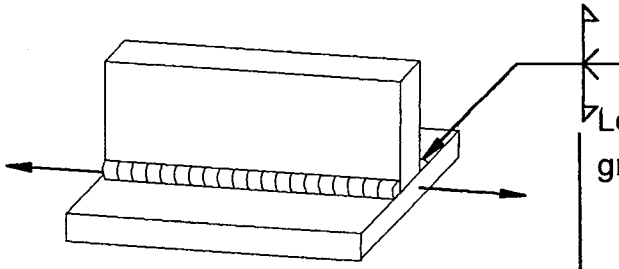	Longitudinally loaded groove weld	2.19	2.19	$\sigma_f = \sigma_n$
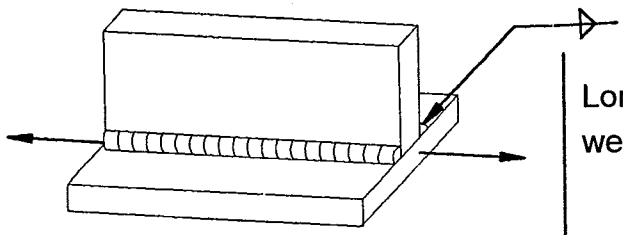	Longitudinally loaded fillet weld	2.19	2.19	$\sigma_f = \sigma_n$

Table 3-1
Basic Weld Configurations and Fatigue Notch Factors (con't.)

Weld Detail	Description	K_f		Fatigue Design Stress σ_f
		Axial	Bending	
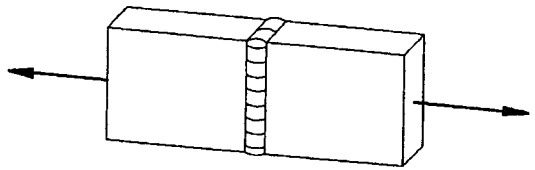	Transversely loaded butt weld	2.46	2.46	$\sigma_f = \sigma_n$
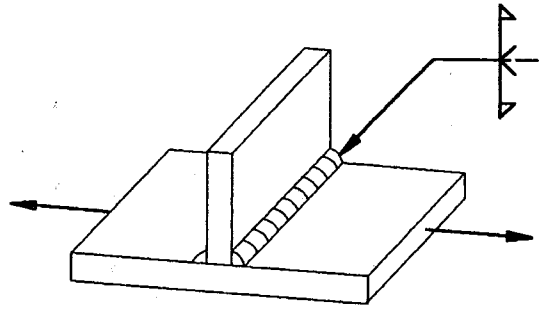	Transversely loaded groove weld.	2.63	2.63	$\sigma_f = \sigma_n$
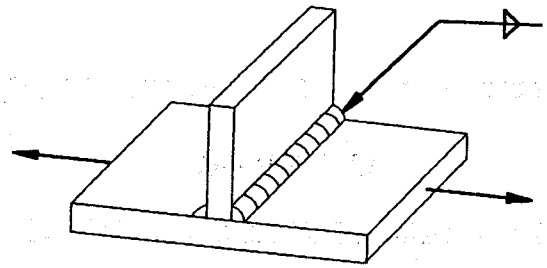	Transversely loaded fillet weld.	2.52	2.93	$\sigma_f = \sigma_n$

Table 3-1
Basic Weld Configurations and Fatigue Notch Factors (con't.)

Weld Detail	Description	K_f		Fatigue Design Stress σ_f
		Axial	Bending	
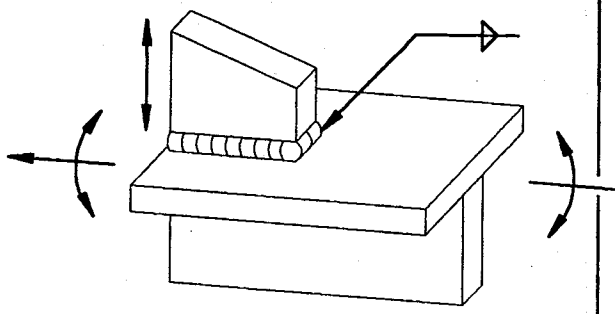	Longitudinally loaded weld termination.	3.6	3.6	Right angle connection using nominal stress (σ_n) in base member and no load in attachment. Axial and bending are the same for attachments to deep sections.
		3.0	3.0	Stress at one t from weld toe with variable geometry and combined stress from reaction in attachment (σ_f).
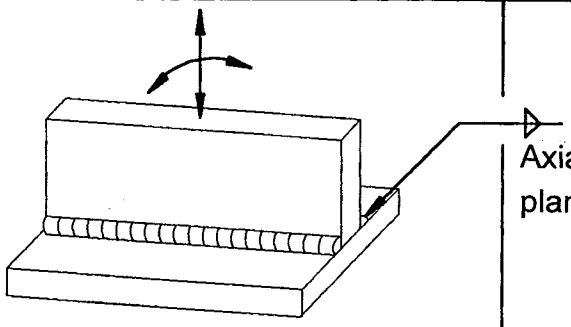	Axial and lateral (out of plane) loaded fillet weld.	5.5	4.4	Use this K_f when out of plane axial and bending stress are much greater than in plane stress. Root failure is likely for axial load.

Table 3-1
Basic Weld Configurations and Fatigue Notch Factors (con't.)

Weld Detail	Description	K_f		Fatigue Design Stress σ_f
		Axial	Bending	
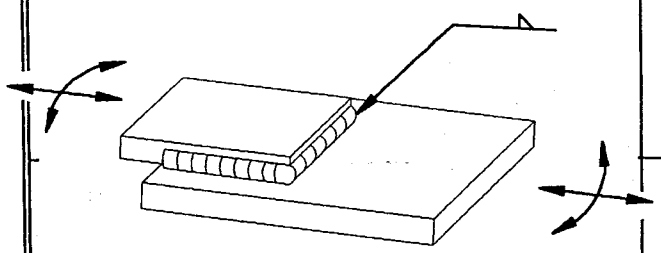	Lap weld in plane load.	2.91	2.91	σ_f = nominal stress at t away from weld toe. Use K_f for axial load in bending. Axial load induces bending.
	Lap weld out of plane load.	5.5	4.4	σ_f = nominal stress at t away from toe of weld. Axial load induces bending.

3.2.2 Design Curves

The mean fatigue strength of a weldment based on its fatigue notch factor and the fatigue strength of the plan plate specimen at the fatigue life in question can be written as:

$$\Delta S_{weld} = \frac{\Delta S_{ss}}{K_{fweld}} = \frac{1.43\ \Delta S_{pp}}{K_{fweld}} \quad (5)$$

Assuming that the scatter in fatigue life data can be described by the standard deviation of the log of the fatigue strength (SD), the design stress would be:

$$\Delta S_{design} = \Delta S_{weld} - 2 \cdot 10^{SD} \quad (6)$$

where:

SD = Log standard deviation of fatigue strength at 10^6 cycles

Thus, at 10^6 cycles

$$\Delta S_{design} = \frac{1.43\ \Delta S_{pp}}{K_{fweld}} - 2 \cdot 10^{SD} \quad (7)$$

This relationship is illustrated in Figure 3-3.

The curves are assumed to be parallel consistent with recent work (2) and current practice in development of fatigue design curves (12, 13) for welded structural details.

The approach used to develop the K_f curves and data is discussed in Appendix A. The welded detail K_f description, loading, and pictographs are presented in Table 3-1.

The basic design curves, which consist of linear relationships between log (ΔS_R) and log (N), are based on a statistical analysis of experimental data as described by Stambaugh (2). Thus the basic design curves are of the form:

$$\log (N) = \log C - m \cdot \log (\Delta S_R)$$

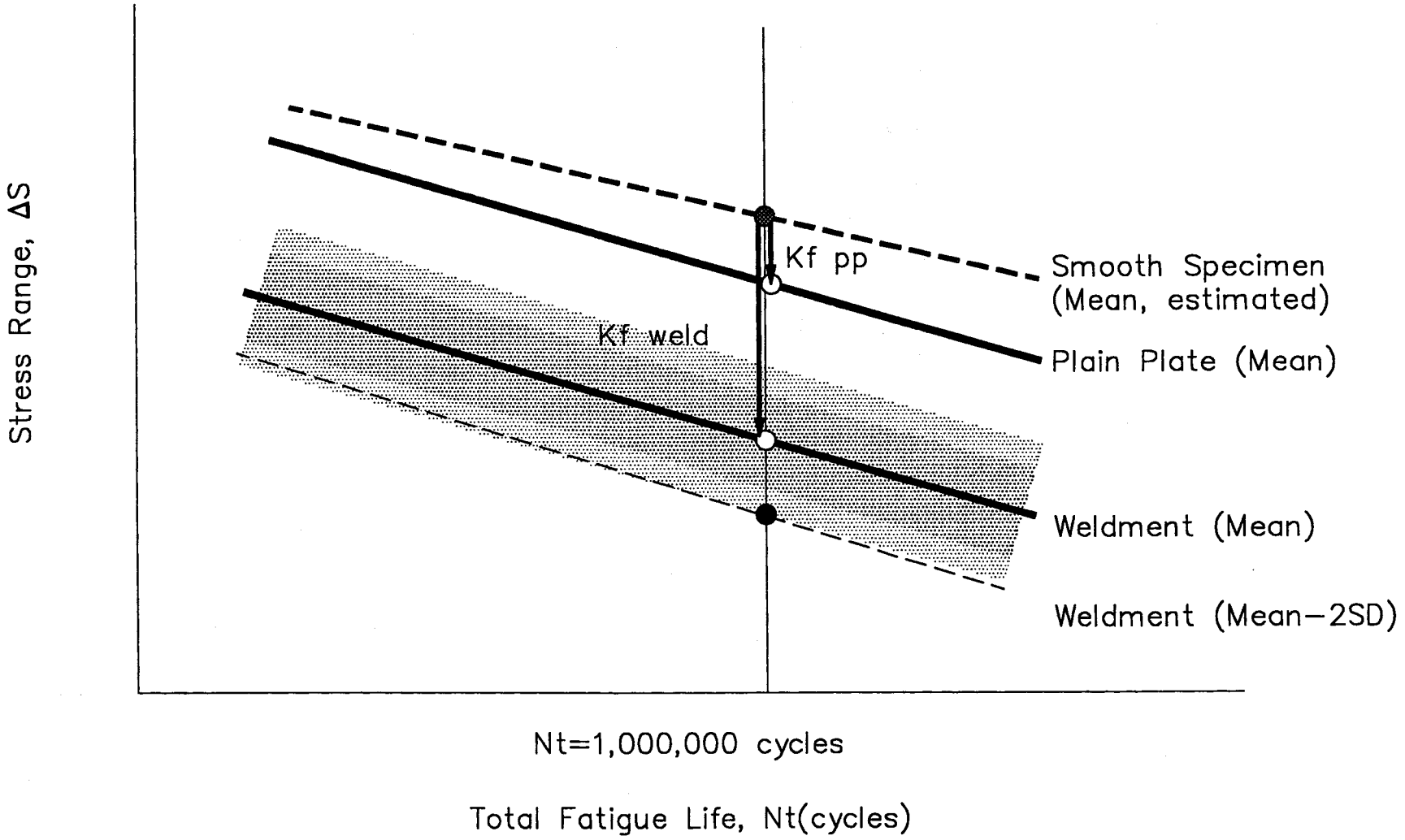

Figure 3-3 Fatigue design curves developed from K_f

or in terms of stress range:

$$\Delta S_R = (C/N)^{1/m}$$

where:

N is the predicted number of cycles for failure under stress range ΔS_R
C is a constant relating to the mean design curve
m is the inverse slope of the design curve

The fatigue design curve shown in Figure 3-4 includes the mean minus two standard deviation adjustment. The relevant statistics are:

logC = 4.38
m = 3
SD = .0696 at N 10^6 cycles

The slope of the design curve is bi-linear to account for the constant amplitude fatigue limit. This limit begins at $5 \cdot 10^6$ cycles. When all nominal stress ranges are less than the constant amplitude fatigue limit for the particular detail, no fatigue assessment is required.

The design curve has a cut off limit at 10^8 cycles. This limit is calculated by assuming a slope corresponding to m=5 below the constant amplitude fatigue limit. All stress cycles in the design spectrum below the cut off limit may be ignored when the structure is adequately protected against corrosion.

Other than as described above, no qualitative adjustments are included in this data set. Adjustments required to account for other factors influencing fatigue response are left to the designer, who should find the research described in the following sections helpful.

3.3 ADJUSTMENTS TO FATIGUE LIFE DATA

3.3.1 Mean Stress

The correction for mean stress ratios other than R=O is based on work by Lawrence (13), who propose an equation to calculate the mean fatigue strength of weldments at long lives.

$$\frac{\Delta S_R}{\Delta S_{R=O}} = \frac{1+(2N)^b}{1+\frac{1+R}{1-R}(2N)^b} \qquad (8)$$

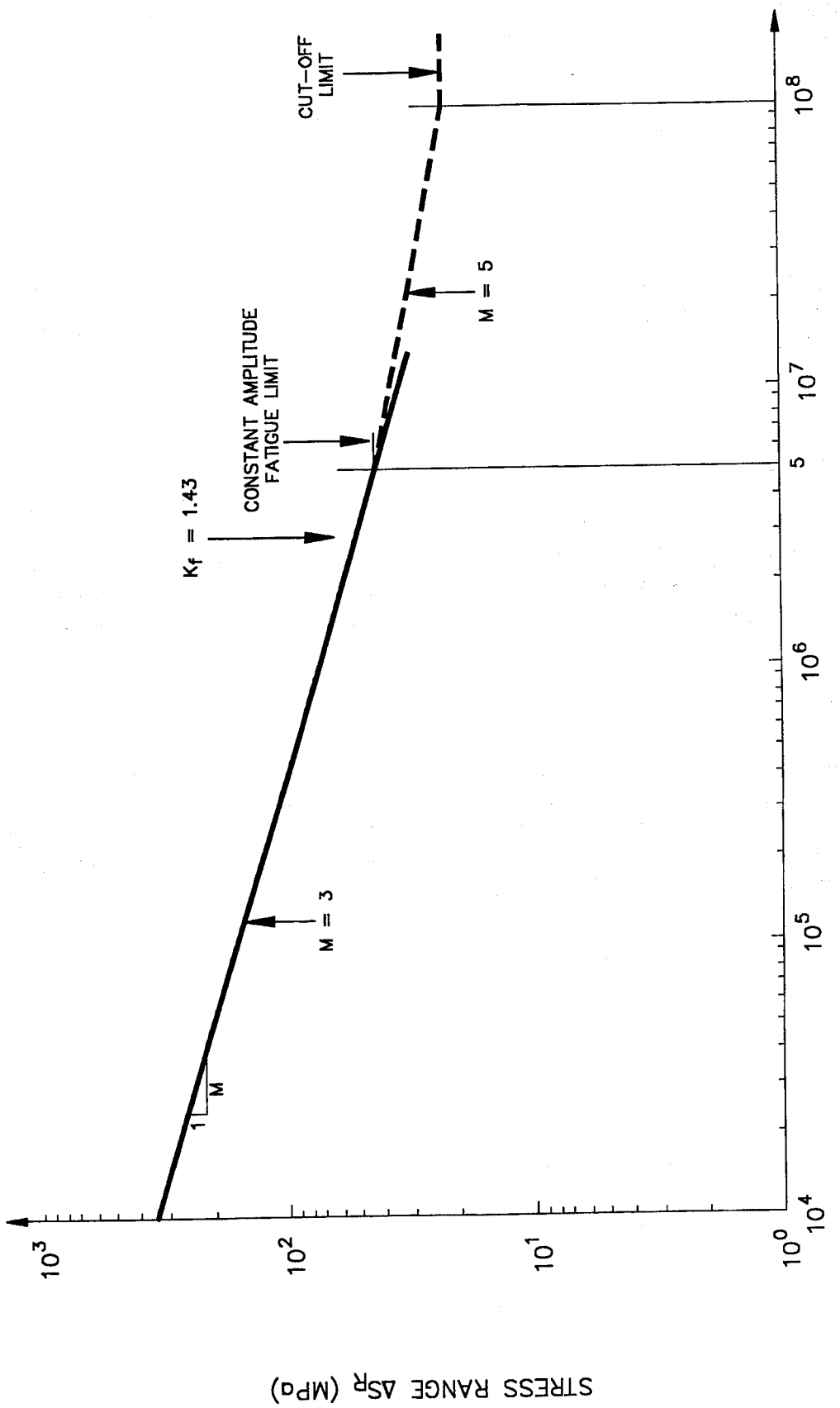

Figure 3-4 Ship detail fatigue stress design curve

This equation is used to predict the mean fatigue strength at any R value at 10^6 cycles from the R=0 fatigue strength at 10^6 cycles. Fatigue strength exponent b is estimated by:

$$b = -\frac{1}{6} log2 \left(1 + \frac{50}{1.5S_u}\right) \quad \textbf{(9)}$$

where S_u is the ultimate strength of base metal. The derivation of this correction is presented by Stambaugh and Lawrence (2) along with its validation using the UIUC fatigue data bank.

3.3.2 Corrosion

Salt water can seriously affect the fatigue life of structural details. The data available (15), (16), (17) indicate that corrosion decreases fatigue life where details are uncoated or do not have cathodic protection. When no consistent protection is provided, evidence suggests that fatigue life should be reduced by a factor of two for all categories. Corrosion also affects fatigue limit, which becomes non-existent when corrosion is present. As noted by UK DOE (18), the design curve must be continued without a change in slope.

3.3.3 Thickness

At present, most agree that for geometrically similar welds larger weldments will sustain shorter fatigue lives. Theoretical (19) and experimental (20) evidence confirm the existence of a size effect, but there is much scatter in the data. Thus, the magnitude of the thickness effect remains in question. Lawrence (11), Gurney (21), and Smith (22) recommend the following relationship:

$$\left[\frac{S_1}{S_2}\right] = \left[\frac{t_2}{t_1}\right]^m \quad \textbf{(10)}$$

where

- t_2 is taken to be 25mm (1 inch)
- t_1 is the thickness of plate (mm)
- S_1 is the design stress at the thickness in question
- S_2 is the design stress for the referenced thickness
- m is 1/4 as recommended by Lawrence (11) for the S-N curves given by Stambaugh and Lawrence (2).

The 25mm reference thickness cited is greater than most structural details constructed of steel plate and shapes. Therefore, the correction need not be applied unless the base plate thickness is greater than 25mm.

3.3.4 Fabrication

The fabrication process is a very important factor in the fatigue life of welded structural details. Data used to develop the fatigue design strategy assume that weld quality is free of critical defects and meets the requirements of regulatory and classification societies. Joint misalignment has a significant effect on fatigue life (23),(24). Weld profile changes by grinding and peening affect fatigue response as noted in the UK DOE (18) design code. Residual stress is a very important factor especially in weld termination. Control of weld geometry and residual stress are effective means of increasing fatigue life. The analytical expressions presented in Appendix C can be used to assess the impact of weld parameter control on fatigue response. Although weld parameter control is often considered expensive, it is worth considering in special cases.

4.0 IMPROVED DETAILS RELATIVE TO FATIGUE

Ship structural detail design depends on many factors that are unique to the specific application. Ship type, size, loading, detail location and many other variables influence their design. However, basic parameters can guide detail designers in selection and application of structural details. These parameters include weld configuration, detail geometry and nominal stress. An understanding of these parameters and their relationship will aid in selecting, evaluating and finalizing detail design as described next.

4.1 DESIGN OBJECTIVE

The approach based on K_f can be used by designers to improve fatigue life of welded ship structural details. Separating geometric effects (K_{scf}) from the fatigue notch factor (K_f) enables ship structural designers to control variables that influenced fatigue response. The designer can determine which parameters he must control within his design constraints (cost and construction capability) when the primary objective is a constant fatigue life for a specific detail. To illustrate this point, the fatigue life (N) based on K_f and K_{scf} can be expressed as:

$$N = f(\sigma_f, K_f)$$

where; $\sigma_f = \sigma_n$ for simple geometries and

$\sigma_f = \sigma_n * K_{scf}$ for more complex geometries (e.g. brackets)

here; σ_n is the nominal stress and

σ_f is the fatigue design stress one plate thickness from the weld toe.

Assuming the designer is working to a constant fatigue life, the important parameters become K_f, K_{scf}, and σ_n. As a practical matter, it is very difficult to design ship structures using K_{scf} because it varies depending on application and FEA is required to determine the fatigue design stress σ_f for fatigue critical locations. All too often detail designers are expected to provide a detail (K_{scf}) that will improve fatigue life; however, K_{scf} alone is insufficient and re-evaluation of the nominal stress σ_n is required in many instances. Nominal stress has a significant influence on fatigue life. Detail designers must assess the trade-off between these parameters because the selection of details depends on the specific application. The reliability approach developed by Munse (1) and K_f presented in Table 4-1 provide guidance in making this assessment when combined to illustrate the trade-off between K_f and K_{scf}. The following can be inferred by inspection of the information provided in Figure 4-1.

Table 4-1

Fatigue Notch Factors for
Panel Stiffener Connections

Ship Detail	K_f	Comments
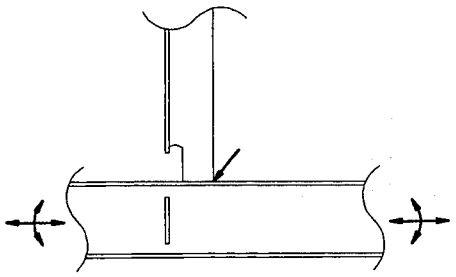	3.0	Connection has high stress concentration factor and is suitable for low nominal stress applications. K_{scf} of 3.3 or greater.
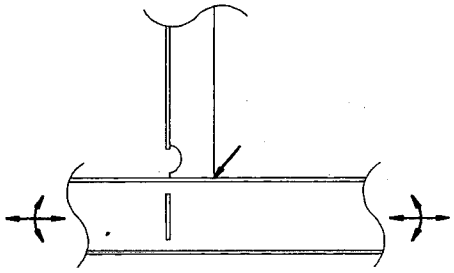	3.0	Connection increases area and reduces stress concentration slightly. K_{scf} of 2.8.
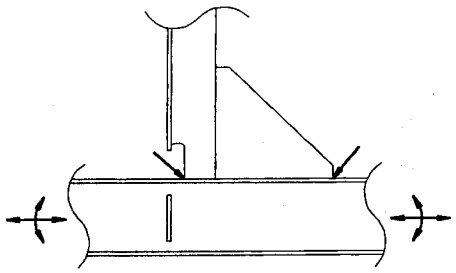	3.0	Connection area and bracket reduce stress at bracket toe. K_{scf} of 2.7. Fatigue critical location depends on effective shear connection to longitudinal.
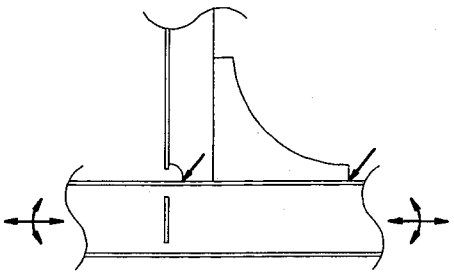	3.0	K_{scf} of 2.3. Fatigue critical location depends on effective shear connection to longitudinal.

Table 4-1
(Cont.)
Fatigue Notch Factors for
Panel Stiffener Connections

Ship Detail	K_f	Comments
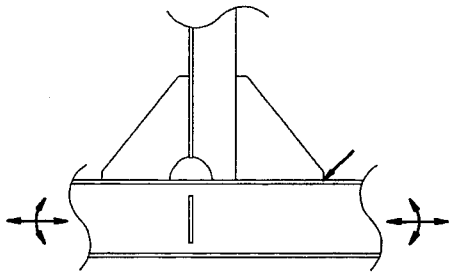	3.0	Straight brackets reduce overall stress in connection. However, K_{scf} of 2.7 is high.
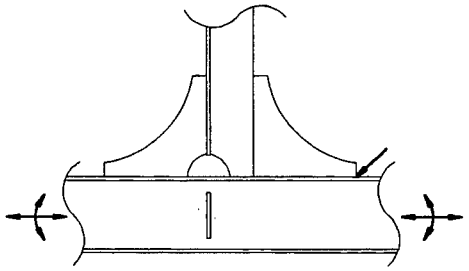	3.0	Double radius bracket is required when using HTS. See discussion in report. K_{scf} of 2.0.
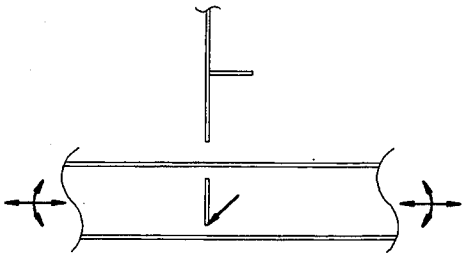	2.46	Shear connection between longitudinal and transverse must be evaluated for specific cutout.
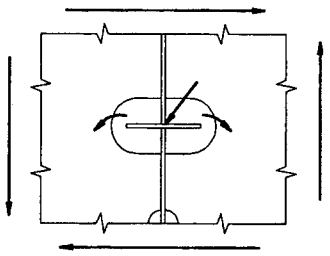	4.4	Out of plane bending on fillet welded attachment increases K_f significantly. K_{scf} and σ_n should be evaluated carefully.

Table 4-1
(Cont.)
Fatigue Notch Factors for
Panel Stiffener Connections

Ship Detail	K_f	Comments
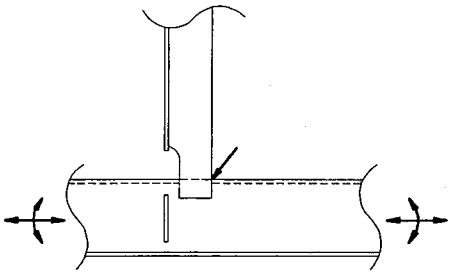	2.62	Lapped attachments have slightly higher K_f than landed attachments. This connection introduces high K_{scf}. Use for low stress (σ_n) applications.
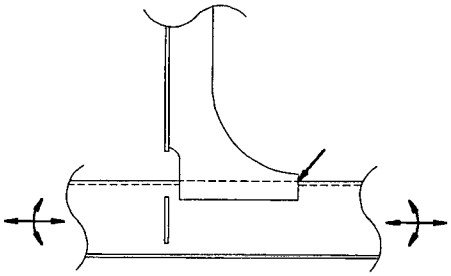	2.62	Fatigue critical location depends on effective shear connection to longitudinal.
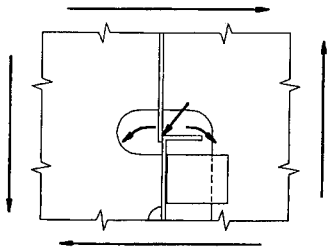	4.4	Asymmetrical flange introduces out of plane bending from shear center load center offset. Corresponding K_f is high reducing fatigue life. Use in low stress (σ_n) applications.

Table 4-1

Fatigue Notch Factors for
Beam Bracket

Ship Detail	K_f	Comments
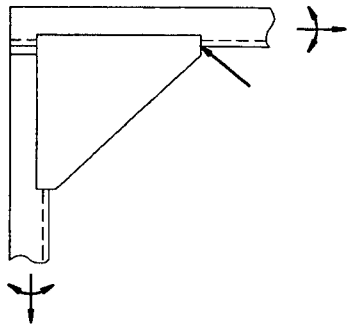	2.91	Lap brackets generally have higher out of plane induced loading. Snipe flange to reduce K_{scf} at flange end.
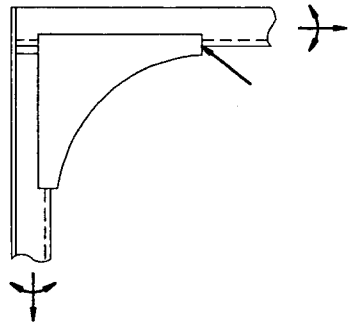	2.91	Radius bracket reduces K_{scf}. See Figure (4-6) for details.
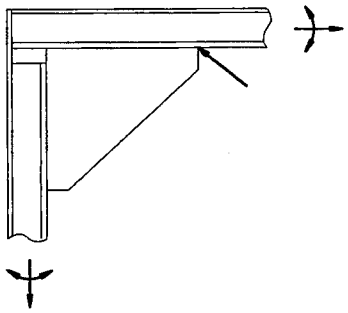	3.0	Flanged brackets have higher K_{scf} than plain but are more susceptible to buckling if not designed correctly.
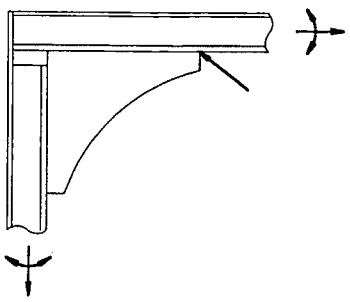	3.0	Radius reduces K_{scf}. Shape flange 5:1 slope to reduce K_{scf}. See Figure (4-6) for details.

Table 4-1

Fatigue Notch Factors for
Deep Bracket

Ship Detail	K_f	Comments
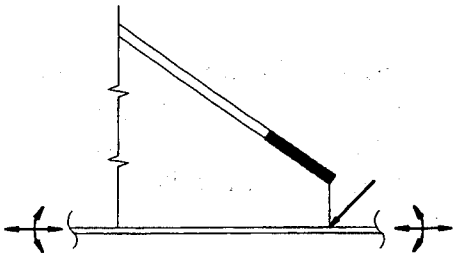	3.0	Stiffener at end of bracket introduces high K_{scf}. Use FEA for high stress applications.
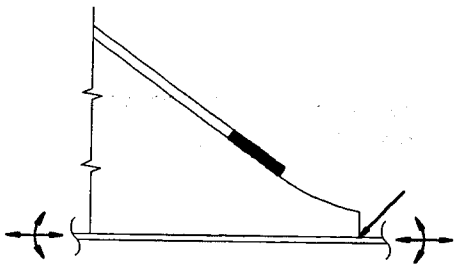	3.0	Most economical means of reducing K_{scf}. See Figure 4-3 for recommended proportions. Use FEA for high stress applications.
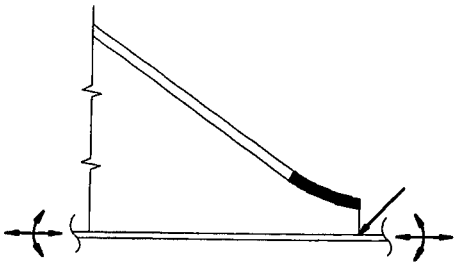	3.0	Slight increase in K_{scf}. Use FEA for high stress applications.
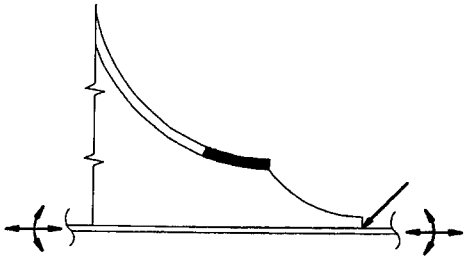	3.0	Best configuration to reduce K_{scf} at bracket toe. Also reduces stress from out of plane bending at toe. Exact geometry should be determined using FEA.

Table 4-1

Fatigue Notch Factors for
Flange Transitions

Ship Detail	K_f	Comments
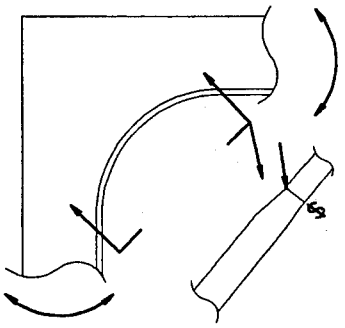	2.58	Tapered flange slope must be > 5:1. Difference in flange widths should be evaluated carefully.
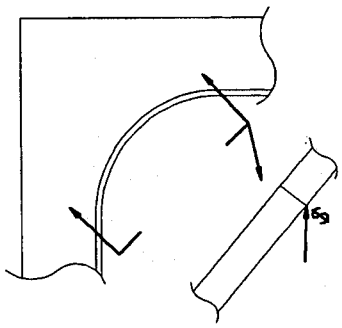	2.04	Weld quality is important to maintain low K_f.

Table 4-1

Fatigue Notch Factors for
Tripping Brackets

Ship Detail	K_f	Comments
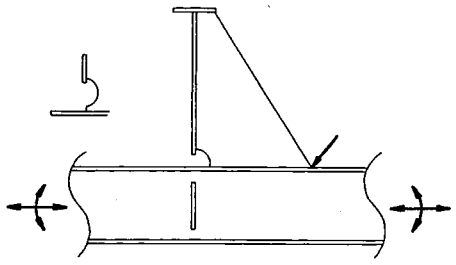	3.0	Straight bracket has high K_{scf}. K_{scf} = 2.7. Effective shear connection between longitudinal and transverse is very important.
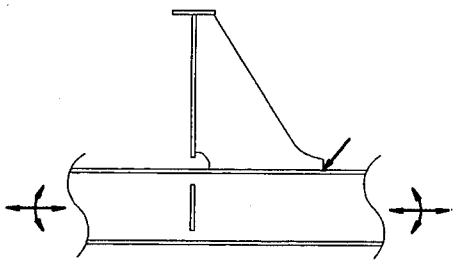	3.0	This configuration reduces K_{scf} at bracket toe; however, heel has high K_{scf}.
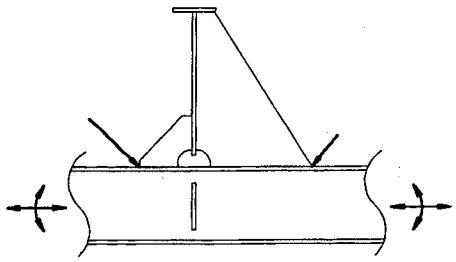	3.0	Heel bracket reduces K_{scf} slightly.
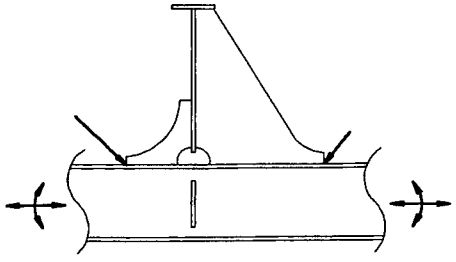	3.0	K_{scf} = 2.0.

Table 4-1

Fatigue Notch Factors for
Tee Cutouts

Ship Detail	K_f	Comments
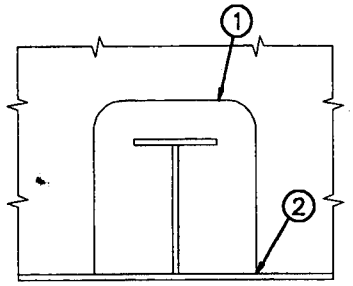	1 - 1.7 2 - 3.0	No effective shear connection is provided on the open cutout. This increases σ_f at point 1 and 2. Should be considered for low stress applications.
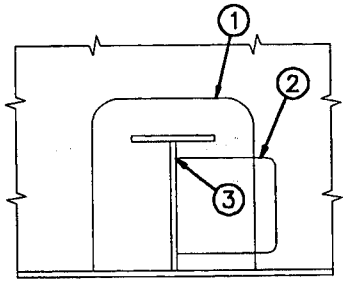	1 - 1.7 2 - 2.62 3 - 3.44	It is important that the lug connection be designed to transfer shear without increasing σ_f at point 2.
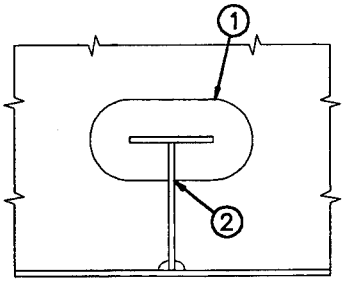	1 - 1.7 2 - 3.44	Most effective method of transferring shear to the transverse structure. This reduces σ_f at point 1.
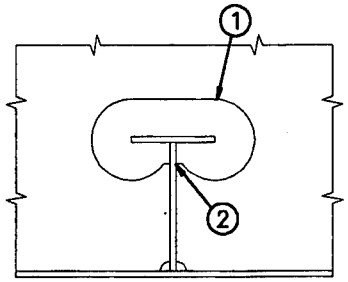	1 - 1.7 2 - 3.44	Note increase in attachment length at web reduces K_{scf} at point 2 and shear stress across the attachment.

Table 4-1

Fatigue Notch Factors for
Angle Cutouts

Ship Detail	K_f	Comments
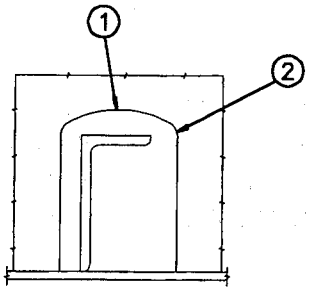	1 - 1.7 2 - 1.7	K_{scf} (Ref. 23) 1 - 2.19 2 - 4.5
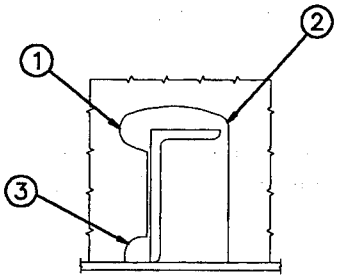	1 - 1.7 2 - 1.7 3 - 3.0	K_{scf} (Ref. 23) 1 - 4.4 2 - 3.3 3 - 4.9
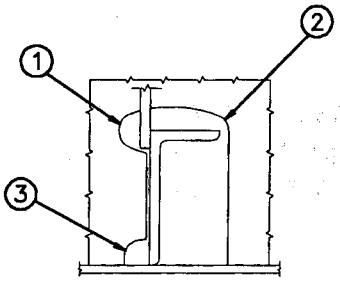	1 - 1.7 2 - 1.7 3 - 3.0	K_{scf} (Ref. 23) 1 - 3.7 2 - 2.8 3 - 4.1
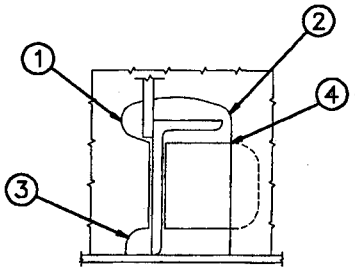	1 - 1.7 2 - 1.7 3 - 3.0 4 - 2.62	K_{scf} (Ref. 23) 1 - 3.5 2 - 2.4 3 - 4.0

Table 4-1

Fatigue Notch Factors for
Bulb Plate Cutouts

Ship Detail	K_f	Comments
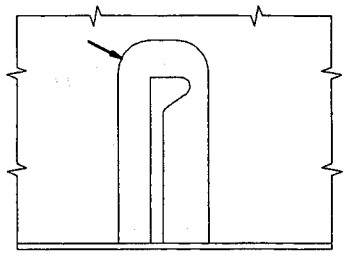	1.7	Small radius increases K_{scf}. Note lack of shear transfer to transverse. Use in low stress applications.
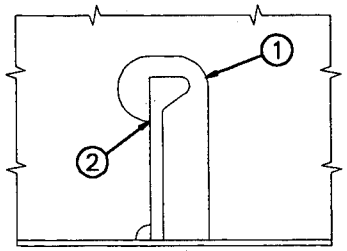	1 - 1.7 2 - 3.44	Geometry must be evaluated carefully to reduce K_{scf}.
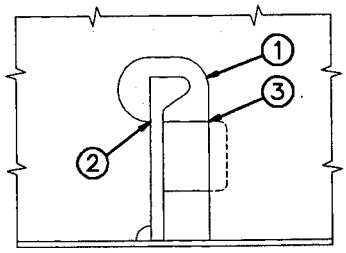	1 - 1.7 2 - 3.44 3 - 2.62	Effective shear connection is important in reducing nominal stress at point 3.
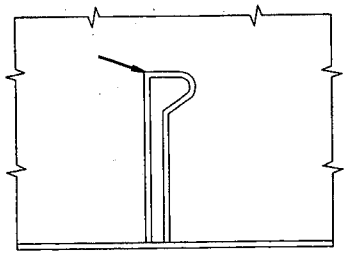	2.93	Weld wrap and quality of weld are important in tight connection.

Table 4-1

Fatigue Notch Factors for
Deck and Side Penetrations

Ship Detail	K_f	Comments
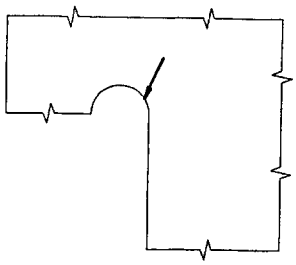	1.7	
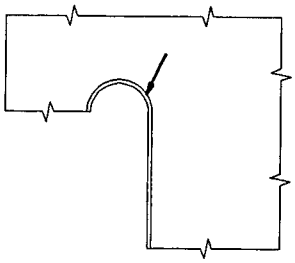	3.0	Face plate introduces weld increasing K_f but reduces K_{scf} in detail. Weld quality is very important in this area.
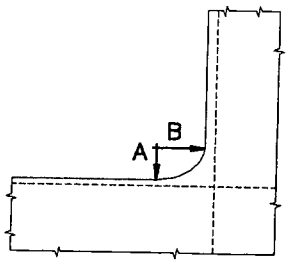	1.7	K_{scf} is very sensitive to opening size and radius. See refs. (25) and (26) for examples.
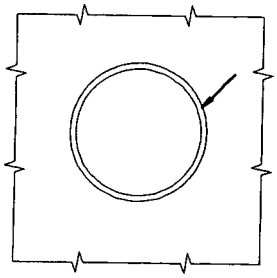	3.0	Weld quality is very important for all main deck and bottom penetrations and attachments.

Table 4-1

Fatigue Notch Factors for
Miscellaneous Cutouts

Ship Detail	K_f	Comments
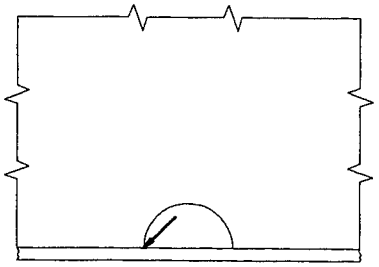	3.0	Size and number of cutouts are important relative to adjacent structure and can increase σ_f at critical location.
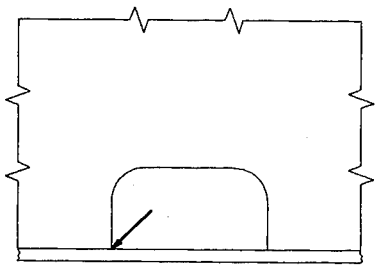	3.0	
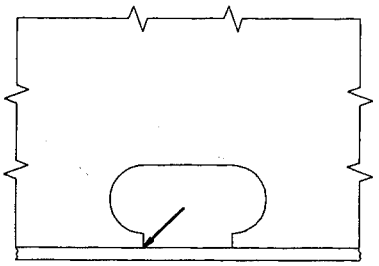	3.0	
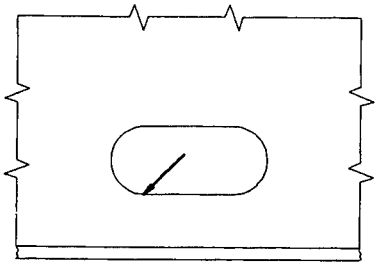	1.7	

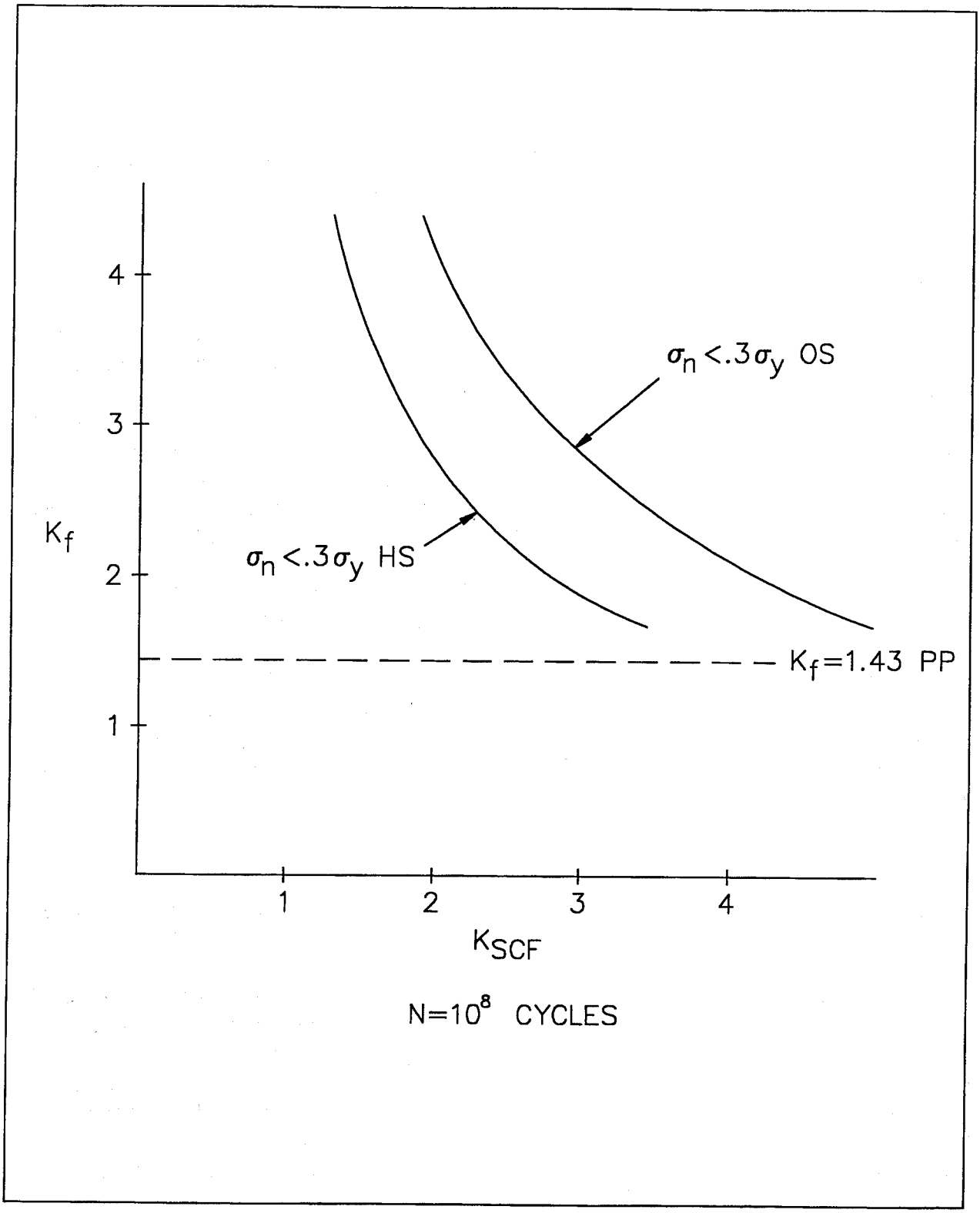

Figure 4-1 Illustration of the relationship between K_f and K_{scf}

$K_{scf} * K_f < 4$ for High Strength Steel ($\sigma_n = .3\sigma_y$ HS)

$K_{scf} * K_f < 8$ for Ordinary Strength Steel ($\sigma_n = .3\sigma_y$ OS)

While these are approximate relationships, they are useful in comparing details and evaluating the trade-off between K_{scf}, K_f, and σ_n. Final determination of σ_f should be based on FEA and K_f presented in Table 3-1.

4.1.1 Reducing Fatigue Notch Factors (K_f)

Improvements in K_f result from changes in weld type, weld geometry, residual stress or mechanical profiling. The effects of these parameters can be significant and used as a technique to improve fatigue life. Weld profiling by grinding and peening improves K_f and extends fatigue life. These techniques are generally used selectively because of there associated increase in fabrication cost. Analytical expressions involving these parameters and effects on K_f are discussed in greater detail in Appendix C. Typical values of K_f are presented in Table 4-1 for ship structural details based on inspection of the details and application of K_f values from Table 3-1.

4.1.2 Reducing Stress Concentration Factors (K_{scf})

Stress Concentration Factors (K_{scf}) have an infinite number of variations. The designer can select from a number of geometries each of them having a significant effect on the fatigue design stress σ_f. Table 4-1 presents typical values of K_{scf} to illustrate the trade-off between K_f and K_{scf}. The K_f, K_{scf} curves shown in Figure 4-1 can be used to screen details and aid the detail designer. Final selection of the detail should be based on FEA to determine σ_f.

4.1.3 Reducing Nominal Stress

Reducing nominal stress in ship structural details is an effective way to reduce fatigue design stress (σ_f) and improve fatigue life.

For example, an increase in frame section modulus will reduce the stress in the detail and weld toe, assuming constant load (which might be typical in using design rules). Similarly, reduction in stiffener or frame span and spacing will reduce nominal stress. The nominal stress in the structure has a significant influence on the fatigue design stress (σ_f) and fatigue response. Therefore, fatigue evaluations should be conducted early in the ship design because structural detail geometry produces stress concentrations that cannot compensate for detrimental effects of high nominal stress.

Another example is shown in Figure 4-2 for the symmetry of the flange on longitudinales. The flange symmetry has significant influence on fatigue strength. It was reported that a second generation VLCC experienced fatigue cracks in

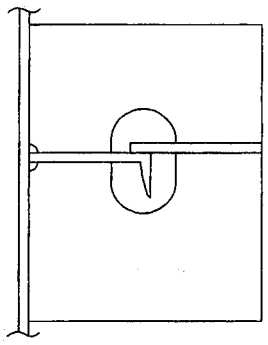

FLAT BAR LAPPED ON ANGLE, CUT CHANNEL OR BULB ANGLE

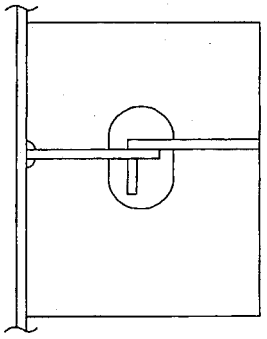

FLAT BAR LAPPED ON BUILT UP ANGLE

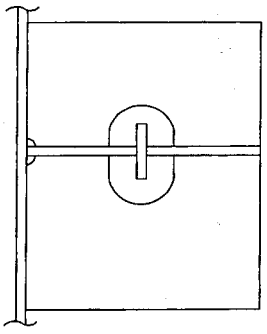

FLAT BAR BUTT TO TEE

TYPICAL WEB FRAME PANEL STIFFENER CONNECTION TO SIDE LONGITUDINAL

Figure 4-2 Frame flange symmetry

asymmetric flanges after three to four years (27). There were no fatigue cracks found in a similar ship with symmetric flanges. An investigation found that the maximum stress in the asymmetric configuration is nearly 70 percent higher than in symmetric flanges. Therefore, use of symmetric Tee sections reduces a component of nominal stress and improves fatigue life.

4.2 RECOMMENDED PROPORTIONS

Numerous examples are provided in Table 4-1 showing the trade-off between K_{scf} and K_f for panel stiffeners, tripping bracket connections, frame cutouts and for shell cutouts. Structural detail proportions are very important in lowering K_{scf} and K_f. Recommended proportions are shown in Figures 4-3 through 4-7 based on the analysis presented in Appendix A.

Recommended panel stiffener ends proportions are presented in Figure 4-3. Both toe and heel brackets are required to achieve a K_{scf} of less than 2.0.

Recommended deep brackets proportions used in double hull tankers are shown in Figure 4-4. The extended bracket toe radius reduces out of plane stress at the weld toe.

Recommended hatch corners and side shell cutouts proportions are shown in Figure 4-5. The exact proportions of these details depend on the specific application (25),(26).

Recommended bulb plate stiffener cutout proportions are shown in Figure 4-6. There are a large number of variations in cutout geometries and Table 4-1 shows K_{scf} for various angle cutouts based on data for standard structural arrangements (24). Additional proportions for cutouts are provided in SSC-266 (26). Generally, small radius corners should be avoided. Effective shear connections are extremely important in reducing K_{scf} in cutouts.

Recommended beam bracket proportions are shown in Figure 4-7. A common feature seen in the figures described above includes 5:1 slope on shaped flanges to reduce K_{scf}. Generally, plain brackets have lower K_{scf} than flanged brackets; however, plain brackets are more susceptible to buckling. Straight brackets are shown because they are more common than radiused brackets. Radiused brackets have much lower K_{scf} than straight brackets and are worth considering for plain brackets

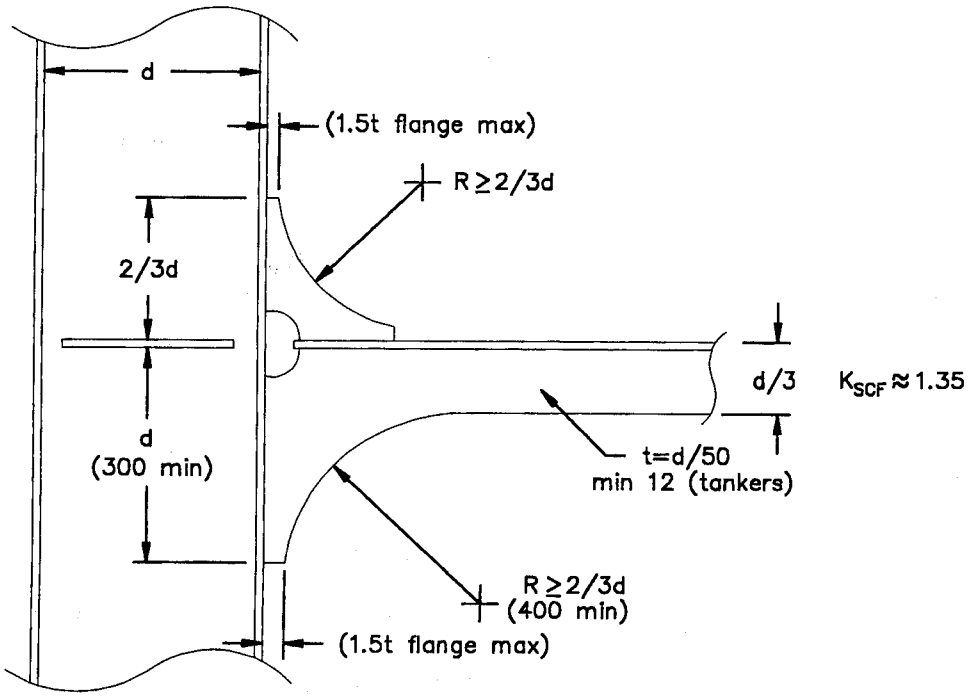

Figure 4-3 Recommended proportions for panel stiffener connections

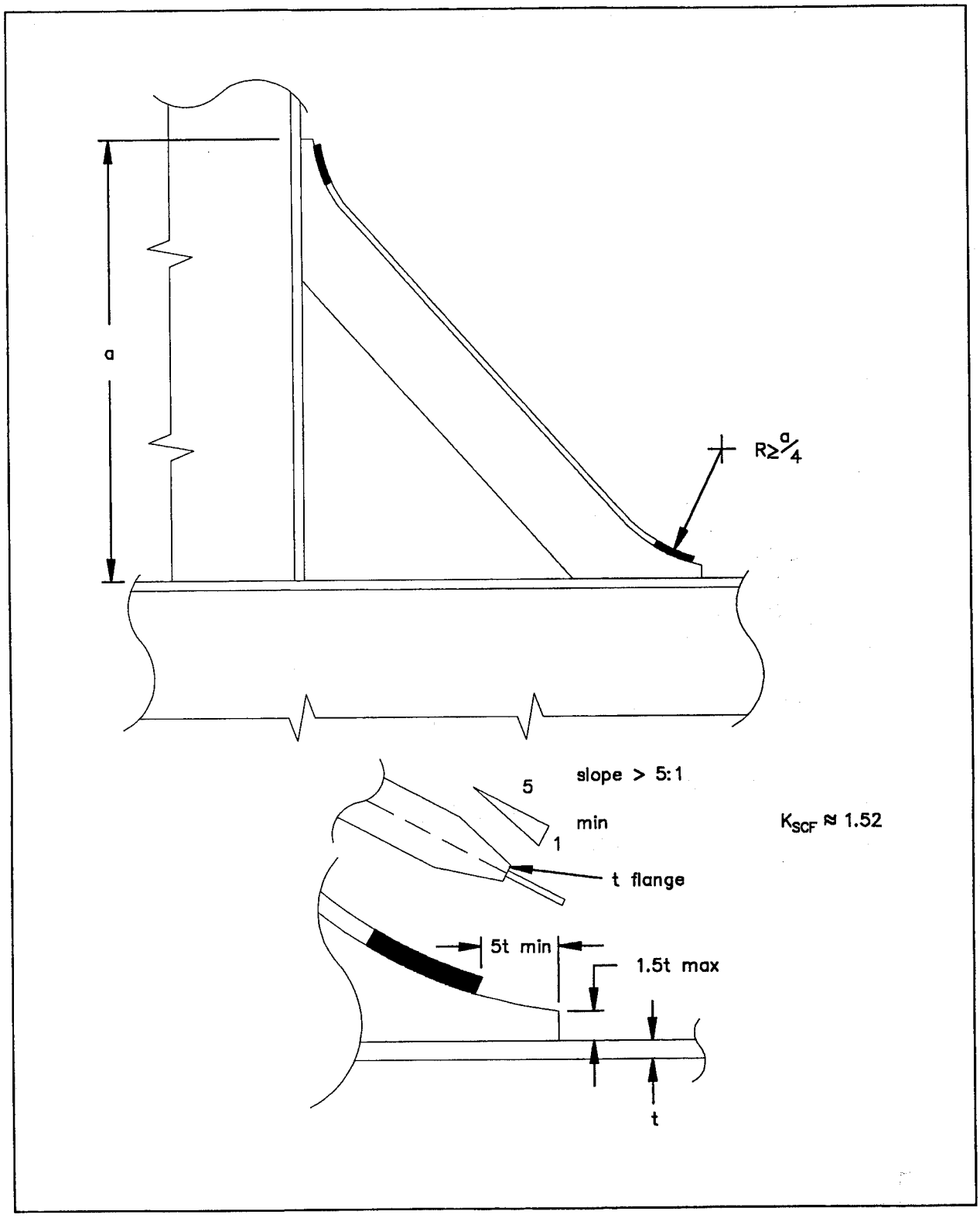

Figure 4-4 Recommended proportions for deep bracket

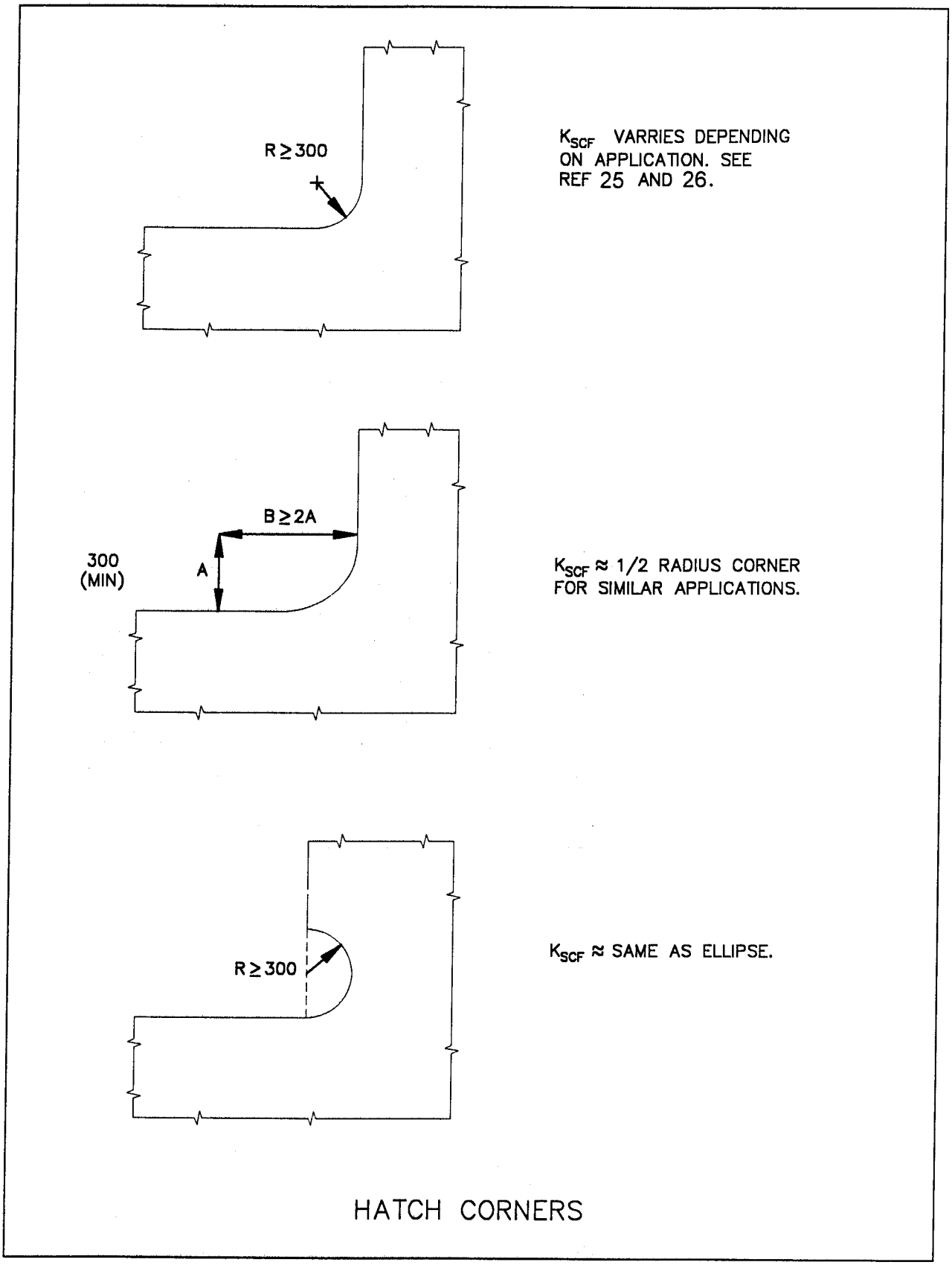

Figure 4-5 Recommended proportions for hatch corners

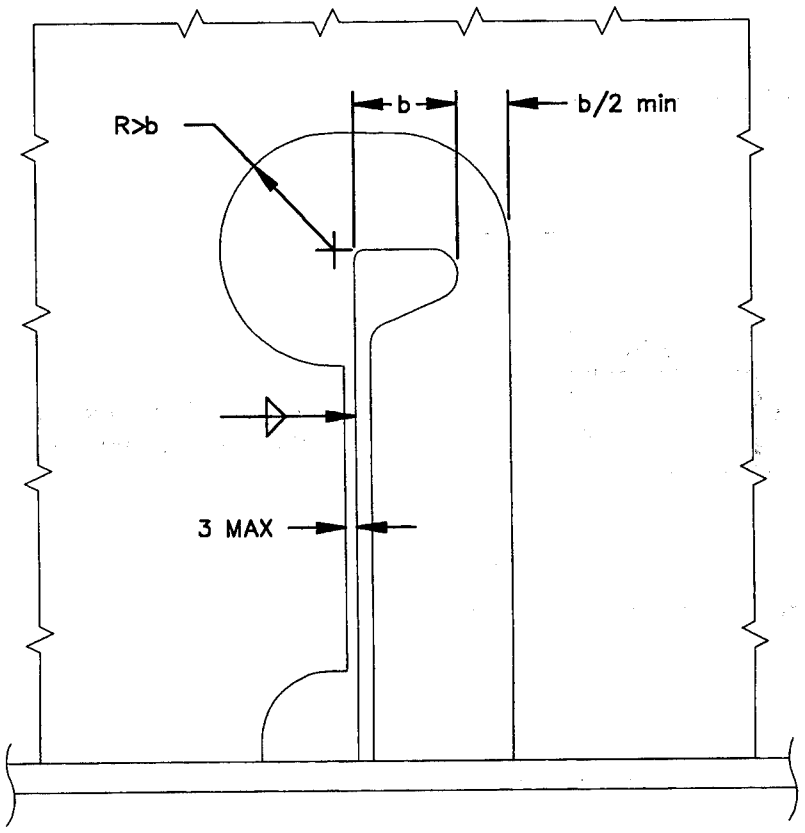

Figure 4-6 Recommended proportions for frame cutout

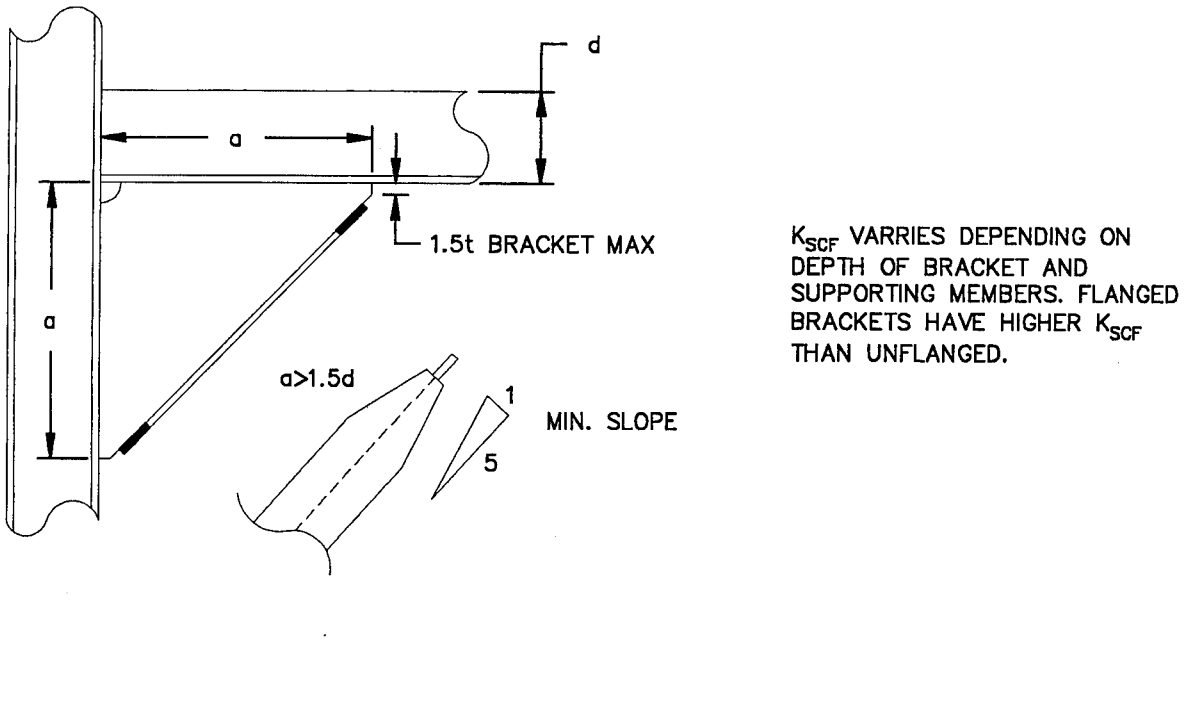

Figure 4-7 Recommended proportions for beam brackets

not requiring rolled flanges. Proportions for panel stiffener connections and deep bracket may be used for radiused brackets. Recommended proportions for bracket thickness, leg length and flange size is presented by Glasfeld (26) and the Tanker Forum (28).

It is extremely important to use good fabrication practices described by Jordan (25) when using the fatigue design strategy and recommended proportions presented in this report. The depth of bracket ends (t<1.5) is extremely important in maintaining a K_f of 3.0.

Clearly, there are various improvements that reduce K_{scf}. The final selection of details and determination of σ_f must be verified by the designer using FEA for specific applications. The cost trade off must be assessed by the designer based on savings of material, labor, and shipyard resources. A guide for estimating the cost of structural details is provided by Jordan in SSC-331 (29).

4.3 APPLICATION OF HIGH STRENGTH STEEL

The application of High Strength Steel (HTS) in ships must be approached carefully. Although the yield strength of HTS is greater, the fatigue strength of welded structural details is approximately the same as ordinary strength steel. When scantlings and resulting section modulus are reduced the nominal stress increases. This translates to an increase in nominal stress at the connecting details. This must be compensated by using details with reduced K_{scf}. For example, in sizing side shell longitudinal stiffeners of AH-36, the section modulus can be reduced to 72% of ordinary strength steel based on the high strength steel factor, Q=.72, by ABS (28). This produces a 40% increase in stress at the detail (assuming constant load). The geometric K_{scf} must reduce the stress by 40% to maintain constant fatigue life. By inspecting the trends in K_{scf} shown in Table 4-1, the double radius bracket is the only detail that produces more than 40% reduction in K_{scf} over straight panel stiffeners. The designer may also choose a smaller increase in nominal stress (say 20%) and compensate with a detail that reduces the K_{scf} by 20%. This trade-off depends on cost for the specific application. Figure 4-1 illustrates the trade-off between K_f and K_{scf} for ordinary and high strength steel. If K_f and K_{scf} are to the left of the respective material curve, the detail is satisfactory for the nominal stress indicated. If not, the nominal stress should be re-evaluated or detail K_f or K_{scf} changed.

(THIS PAGE INTENTIONALLY LEFT BLANK)

5.0 CONCLUSIONS AND RECOMMENDATIONS

1. Recent advances in computer technology and development of pre-processors for finite element programs allows designers to analyze the stresses in ship structural details quickly. Variations can be evaluated and parametric analysis of detail configurations can be performed to guide the designer in assessing fatigue critical details. However, similar techniques are required to guide the designer in developing load histories quickly. The reliability approach developed by Munse (1) can be applied easily; however, its application has not been verified and calibrated for general use. Further development of this type of approach, combined with the fatigue design strategy presented here, will expedite detail design and fatigue analysis of more details requiring attention by designers.

2. The fatigue design strategy presented here should be used to re-evaluate stiffened panel design criteria in light of the fatigue notch factors and stress concentration factors for typical welded structural details. This evaluation should include the effects of high strength steel and non-linear effects of torsion in panel stiffeners.

3. The approach used to predict effects of weld parameters for weld terminations has been developed using existing data for attachments; however, the technique should be verified for combined loading and sheer loading typical of terminations found in welded ship structural details. This effort should include both testing and analytical evaluations (using FEA) of the test specimens. Three dimensional effects at the weld should be evaluated both experimentally and analytically.

(THIS PAGE INTENTIONALLY LEFT BLANK)

6.0 REFERENCES

1. Munse, W.H., Wilbur, T.W., Tellalian, M.L., Nicolle, K., and Wilson, K., "Fatigue Characterization of Fabricated Ship Details for Design," SSC-318, 1983.

2. Stambaugh, K., Lesson, D., Lawrence, R., and Banas, "Reduction of S-N Curves for Ship Structures," SSC-369, 1992.

3. Jordan, C.R. and Cochran, C.S., "In-Service Performance of Structural Details," SSC-272, 1978.

4. Jordan, C.R. and Knight, L.T., "Further Survey of In-Service Performance of Structural Details," SSC-294, 1980.

5. Stambaugh, K. and Wood, W., "Ship Fracture Mechanisms Investigation," SSC-337, March 1987.

6. Exxon Corporation, "Large Oil Tanker Structural Survey Experience," Position Paper, June 1, 1982.

7. White, G.J. and B.M. Ayyub, "Reliability Based Fatigue Design for Ship Structures," ASNE Journal, May 1985.

8. Wirsching P.H., Chen Y.-N., "Considerations of Probability-Based Fatigue Design for Ship Structures," ASNE Journal, May 1985.

9. Stambaugh, K. and Munse, W.H., "Fatigue Performance under Multi-axial Loading Conditions," SSC-367, 1990.

10. Liu, D. and A. Bakker, "Practical Procedures for Technical and Economic Investigations of Ship Structural Details," Marine Technology, January 1981.

11. Lawrence, F.W., "Fatigue Characterization of Fabricated Ship Details -- Phase II," Ship Structure Committee Project SR-1298, University of Illinois, Urbana, Illinois (awaiting publication).

12. "Guidance for the Survey and Construction of Steel Ships," Nippon Kaiji Kyokai, 1989.

13. "Recommendation for the Fatigue Design of Steel Structures," ECCS, 1985.

14. Miner, M.A., "Cumulative Damage in Fatigue," Journal of Applied Mechanics, Vol. 12, 1945.

15. Marshall, P., "Basic Considerations for Tubular Joint Design in Offshore Construction," Welding Research Council Bulletin 193, April 1974.

16. Burnside, O.H., S.J. Hudak, Jr., E. Oelkers, K. Chen, and Dexter R.J., "Long-Term Corrosion Fatigue of Welded Marine Steels, "SSC-326, 1984.

17. Albrecht, P., Sidani M., "Fatigue Strength of Weathering Steel for Bridges," University of Maryland Department of Civil Engineering, October 1987.

18. U.K. Department of Energy (DEn), "Offshore Installations: Guidance on Design and Construction," January,1990.

19. Gurney, T.R., "The Influence of Thickness on the Fatigue Strength of Welded Joints," Proceedings 2nd International Conference on Behaviour of Offshore Structures (BOSS), London, 1979.

20. Maddox, S.J., "The Effect of Plate Thickness on the Fatigue Strength of Fillet Welded Joints," The Welding Institute, 1987.

21. Gurney, T.R., "Revised Fatigue Design Rules," Metal Construction 15, 1983.

22. Smith, I.J., "The Effect of Geometry Change Upon the Predicted Fatigue Strength of Welded Joints," Proc. 3rd Int. Conf. on Numerical Methods in Fract. Mech., pp. 561-574.

23. General Dynamics Corp., "Standard Structural Arrangements," NSRP, July 1976.

24. "Guide for the Fatigue Strength Assessment of Tankers," American Bureau of Shipping, June 1992.

25. Comstock, E., ed., "Principles of Naval Architecture," SNAME, 1969.

26. Glasfeld, R., Jordan, D., Kerr, M., Zoller, D., "Review of Ship Structural Details," SSC-266, 1977.

27. Tanker Structure Cooperative Forum, "Workshop Report: Fatigue Life of High Tensile Steel Structures," 1991.

28. American Bureau of Shipping, "Rules for Building and Classing Steel Vessels," 1990, Paramus, New Jersey.

29. Jordan, C.R., Krunpen, R.P., "Design Guide for Ship Structural Details," SSC-331, 1990.

(THIS PAGE INTENTIONALLY LEFT BLANK)

Appendix A

Analysis of Ship Structural Details Used In Case Studies

(THIS PAGE INTENTIONALLY LEFT BLANK)

A.1 CASE STUDY INTRODUCTION

The case studies presented below are used to illustrate the complex loading on ship structure details. Linear Finite Element Analysis (FEA) was used to determine the fatigue design stress (σ_f) and resulting stress concentration factors (K_{scf}). The principal stress is used to characterize the stress and estimate stress concentration factors as described in this report. The stresses and details shown are application dependent and are used as a guide to develop the fatigue design strategy.

The following case studies are used to evaluate stress concentration factors.

1) Double hull tanker frame cutout for a longitudinal and a deep bracket in a transverse frame.

2) Roll on-Roll off (Ro/Ro) ship side port.

3) Double hull barge transverse floor cutout for a longitudinal.

4) Small Water Plane Twin Hull (SWATH) beam bracket in the haunch area.

A.2 CASE STUDY ANALYSIS

The first case study includes two details in a double hull tanker shown in Figures A-1 and A-2. The midship section of the double hull tanker is shown in Figure A-3. This is representative of a mid size tanker (A-1). Hull loading for the double hull tanker case study is developed following the ABS Guide For Fatigue Assessment of Tankers (A-2). The structural loading developed using this guide is calibrated to a long term stress distribution parameter. Hydrodynamic loading for similar sized tankers predicted by Bea, et al. (A-3) and Franklin (A-4) compares favorably with the pressure developed using ABS guidelines. The frame cutout and deep knee bracket are of interest because they experience fatigue failure (A-5). ABS guide recommends fatigue analysis for both details (A-2). Typical frame cutout loading is shown in Figure A-4. Detail geometry and FEA models of the hull sections frame cutout and a deep knee bracket are shown in Figures (A-5) through (A-9). Stress concentration factors are shown in Tables (A-1 and A-2) for panel stiffeners and deep brackets.

The Ro/Ro ship side port case study is of a detail common to Sealift ships being built in the United States (A-6). The Ro/Ro ship and side port are shown in Figures A-10 and A-11. The basic FEA model is shown in Figure A-12. Stress concentration factors are shown in Table A-3 for side cutouts.

The double hull barge case study is a cut out in the double bottom floor. Loading and response data are presented by Fricke (A-7). The midship section and detail are shown in Figures A-13 and A-14. Stress in this cutout is shown in A-14.

The SWATH case study is a beam bracket in the haunch area of the strut. Loading data will be based on the data published by Sikora (A-8). Improved detail will be based on the investigators knowledge of this type of detail in SWATH ships. The SWATH ship, midship section and beam bracket are shown in Figures A-15, A-16, and A-17. The basic FEA model is shown in Figure A-18. Stress concentraction factors are shown in Table A-4 for typical beam brackets.

It is interesting to note that the chocked beam bracket has the lowest K_{scf} (1.57). This must be compared to the K_f to fully understand evaluate its application. The K_f for the weld between the bracket flange and beam flange is very important. The weld is loaded axially. K_f for an axially loaded fillet weld is 5.5 and K_f for an axially loaded groove weld is 2.63. Using the guidance provided in Section 4.1:

Groove weld $K_f * K_{scf} = 1.57 * 2.63 = 4.1$

Fillet weld $K_f * K_{scf} = 1.57 * 5.53 = 8.63$

Clearly, the fillet weld has a high combined K_f and K_{scf} at $\sigma_n = .3\sigma y$. For a plain beam bracket:

Fillet weld $K_f * K_{scf} = 3.0 * 2.25 = 6.75$

The plane bracket has a higher combined K_f and K_{scf} than a groove welded flange bracket, but better than a fillet welded bracket for this application.

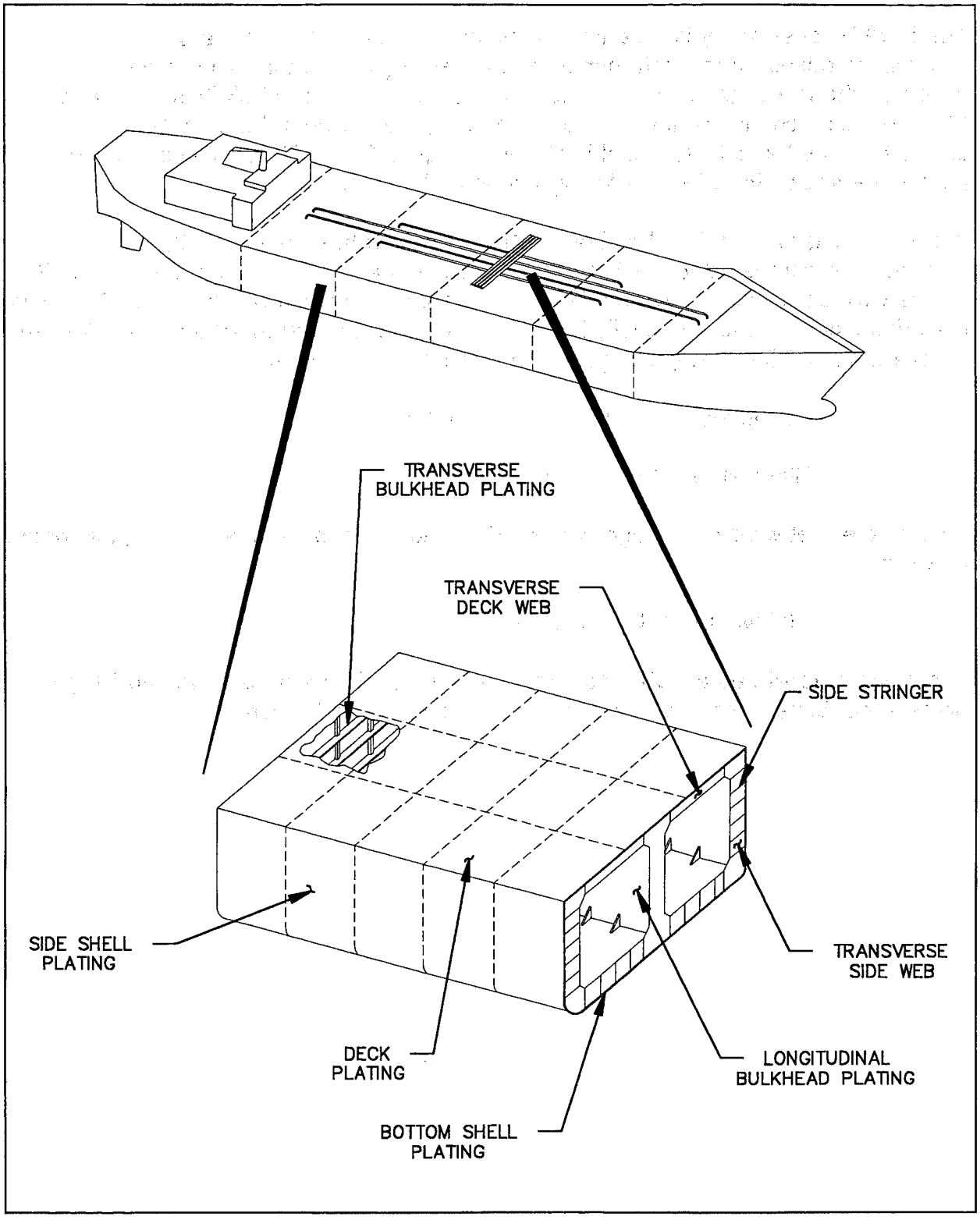

Figure A-1 Double hull tanker

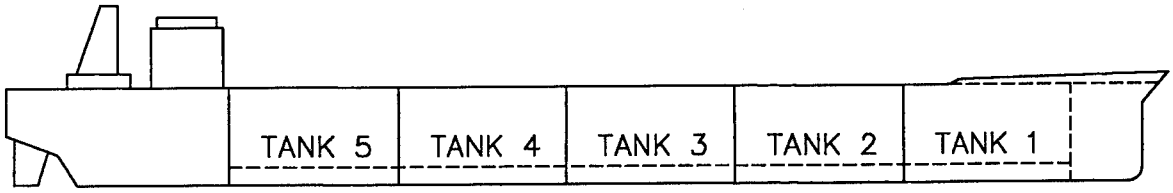

PROFILE

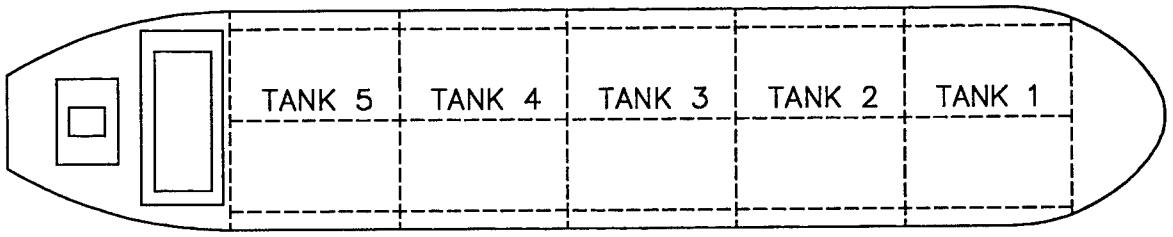

PLAN

DWT	150,000 t
LBP	250 m
LOA	260 m
BREADTH	40 m
DEPTH	20 m
CONSTRUCTION	DOUBLE HULL

Figure A-2 Double hull tanker characteristics

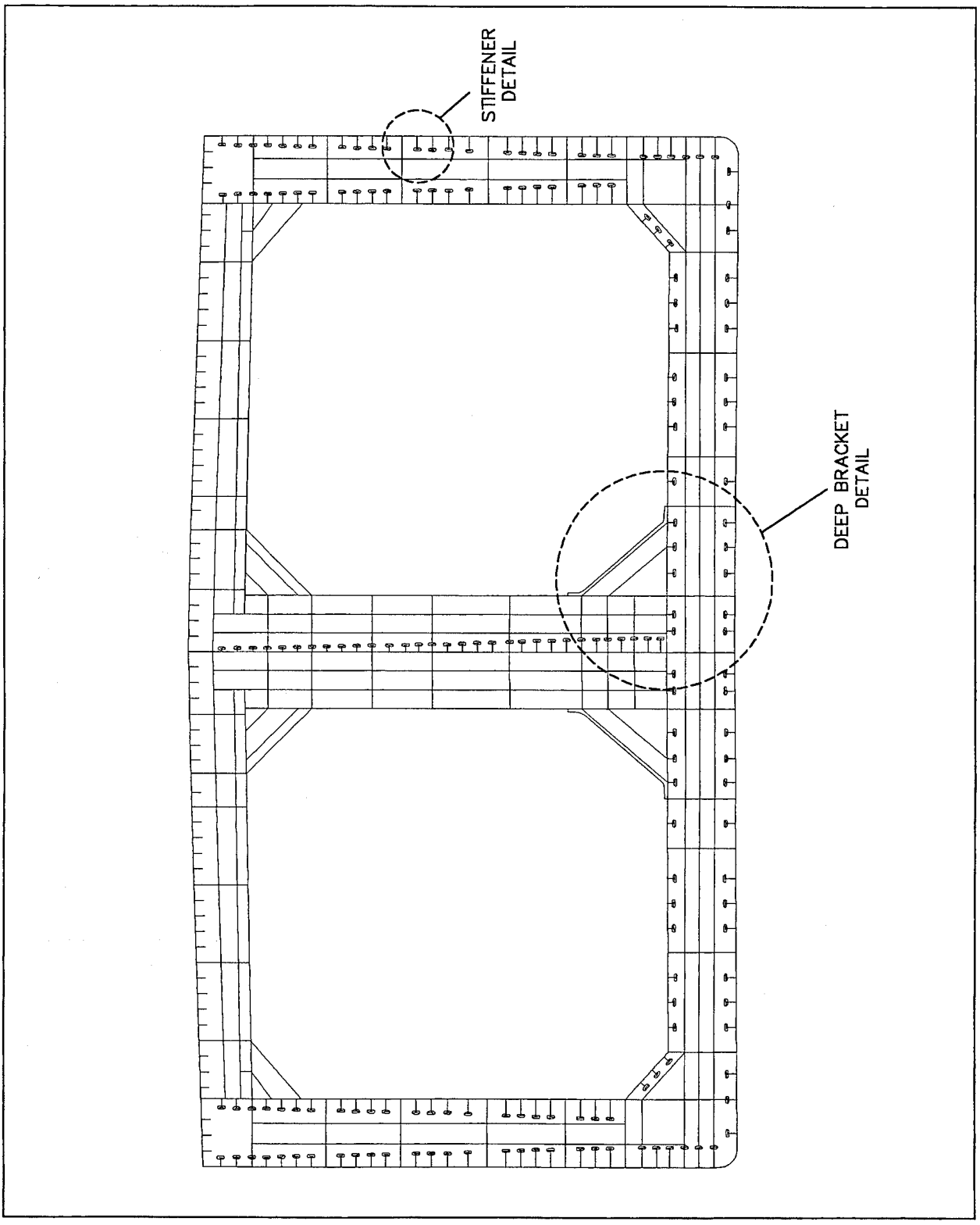

Figure A-3 Double hull tanker midship section

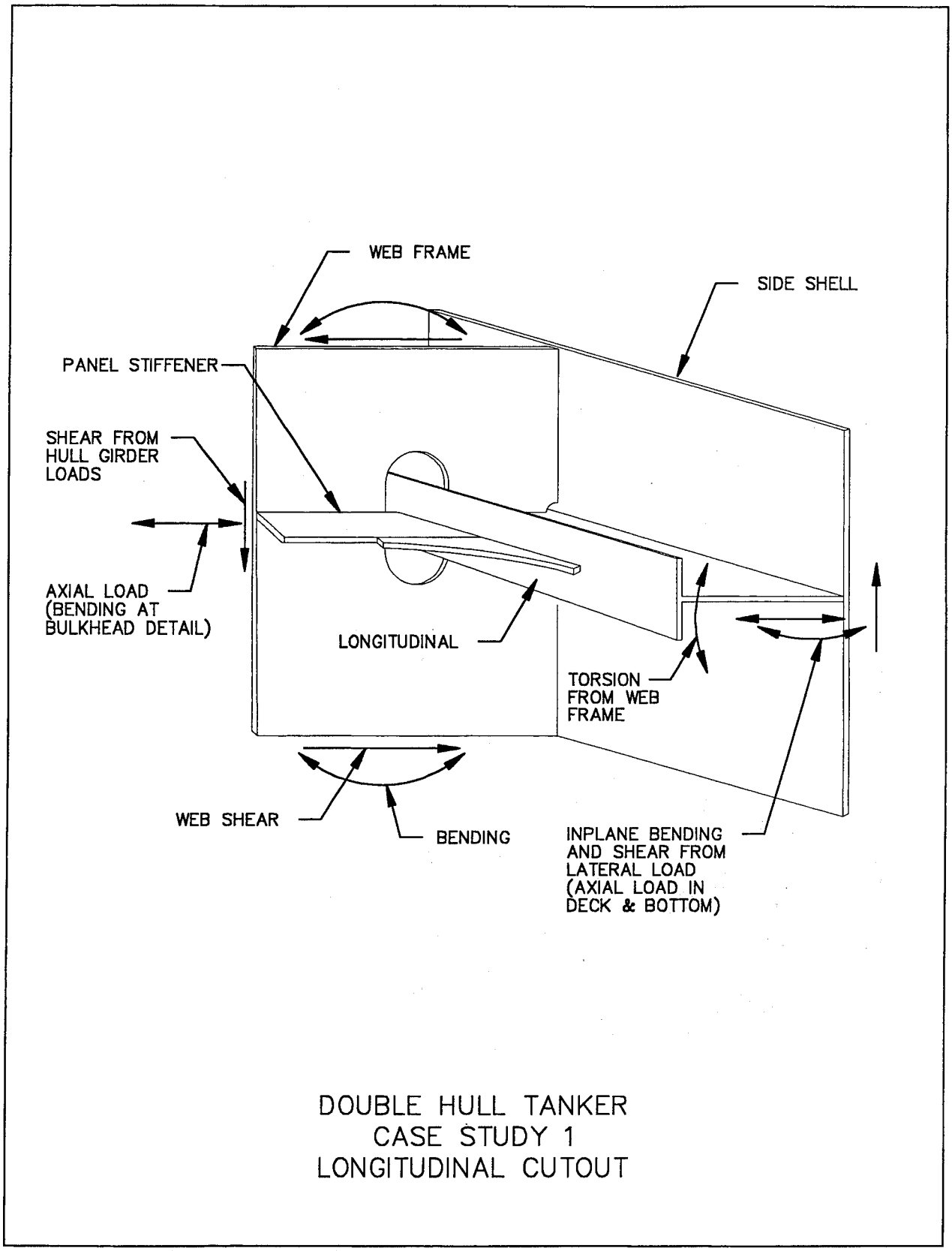

Figure A-4 Loading on side shell frame cutout

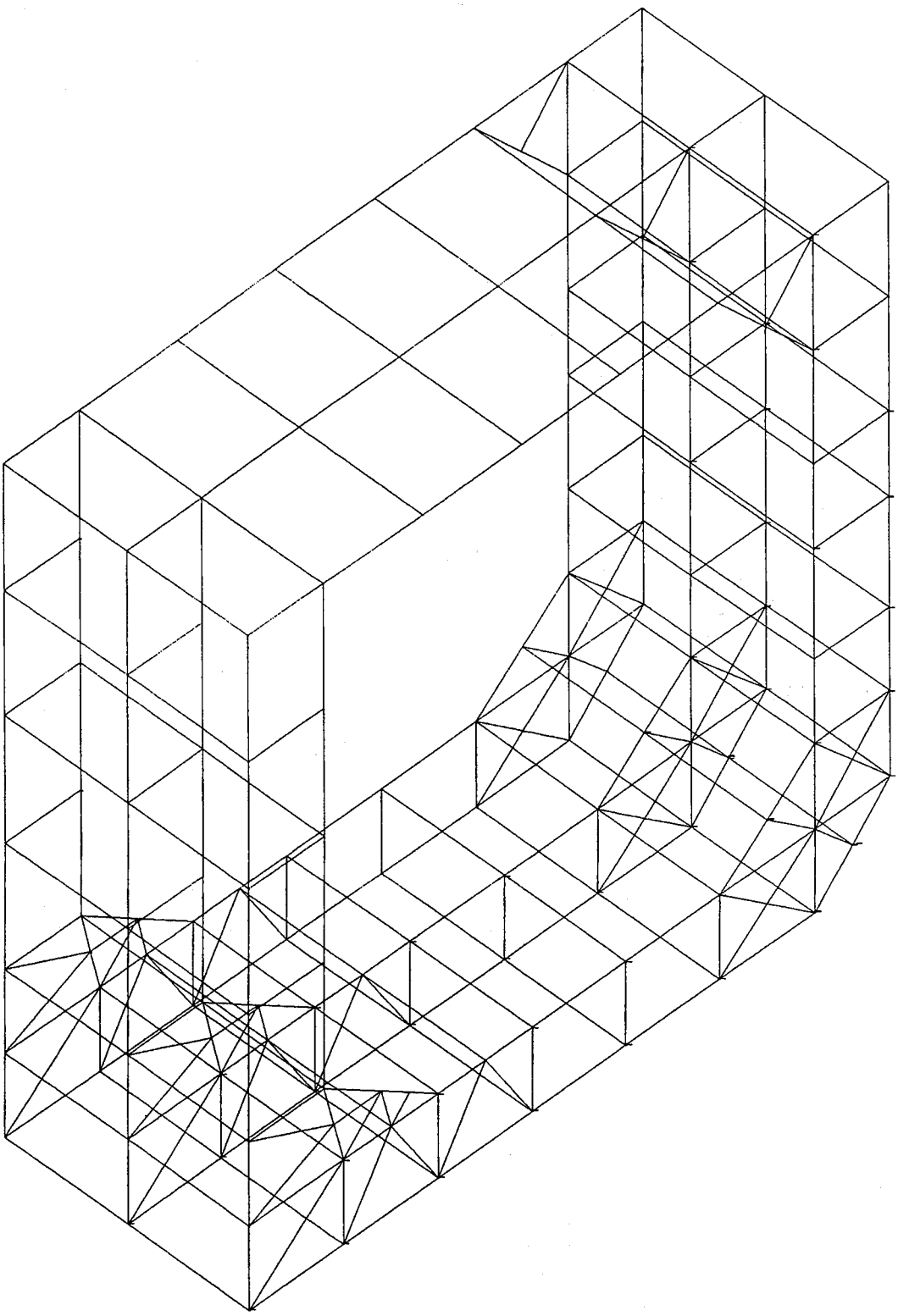

Figure A-5 Course mesh FEA model of double hull tanker

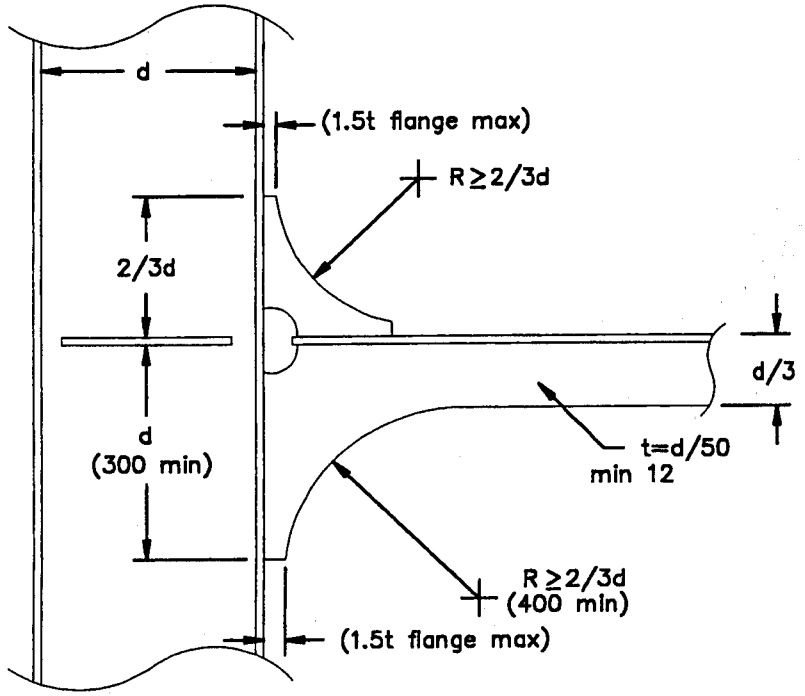

Figure A-6 Detail geometry of panel stiffener

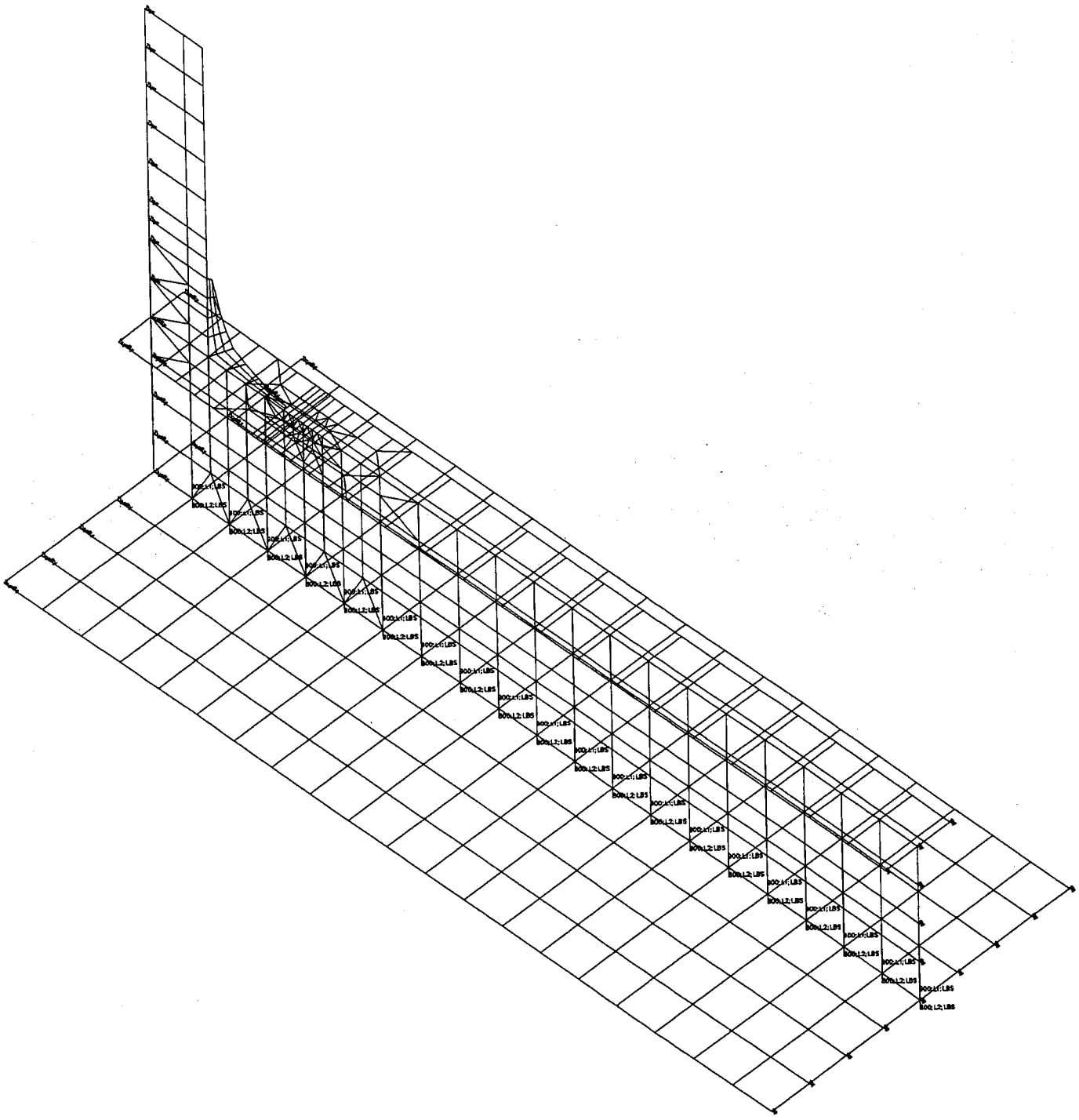

Figure A-7 FEA model of panel stiffener

Table A-1 Stress Concentration Factors for Panel Stiffeners

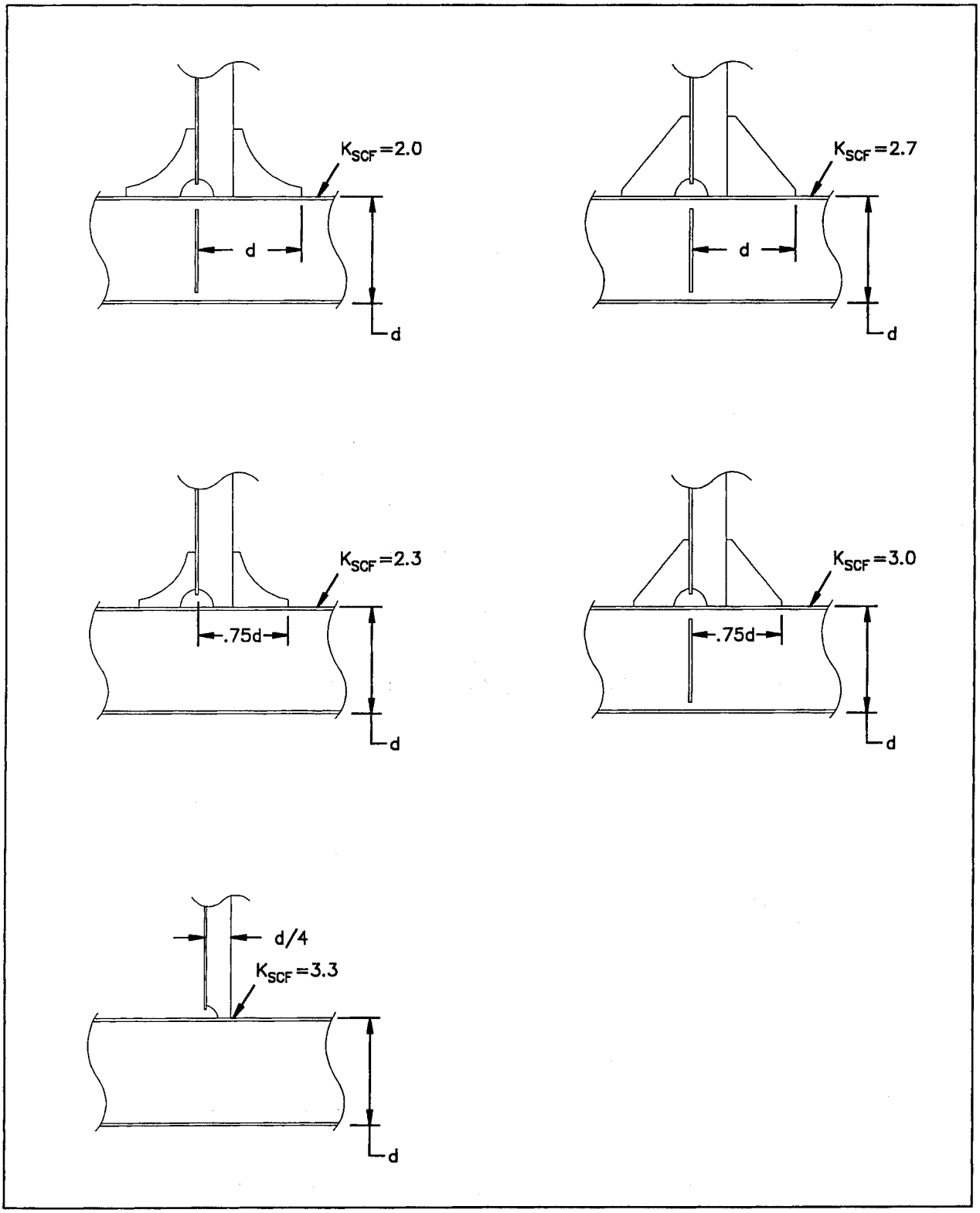

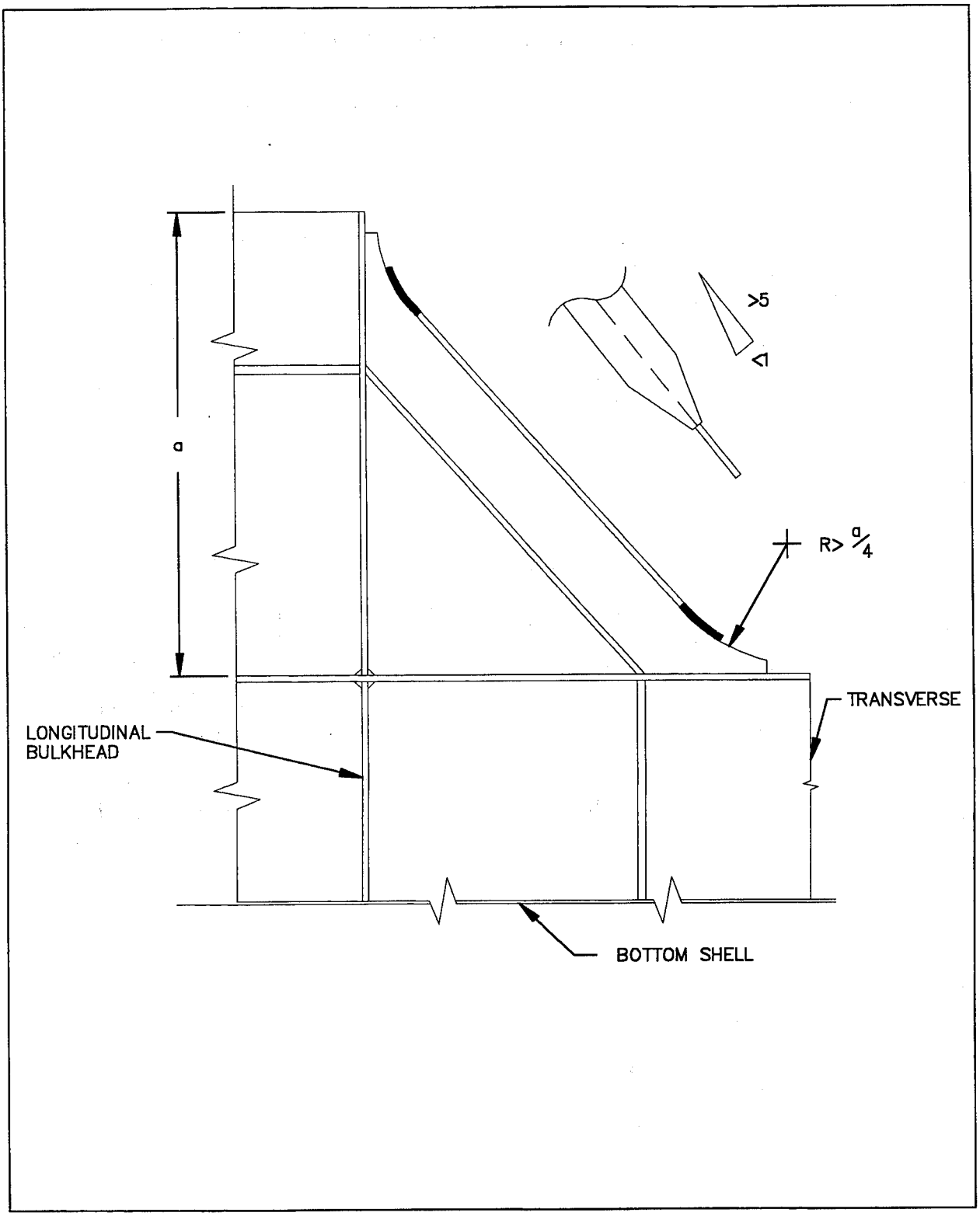

Figure A-8 Detail geometry for deep bracket

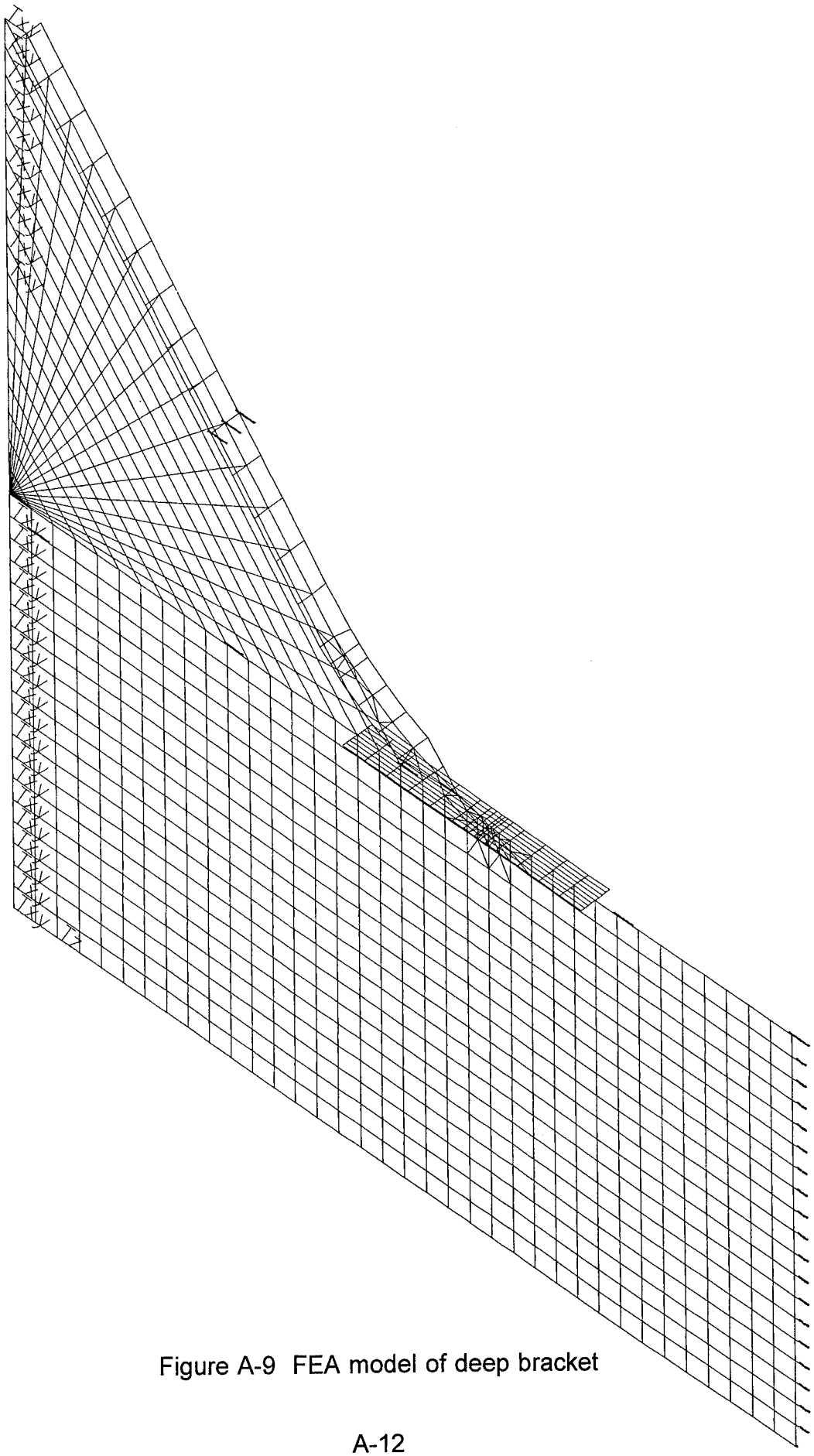

Figure A-9 FEA model of deep bracket

Table A-2 Stress Concentration Factors of Deep Bracket

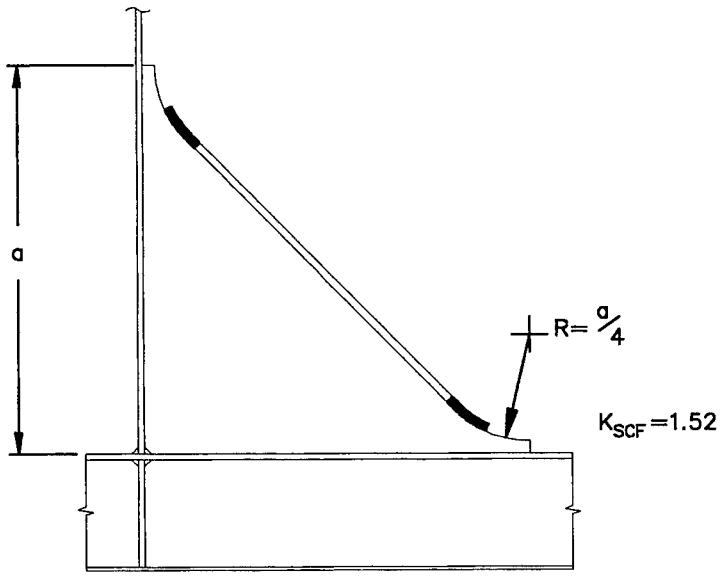

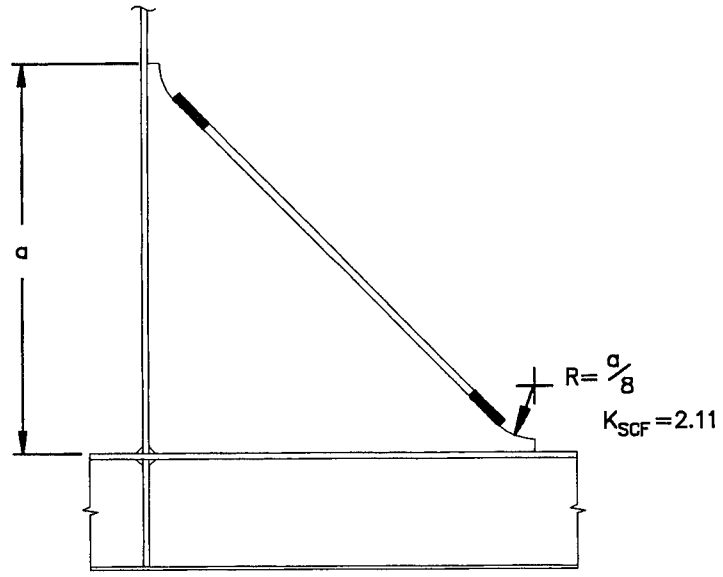

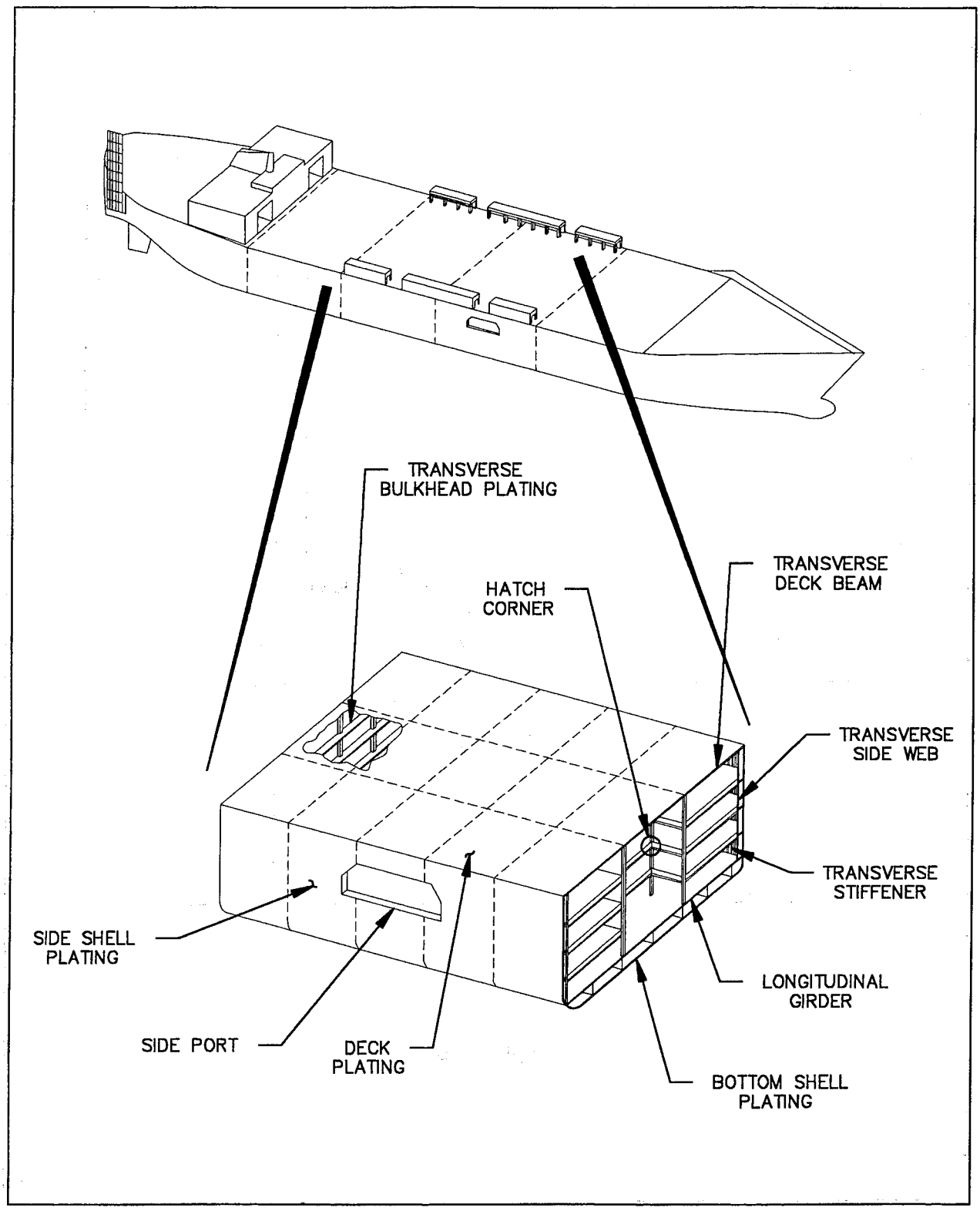

Figure A-10 Ro/Ro side port cutout

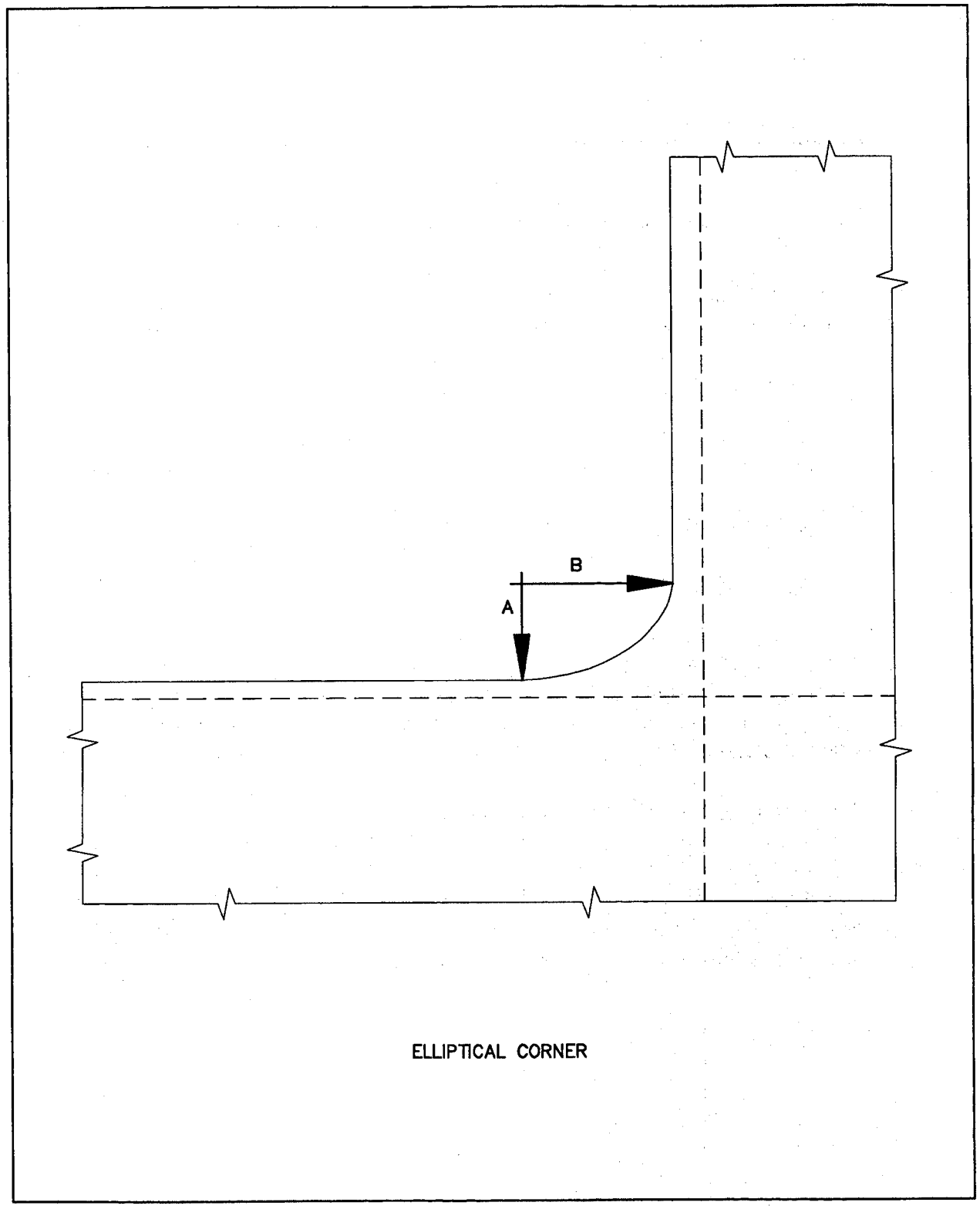

Figure A-11 Ro/Ro side port cutout detail

Table A-3 Stress Concentration Factors for Side Port Cutout

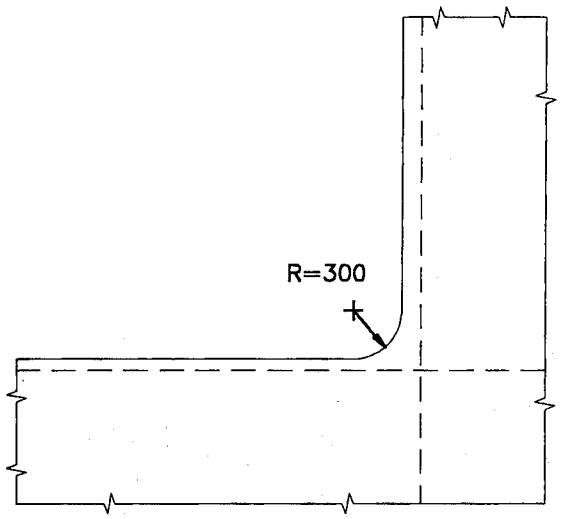

$K_{SCF} \simeq 2.0$

RADIUS CORNER

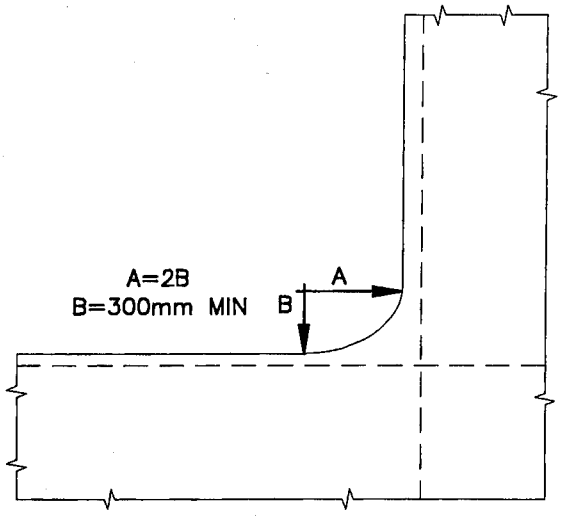

$K_{SCF} \simeq 1.5$

ELLIPTICAL CORNER

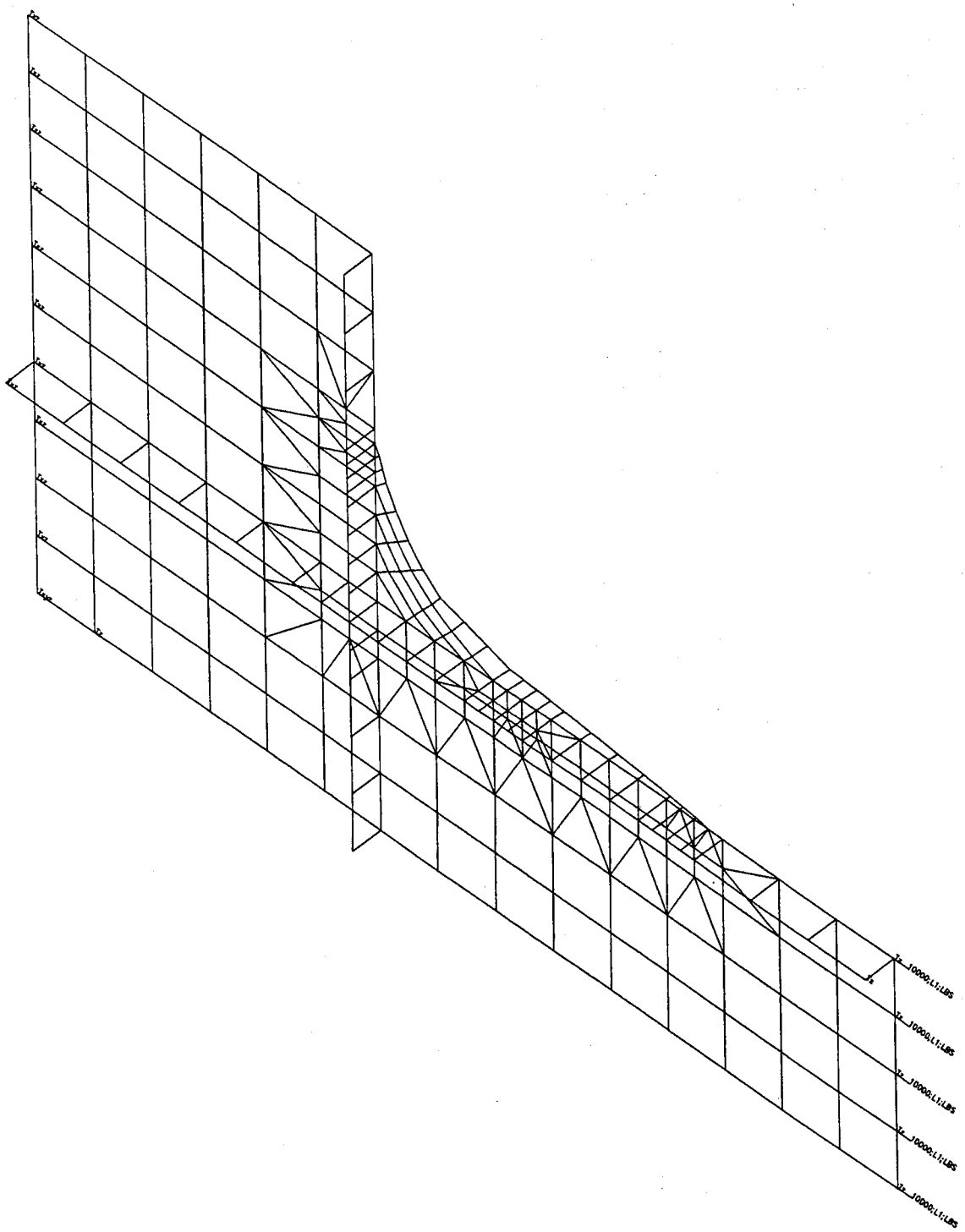

Figure A-12 FEA model of side port cutout

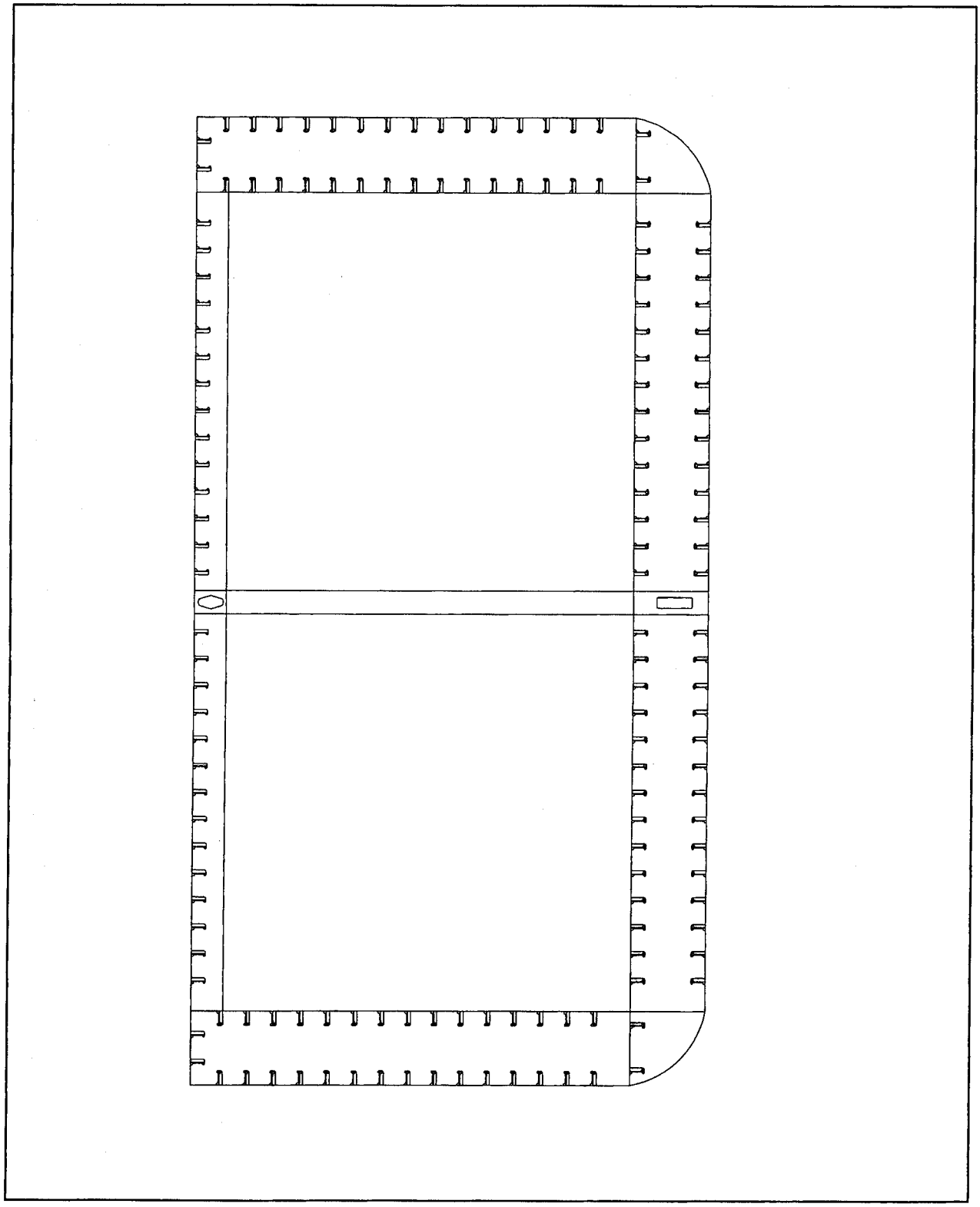

Figure A-13 Double hull barge midship section

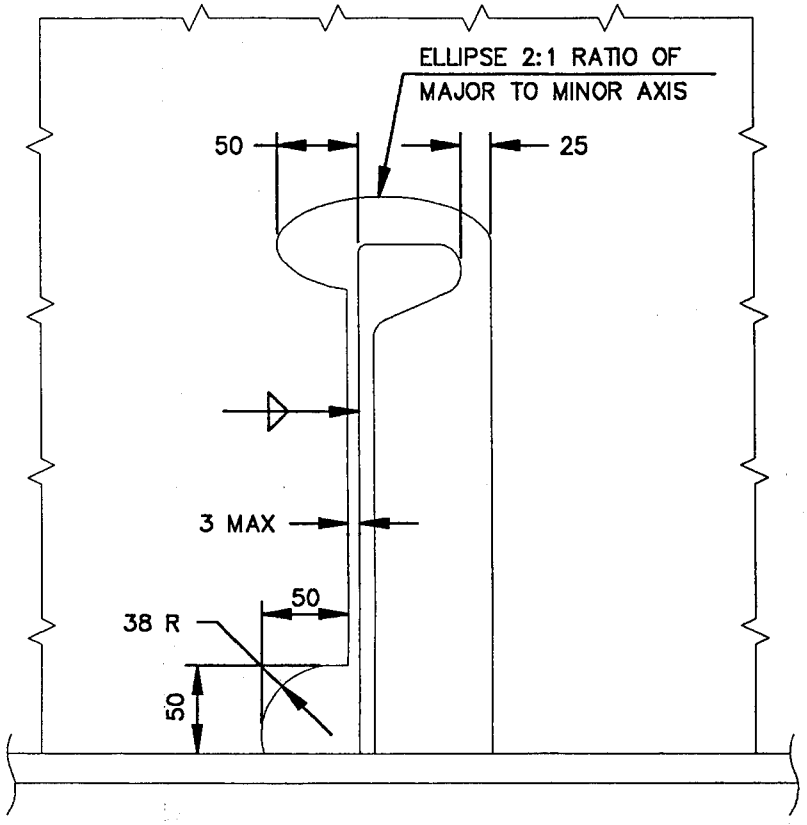

Figure A-14 Detail geometry for bulb plate cutout

Table A-4
Stress Concentration Factors for Bulb Plate Cutout

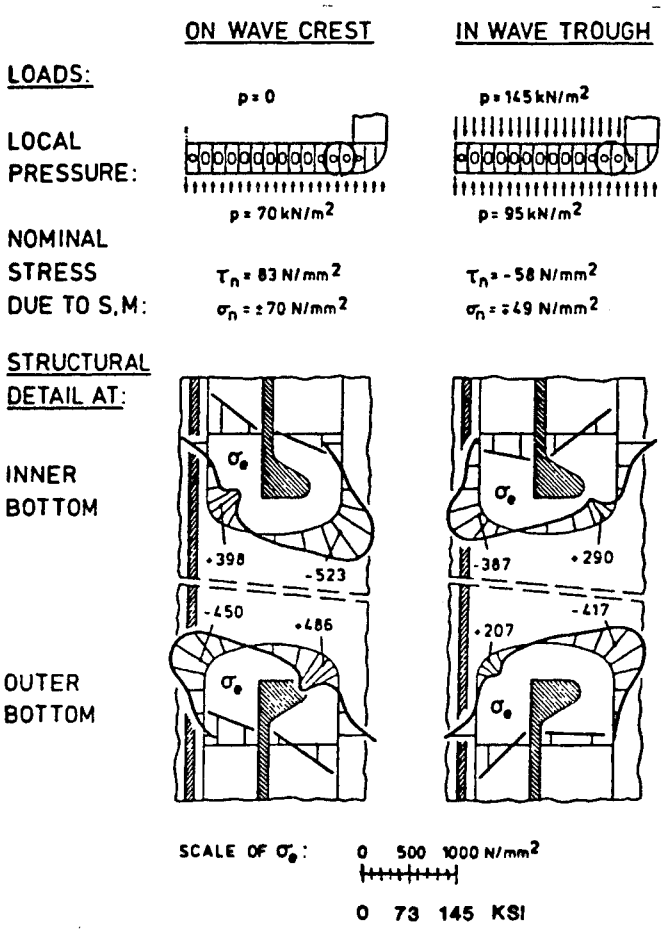

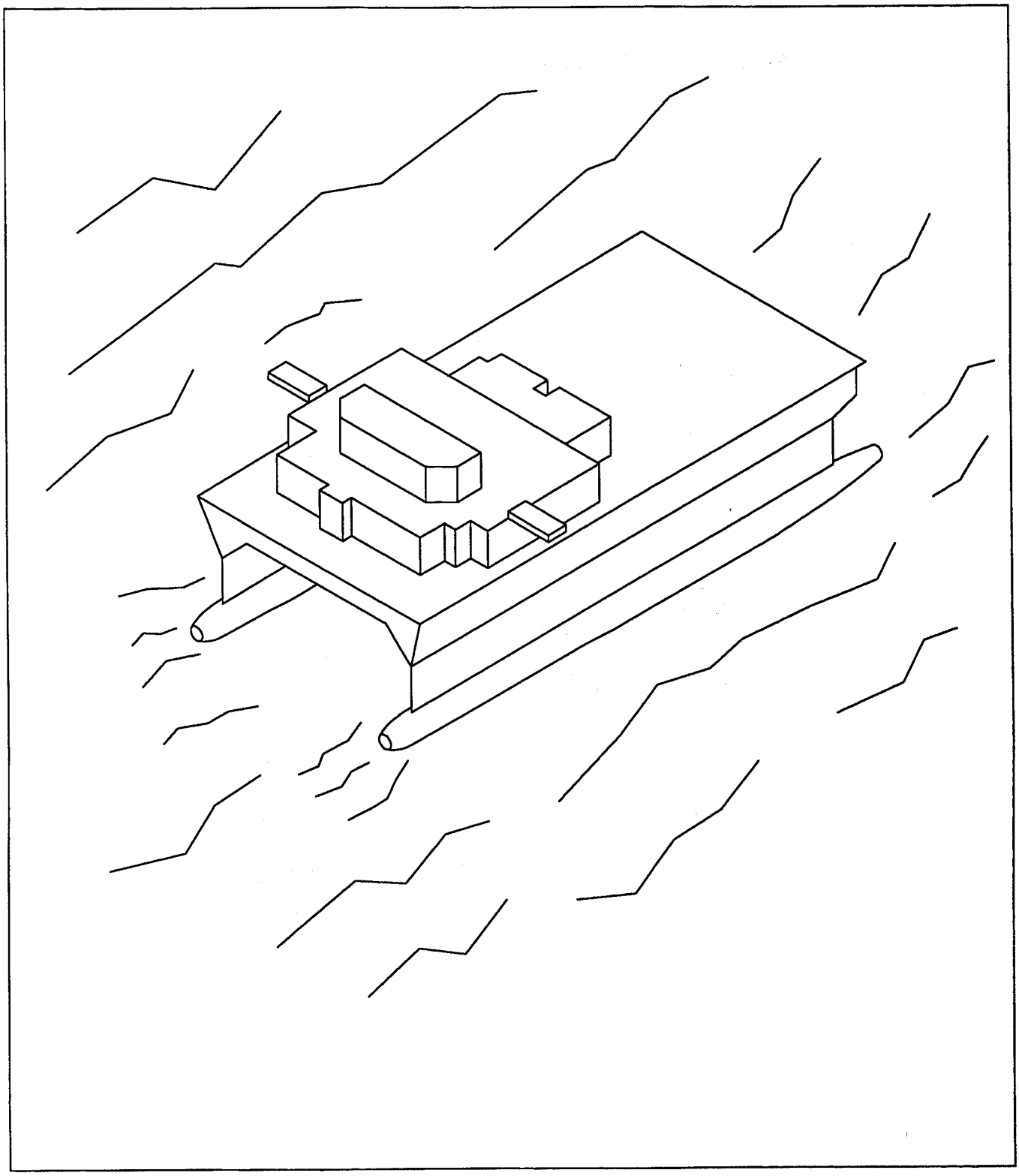

Figure A-15 SWATH ship

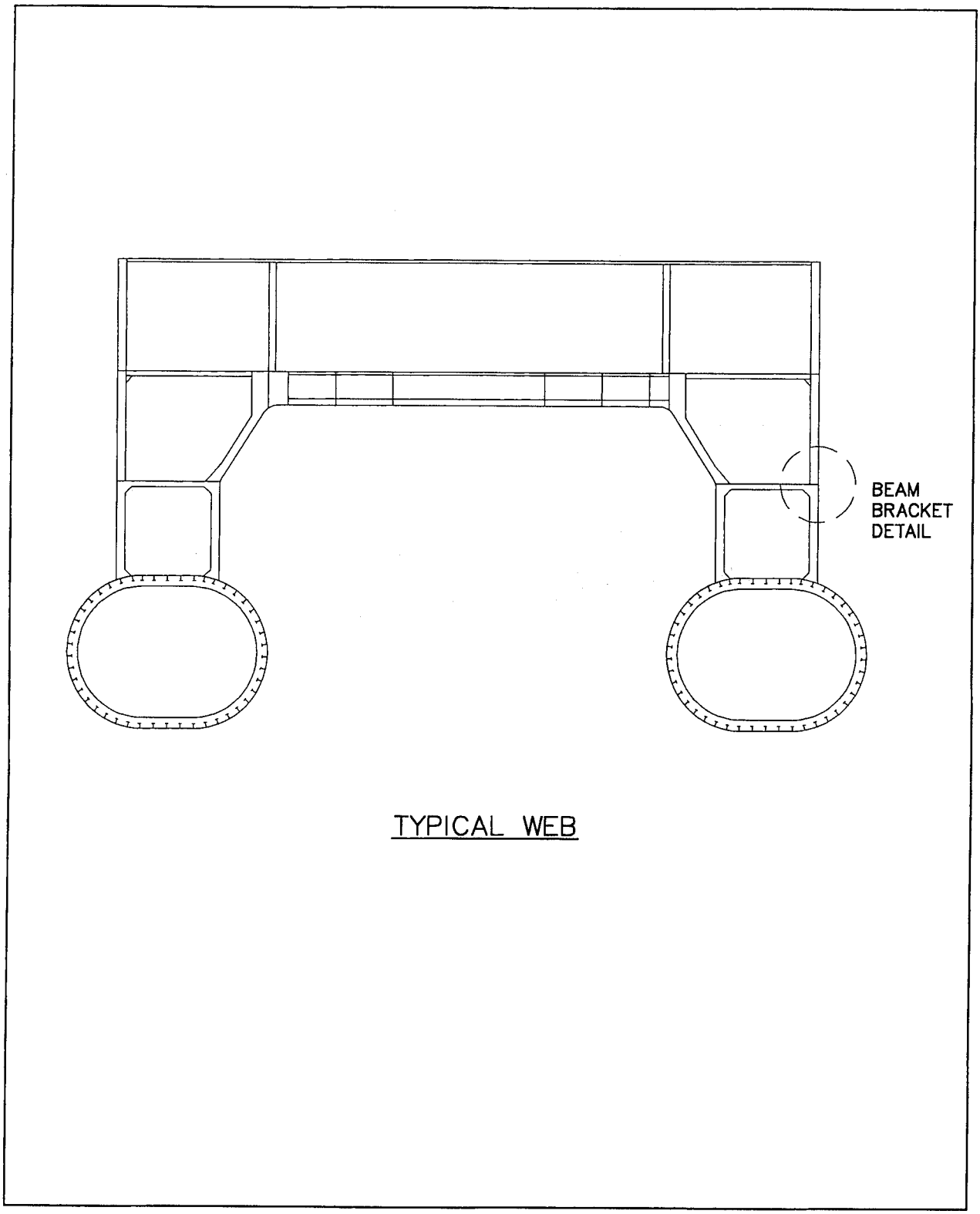

Figure A-16 SWATH ship midship section

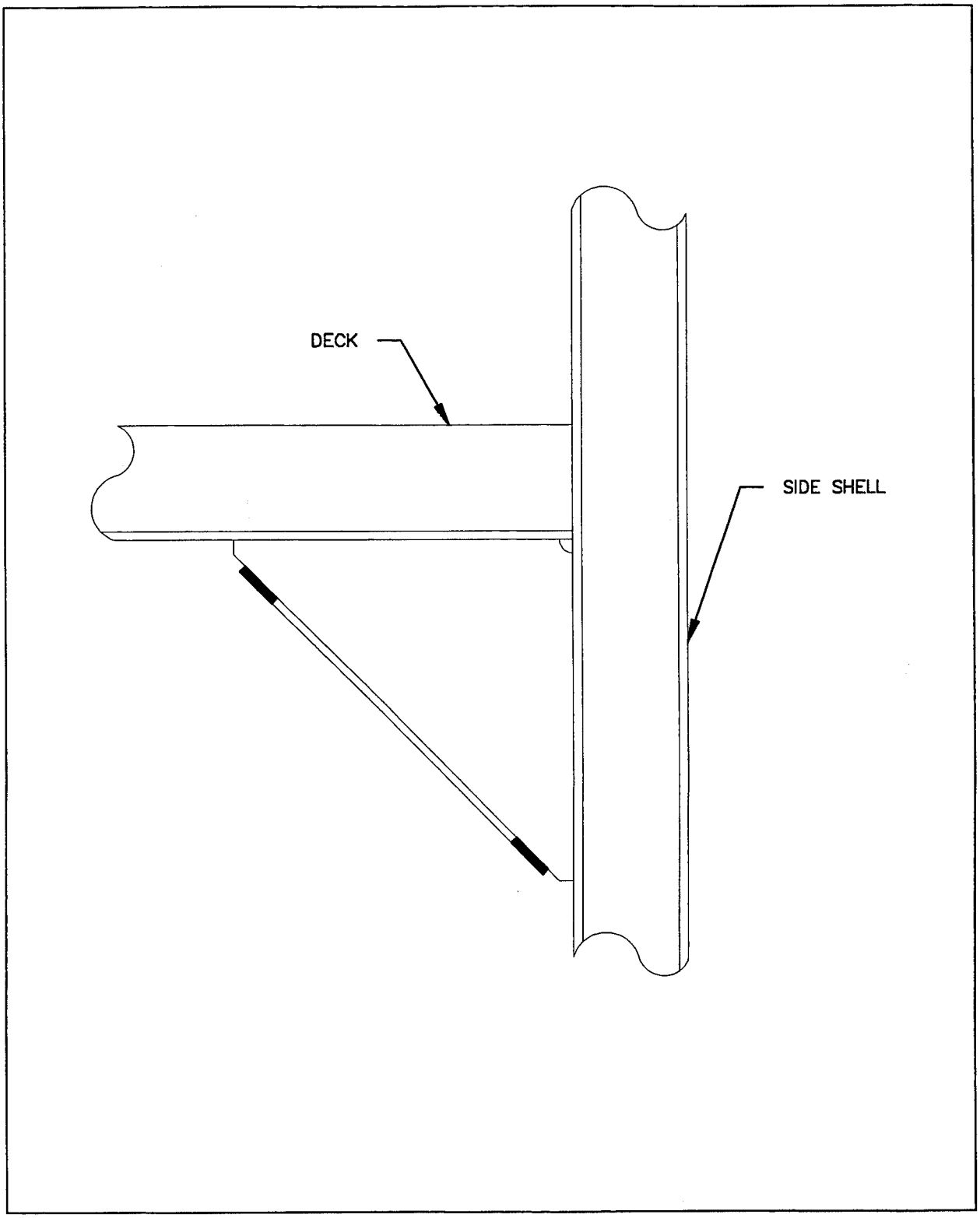

Figure A-17 Detailed geometry for SWATH ship beam bracket

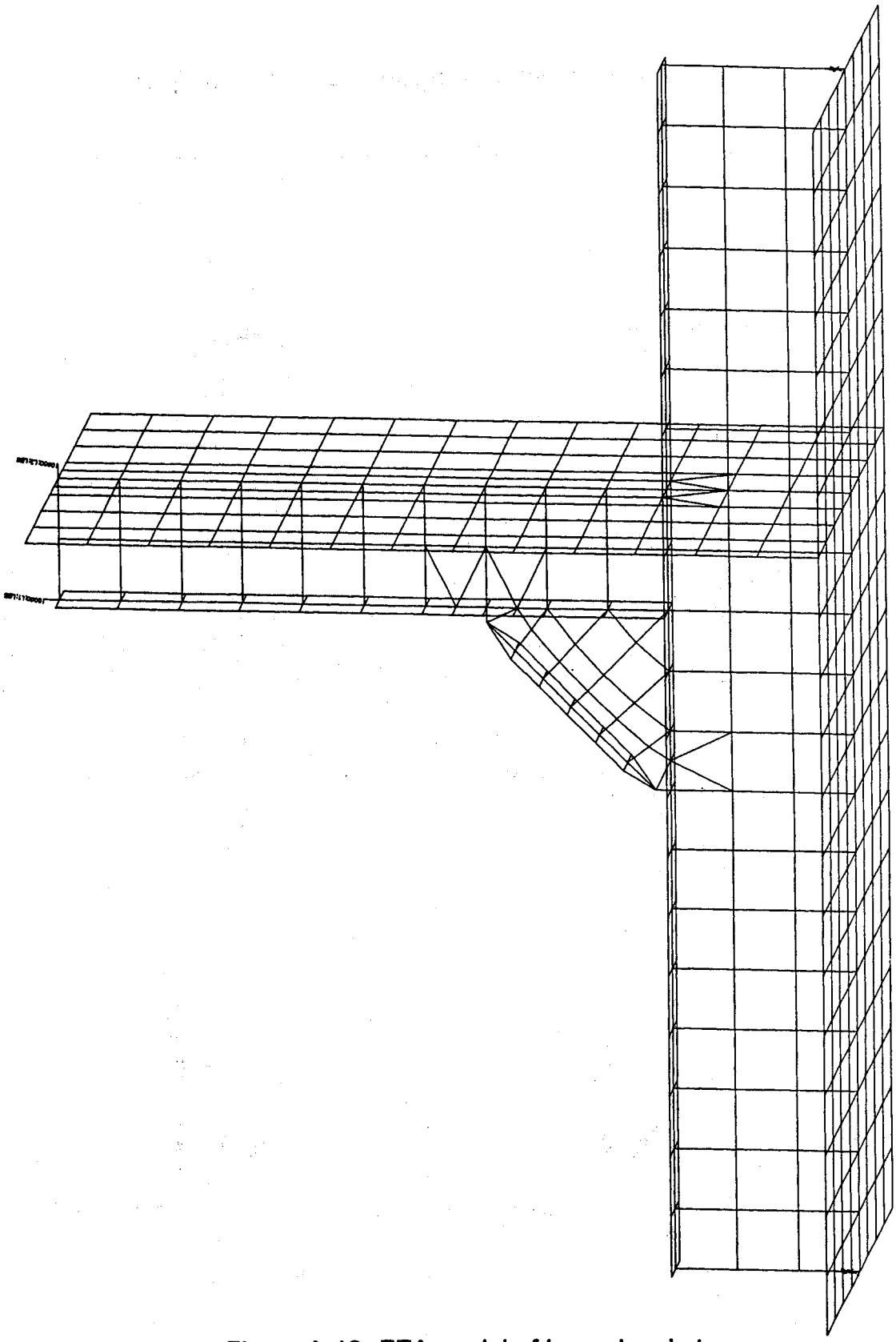

Figure A-18 FEA model of beam bracket

Table A-4 Stress Concentration Factors for Beam Brackets

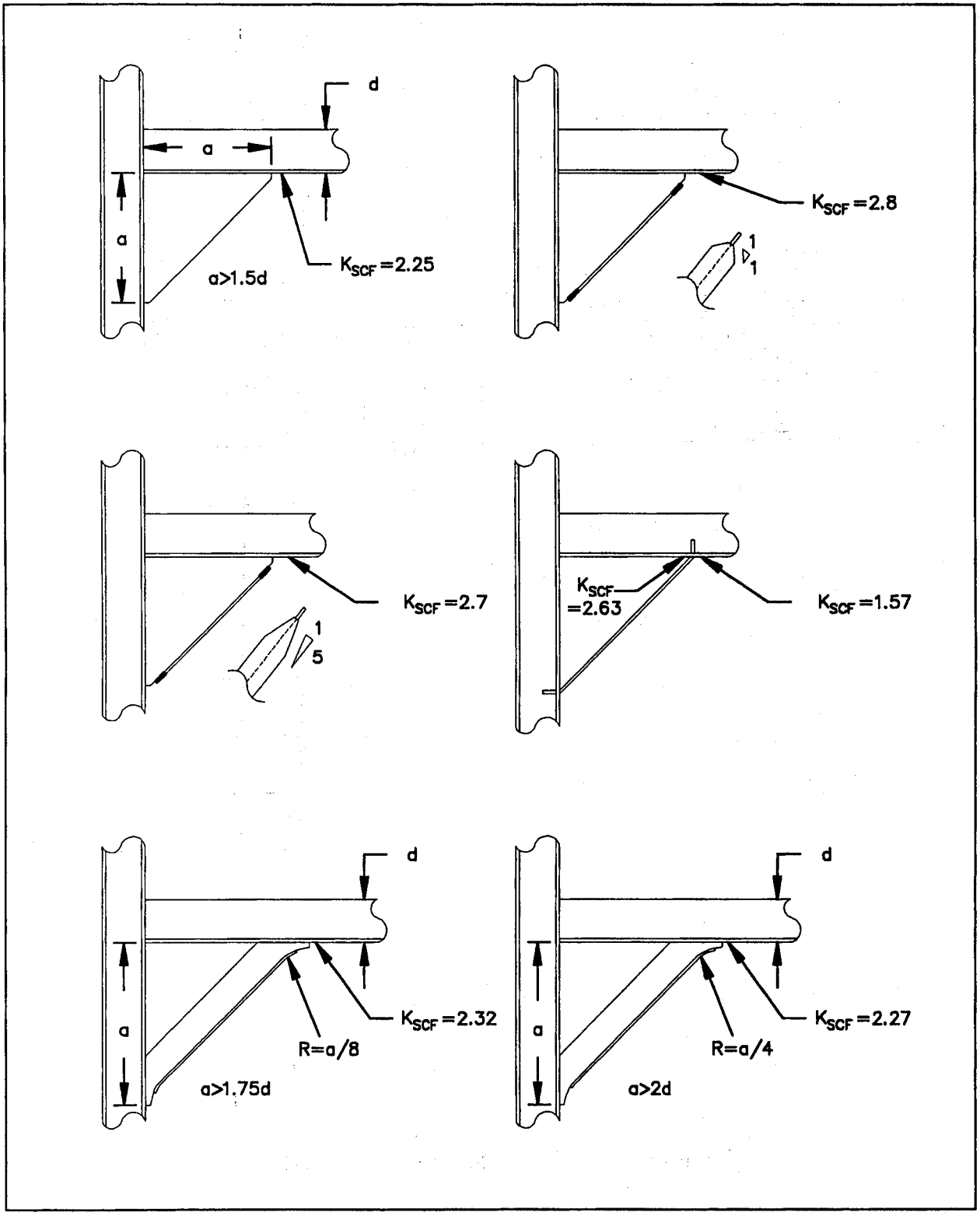

A.3 REFERENCES

A-1 Chen, H.H., Jan, H.Y., Conlon, J.F., and Liu, D., "New Approach for the Design and Evaluation of Double Hull Tanker Structures," SNAME Transaction, 1993.

A-2 "Guide for the Fatigue Strength Assessment of Tankers," American Bureau of Shipping, June 1992.

A-3 Schulte-Strathus, R., and R. G. Bea, 1993, "Fatigue Classification of Critical Structural Details in Tankers: Development of Calibrated S-N Curves and System for the Selection of S-N Curves," Report No. FACTS-1-1, University of California, Berkeley.

A-4 Franklin, P. and Hughes, O., "An Approach to Conducting Timely Structural Fatigue Analysis of Large Tankers," SNAME T&R-R41, September, 1993.

A-5 Exxon Corporation, "Large Oil Tanker Structural Survey Experience," Position Paper, June 1, 1982.

A-6 Wood, W., Edinberg, D., Stambaugh, K., and Oliver, C., "Prediction of Fatigue Response in TAK-X Side Port Structural Details," Giannotti & Associates, 1982 (Proprietary).

A-7 Fricke, W. and Daetzold, H., "Application of the Cyclic Strain approach to the Fatigue Failure of Ship Structural Details," Journal of Ship Research, September 1987.

A-8 Sikora, J.P., Dinsenbacher, A., and Beach, J.E., "A Method for Estimating Lifetime Loads and Fatigue Lives for SWATH and Conventional Monohull Ships," Naval Engineers Journal, ASNE, May 1983, pp. 63-85.

Appendix B

Development of Fatigue Notch Factors

(THIS PAGE INTENTIONALLY LEFT BLANK)

B.0 FATIGUE NOTCH FACTORS

B.1 DETAIL

Ship structural details vary in geometry and loading making it difficult to correlate them to existing data developed for structural details in published literature. In order to correlate the ship structural details geometries with test data, it is necessary to define basic weld configurations that are, to the extent practical, independent of detail geometry. The basic weld configurations associated with ship structural details can be defined as:

1) Weld ripple of longitudinally loaded groove or fillet welds,
2) Weld toes of transversely loaded groove welds,
3) Weld toes of transversely loaded non-local carrying fillet welds,
4) Weld toes of transversely loaded load carrying fillet welds and,
5) Weld toes of fillet weld terminations.

Each of these five basic weld configurations and associated failure location is correlated to an equivalent detail from the fatigue data presented in Tables B-1 and B-2 from SSC-318 (B-I) and SSC-369 (B-2). The K_f values for each detail are also shown in Table B-1 and summarized in Table 3-1 for the basic weld configurations.

The definition of stress and K_f associated with the basic weld configurations is the nominal stress range as documented in Section 3.0 of this report. However, stress and K_f associated weld termination common in ship details (shown in Table 4-1) requires re-evaluation to be generic in application. The weld termination associated with the straight attachment of detail 30 shown in Table B-2 is used to establish K_f of 3.6 at one plate thickness from the weld toe. FEA from the University of California Berkeley (B-3) presents K_t at various distances from the weld toe for a pair of similar attachment details as shown in Figures B-1 and B-2. A stress concentration factor can be inferred at one plate thickness from the weld toe. With this information, it is possible to estimate K_f of 3.0. This is independent of attachment geometry. Because this new K_f is independent of attachment geometry, it can be used with stress concentration factors associated with other detail geometries. This assumes that the designer has knowledge of the state of stress at one plate thickness from the weld toe. This must be obtained from FEA of the detail or from the nominal stress and an associated K_{scf} as described earlier in this report.

Table B-1

Fatigue Strength of Welded Details

SSC - 318 Weldment Details	Mean Fatigue Strength (ΔS) at 1E+06 Cycles (ksi)				Standard Deviation of Log ΔS (ksi units)		Kf	Fatigue Crack Initiation Sites
	SSC - 318	All R , All Sy	R = 0	R = 0 , Sy < 50 ksi	R = 0	R = 0 , Sy < 50 ksi		
1Q	51	51.8	51	----	0.074	----	1.43*	----
1H	48.5	48.2	45.6	39.3	0.06	0.04	1.43*	----
1.All	46.5	44.9	42.1	38.2	0.104	0.042	1.43*	----
1M	38.3	37.1	36.2	36.2	0.04	0.04	1.43*	----
8	39.2	39.8	39.1	35.4	0.094	0.079	1.54	----
2	42	42.1	41	35	0.076	0.017	1.43*	----
10(G)	36.1	35.2	32.8	31.6	0.136	0.127	1.82	Weld
10Q	31.2	31.5	32.7	----	0.114	----	1.84	Toe
3(G)	31.3	31.2	31	31	0.084	0.081	1.94	Weld
1(F)	41.5	38.4	38.4	30.5	0.117	0.057	1.43*	----
10A	30.9	31.1	28.8	29.7	0.115	0.066	2.04	Toe
25A	38.1	35.8	29.3	29.6	0.109	0.12	2.05	Toe
3	30.3	29	29.1	29.2	0.049	0.044	2.07	Ripple
13	28	27.8	27.3	28.5	0.055	0.057	2.15	Toe
2S	29.8	29.8	28.4	28.1	0.097	0.045	2.11	----
12(G)	27.2	27.2	27.2	27.2	0.072	0.072	2.16	Weld
10H	34	35.2	33.1	25.8	0.102	0.101	1.84	Toe
4	28.3	27.3	26.8	25.7	0.092	0.095	2.19	Ripple
6	28.3	27.3	26.8	25.7	0.092	0.095	2.19	Ripple
9	25.7	25.7	25.8	25.5	0.079	0.085	2.33	----
10M	25.2	26.4	24.5	24.5	0.093	0.093	2.46	Toe
16(G)	23.6	22.7	24.5	24.5	0.215	0.215	2.46	Root
25	24	24.1	23.9	24.5	0.09	0.08	2.52	Toe
7(B)	24.3	23.8	23.8	24.4	0.083	0.11	2.46	Toe or D. T.**
19	17	23.2	23.1	----	0.157	----	2.61	Toe
30A	23	23	23	23	0.014	0.014	2.62	D. T.
26	17.1	17.4	23	23	0.054	0.054	2.62	Toe
14	29.8	25.9	22.9	22.9	0.115	0.109	2.63	Toe
11	22.3	22.7	22.7	22.1	0.078	0.08	2.58	Toe
21	21.8	21.8	21.8	21.8	0.117	0.117	2.69	Toe
7(P)	20.4	21.5	21.5	----	0.075	----	2.73	Toe or D. T.
36	20.6	20	20	20	0.062	0.062	3.01	D. T.
25B	20.6	20	20	20	0.062	0.062	2.93	Toe or D. T.
12	19.6	19.7	19.7	19.7	0.055	0.055	2.98	Toe
16	19.9	19.6	19.6	19.6	0.104	0.104	3.07	Toe or Root
22	19.2	19.1	19.5	19.4	0.045	0.044	3.01	Toe
21(3/8")	18.1	17.9	17.9	17.9	0.037	0.037	3.28	Toe
20	16.1	17.5	17.5	17.5	0.099	0.099	3.44	Toe
23	17.2	18.3	----	----	----	----	----	Toe
24	17.2	18.3	----	----	----	----	----	Toe
30	16.7	16.7	16.7	16.7	0.051	0.051	3.6	D. T.
38	16	16	16	16	0.058	0.058	3.66	Toe
17A	15.6	16.2	15.8	15.8	0.051	0.051	3.81	D. T.
17	15	14.6	14.6	14.6	0.046	0.046	4.26	D. T.
18	11.5	12.2	12.8	14.5	0.107	0.148	4.7	D. T.
32A	14.1	14.1	14.1	14.1	0.055	0.055	4.16	D. T.
27	12	12.8	13.5	13.5	0.101	0.101	4.46	----
33	11.4	11.6	12.9	12.9	0.055	0.055	4.67	Toe at C.T. or D. T.**
31A	15.7	15.6	15.8	----	0.12	----	3.71	Toe
46	11.9	11.9	----	----	----	----	----	D.T.
40	11.2	11.2	----	----	----	----	----	Toe and D. T.
32B	11.2	11.2	----	----	----	----	----	Toe and D. T.

*Plain Plate

* C. T. - Continuous Termination , D. T. - Discontinuous Termination

Table B-1

Fatigue Strength of Welded Details (con't.)

SSC - 318 Weldment Details	Mean Fatigue Strength (ΔS) at 1E+06 Cycles (ksi)				Standard Deviation of Log ΔS (ksi units)		Kf	Fatigue Crack Initiation Sites
	SSC - 318	All R , All Sy	R = 0	R = 0 , Sy < 50 ksi	R = 0	R = 0 , Sy < 50 ksi		
21(S)	31	31	30.5	30.5	0.031	0.031	1.97	Toe
18(S)	20	20	21	21	0.042	0.042	2.87	Toe and D. T.
33(S)	20.5	20.5	20.7	20.7	0.06	0.06	2.91	Toe
17(S)	21	21	19.6	19.6	0.041	0.041	3.07	Toe
17A(S)	21	21	19.6	19.6	0.041	0.041	3.07	Toe
20(S)	19.6	21.2	16.9	17.3	0.159	0.168	3.56	Toe
19(S)	20.3	18.2	15.4	15.4	0.124	0.124	3.91	Toe
38(S)	13	13.3	13.5	13.5	0.113	0.113	4.46	Toe

Table B-2

Welded Detail Classification

CATEGORY	DETAIL NUMBER	DESCRIPTION, LOADING	PICTOGRAPH
A	1	Plain plate, machined edges, Axial	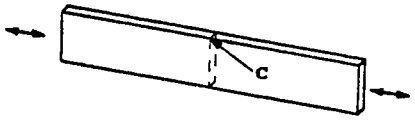
	2	Rolled I-Beam, Bending	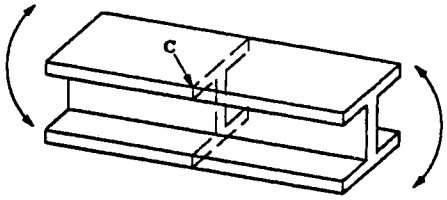
	8	Double shear bolted lap joint, Axial	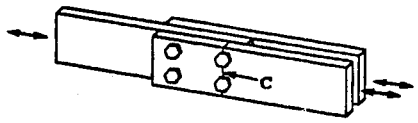
B	1(F)	Plain plate flame-cut edges, Axial	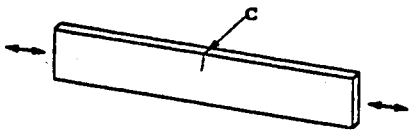

Key to symbols is presented on Page B-16

Table B-2

Welded Detail Classification (con't.)

CATEGORY	DETAIL NUMBER	DESCRIPTION, LOADING	PICTOGRAPH
B	3	Longitudinally welded plate, as-welded, Axial	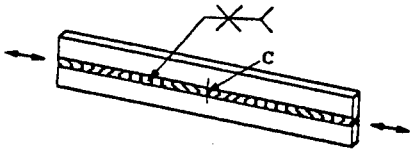 (As-welded)
	3(G)	Longitudinally welded plate, weld ground, Axial	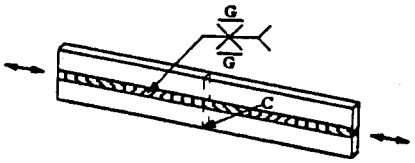 (Ground faces of the weld)
	10(G)	Transverse butt joint, weld ground, Axial	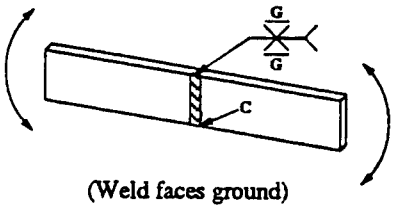 (Weld faces ground)
	10A	Transverse butt joint, as welded, In-plane bending	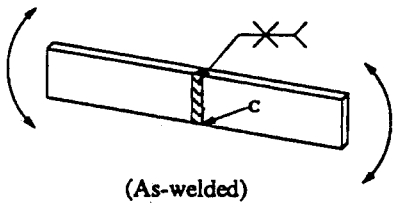 (As-welded)

Key to symbols is presented on Page B-16

Table B-2

Welded Detail Classification (con't.)

CATEGORY	DETAIL NUMBER	DESCRIPTION, LOADING	PICTOGRAPH
B	25A	Lateral attachment to plate, Axial	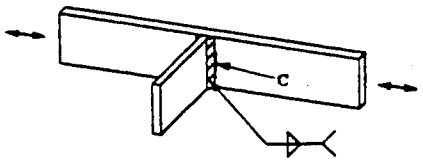
	13	Flange splice (unequal width), as-welded, Bending	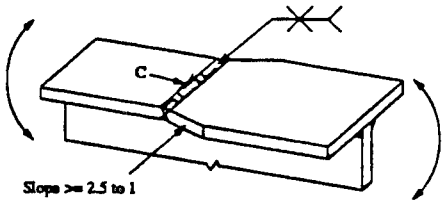 (As-welded)
	28	Plain plate with drilled hole, Axial	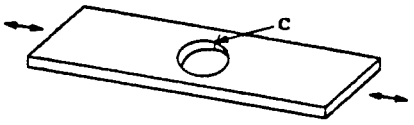 (Drilled hole)
C	12(G)	Flange splice (unequal thickness), weld ground, Bending	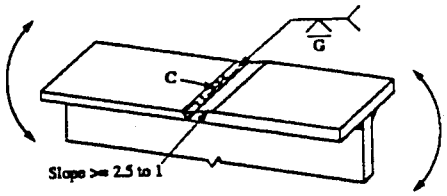 (Weld faces ground)

Key to symbols is presented on Page B-16

Table B-2

Welded Detail Classification (con't.)

CATEGORY	DETAIL NUMBER	DESCRIPTION, LOADING	PICTOGRAPH
C	4	Welded I-beam continuous weld, Bending	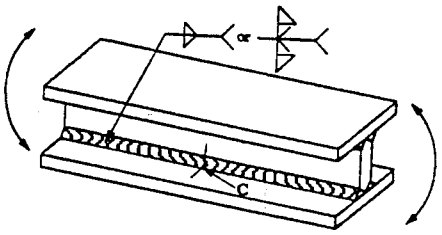
	6	Welded I-beam with longitudinal stiffeners welded to web, Bending	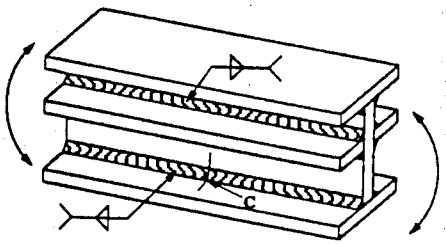
	9	Single shear riveted lap joint, Axial	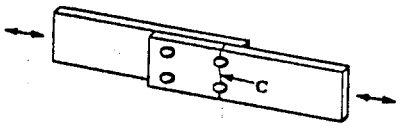 (Riveted)
	16(G)	Partial penetration butt weld, weld ground, Axial	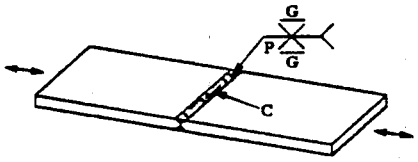 (Partial penetration - weld ground)

Key to symbols is presented on Page B-16

Table B-2

Welded Detail Classification (con't.)

CATEGORY	DETAIL NUMBER	DESCRIPTION, LOADING	PICTOGRAPH
C	25	Lateral attachments to plate, Axial	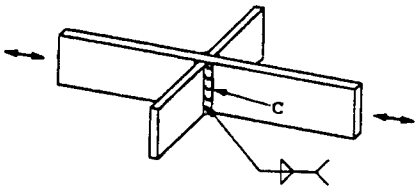
	7(B)	I-beam with welded stiffeners, Bending stress in web	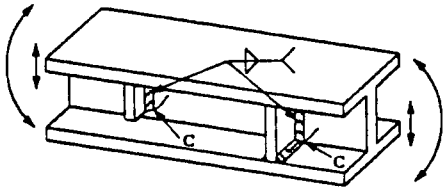
D	30A	Lateral attachments to plate, Bending	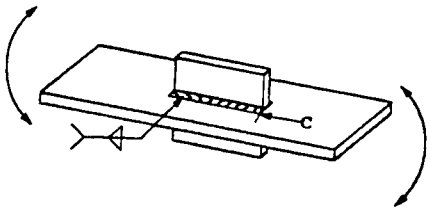
	26	Doubler plate welded to plate, Axial	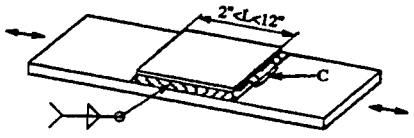

Key to symbols is presented on Page B-16

Table B-2

Welded Detail Classification (con't.)

CATEGORY	DETAIL NUMBER	DESCRIPTION, LOADING	PICTOGRAPH
D	14	Cruciform joint, Axial	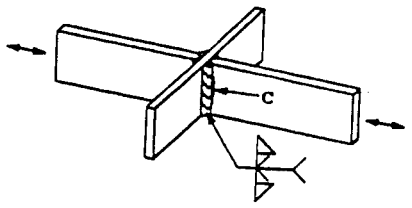
	11	Transverse butt welded I-beam, as-welded, Bending	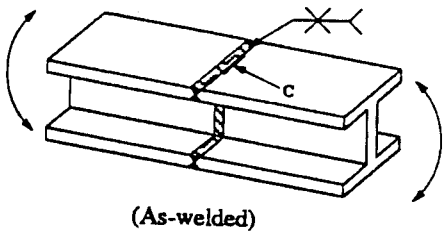 (As-welded)
	21	Cruciform joint, 1/4" weld, In-plane bending stress at weld toe, C	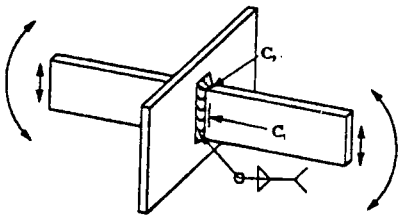
	7(P)	I-beam with welded stiffeners, Principal stress in web	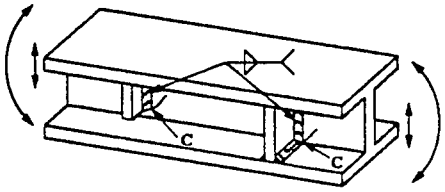

Key to symbols is presented on Page B-16

Table B-2

Welded Detail Classification (con't.)

CATEGORY	DETAIL NUMBER	DESCRIPTION, LOADING	PICTOGRAPH
D	36	Welded beam with intermittent welds and cope hole in the web, Bending	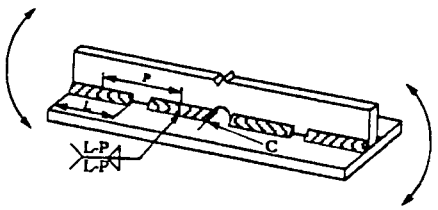
	25B	Lateral attachment to plate with stiffener, Axial	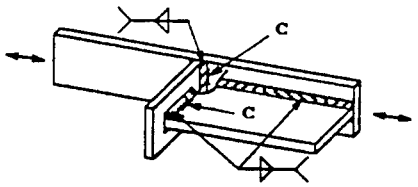
	12	Flange Splice (unequal thickness), as-welded, Bending	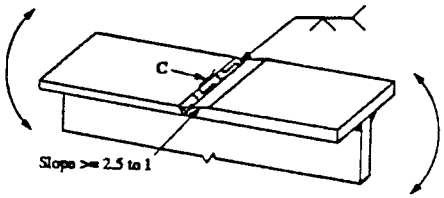 (As-welded)
	16	Partial penetration butt weld, as-welded, Axial	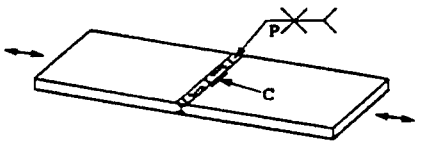 (Partial penetration - as-welded)

Key to symbols is presented on Page B-16

Table B-2

Welded Detail Classification (con't.)

CATEGORY	DETAIL NUMBER	DESCRIPTION, LOADING	PICTOGRAPH
D	22	Attachment of stud to flange, Bending	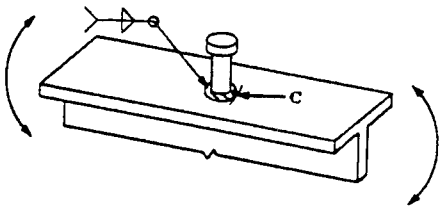
E	21(3/8")	Cruciform joint, 3/8" weld, Bending stress on throat weld	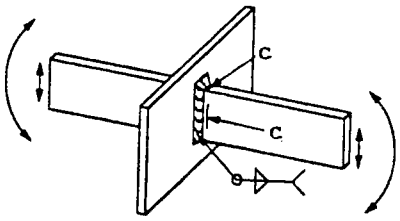
	20	Cruciform joint, Axial, Stress on plate at weld toe C	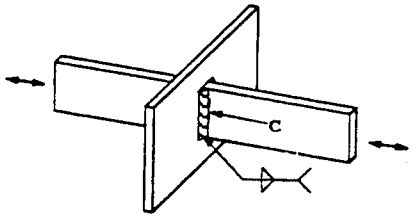
	23	Attachment of channel to flange, Bending	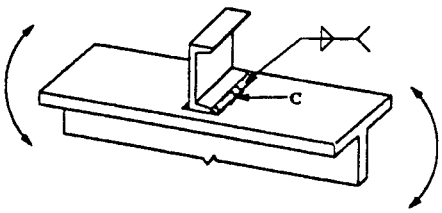

Key to symbols is presented on Page B-16

Table B-2

Welded Detail Classification (con't.)

CATEGORY	DETAIL NUMBER	DESCRIPTION, LOADING	PICTOGRAPH
	24	Attachment of bar to flange (L<=2"), Bending	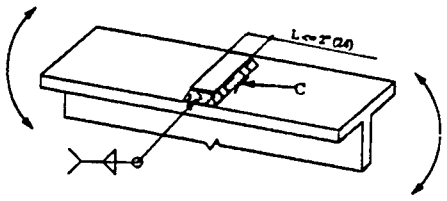
E	19	Flat bars welded to plate, lateral welds only, Axial	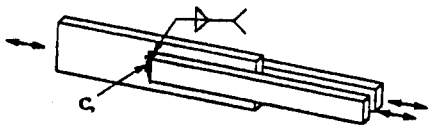
	30	Lateral attachments to plate, Axial	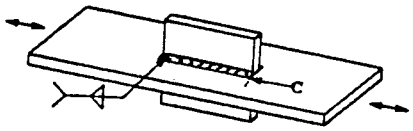
F	38	Beam connection with horizontal flanges, Bending	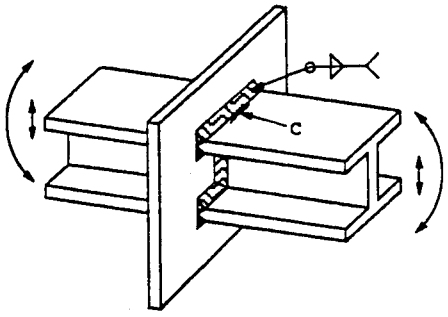

Key to symbols is presented on Page B-16

Table B-2

Welded Detail Classification (con't.)

CATEGORY	DETAIL NUMBER	DESCRIPTION, LOADING	PICTOGRAPH
F	17A	Channel welded to plate, longitudinal weld only, Axial	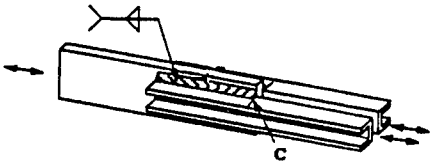
	31A	Attachments of plate to edge of flange, Bending	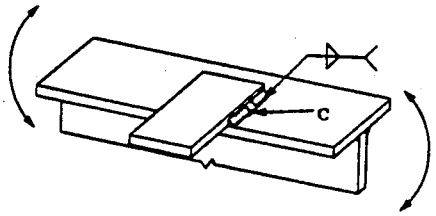
	17	Angles welded on plate, longitudinal welds only, Axial Stress in angle end of weld, C	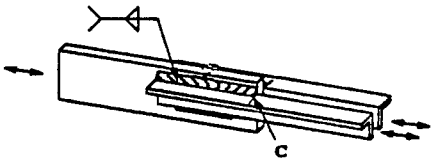
	18	Flat bars welded to plate, longitudinal weld only, Axial Stress in plate, C	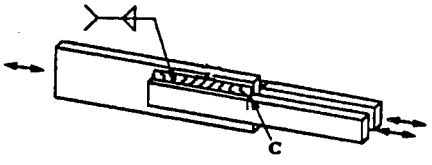

Key to symbols is presented on Page B-16

Table B-2

Welded Detail Classification (con't.)

CATEGORY	DETAIL NUMBER	DESCRIPTION, LOADING	PICTOGRAPH
F	32A	Groove welded attachment of plate to edge of flange, Bending stress in flange at end of attachment, C	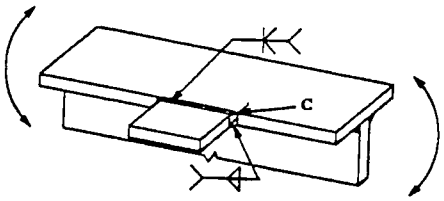
G	27	Slot or plug welded double lap joint, Axial	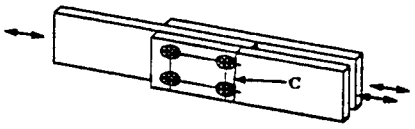 (Slot or Plug Welds)
	33	Flat bars welded to plate, lateral and longitudinal welds, Axial	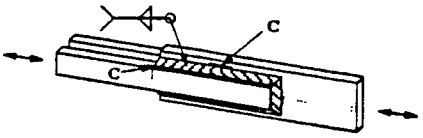
	46	Triangular gusset attachments to plate, Axial	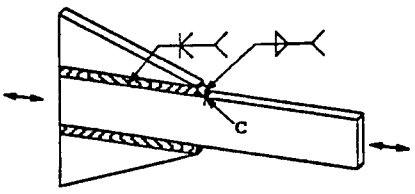

Key to symbols is presented on Page B-16

Table B-2

Welded Detail Classification (con't.)

CATEGORY	DETAIL NUMBER	DESCRIPTION, LOADING	PICTOGRAPH
G	40	Interconnecting beams, Bending in perpendicular directions	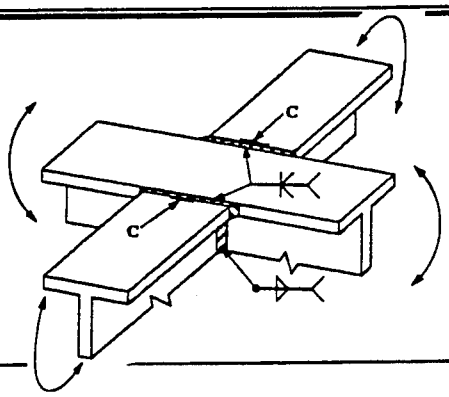
	32B	Butt welded flange (unequal width), Bending	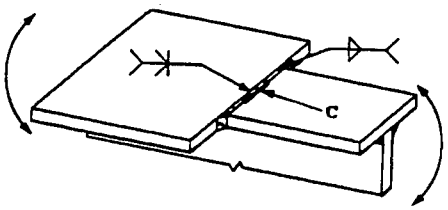
S	21(S)	Cruciform joint, In-plane bending, Shear stress on the weld, C_s	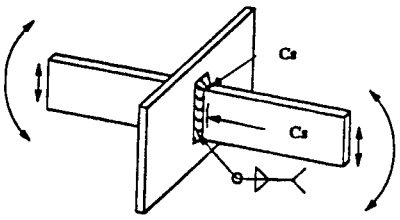
	18(S)	Flat bars welded to plate, longitudinal weld only, Axial, Shear stress on weld, C_s	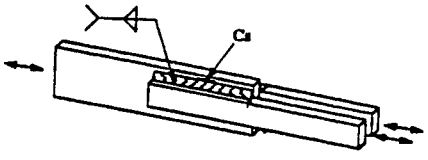

Key to symbols is presented on Page B-16

Table B-2

Welded Detail Classification (con't.)

CATEGORY	DETAIL NUMBER	DESCRIPTION, LOADING	PICTOGRAPH
S	33(S)	Flat bars welded to plate, lateral and longitudinal welds, Axial, Shear stress on weld, C_s	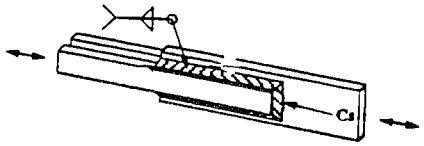
	17(S)	Angle welded to plate, longitudinal weld only, Axial, Shear stress on weld, C_s	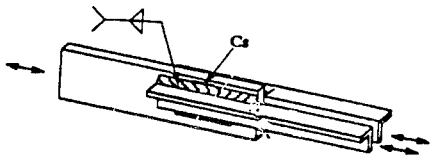
	17A(S)	Channel welded to plate, longitudinal weld only, Axial, Shear stress on weld, C_s	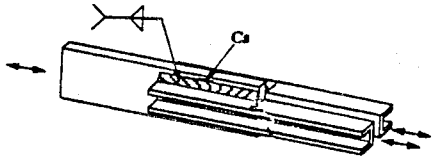
	20(S)	Cruciform joint, Axial, Shear stress on weld, C_s	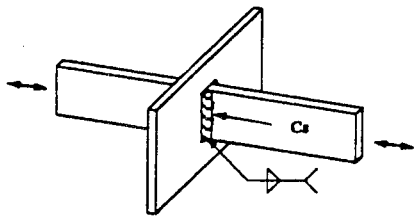

Key to symbols is presented on Page B-16

Table B-2

Welded Detail Classification (con't.)

CATEGORY	DETAIL NUMBER	DESCRIPTION, LOADING	PICTOGRAPH
S	19(S)	Flat bars welded to plate, lateral welds only, Axial, Shear stress on weld, C_s	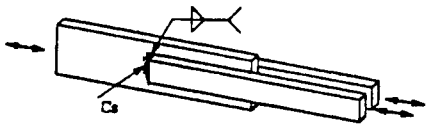
	38(S)	Beam connection with horizontal flanges, Shear stress on weld, C_s	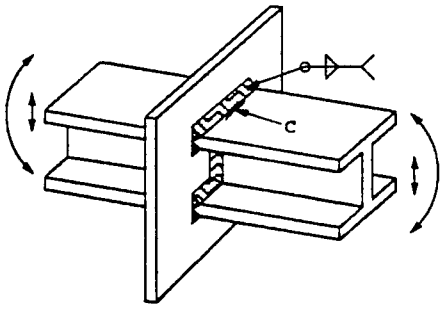

Key to Symbols

(F) - Flame cut edges
(G) - Weld ground
(B) - Bending stresses
(P) - Principal stresses
(S) - Shear stresses
A,B,C, .. Additional description within the same detail number
C→ - Crack initiation site due to tensile stresses
C_s→ - Crack initiation site due to shear stresses
L - Length of intermittent weld
P - Pitch between to intermittent welds
R - Radius
t - Thickness of plate

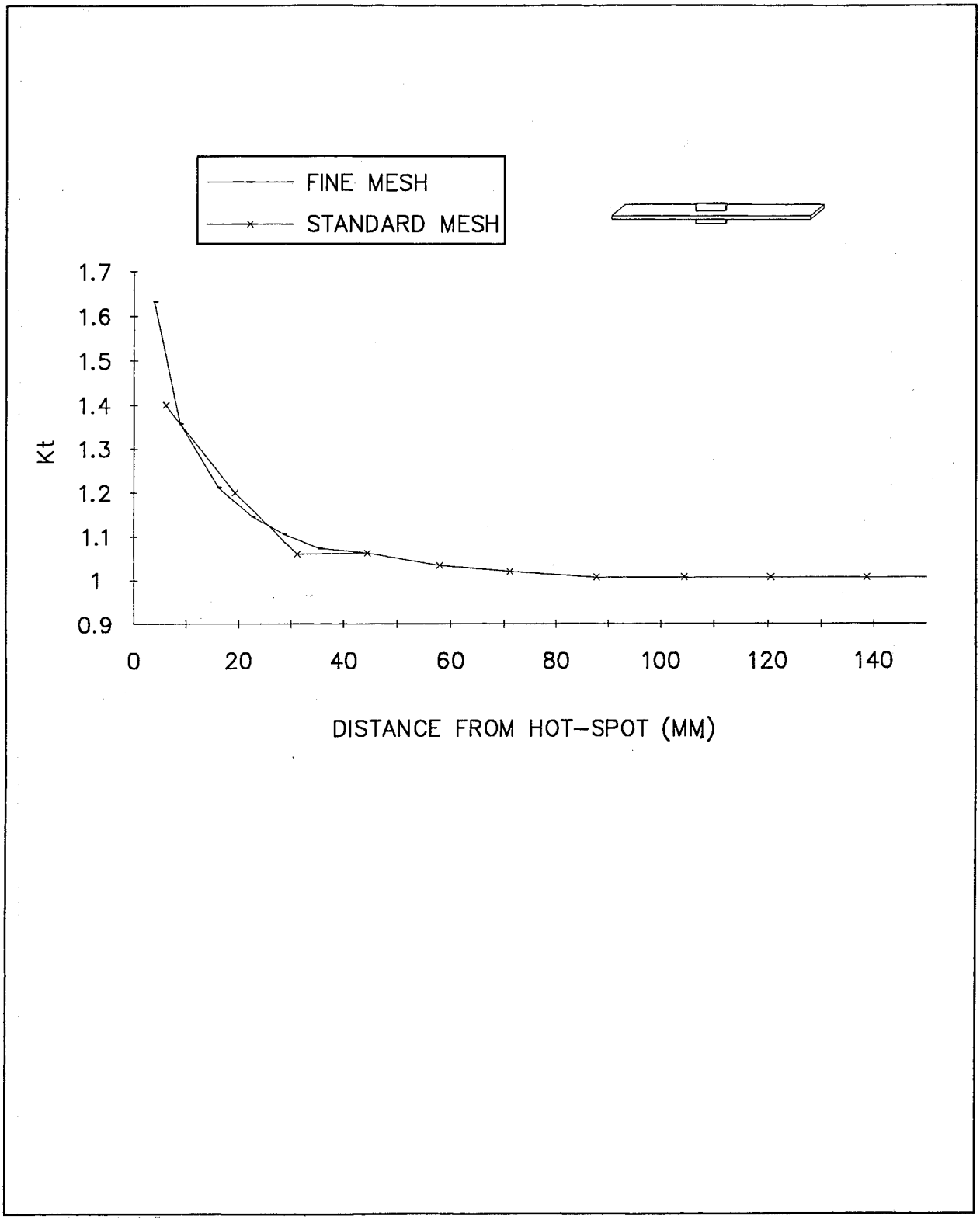

Figure B-1 FEA of attachment detail I

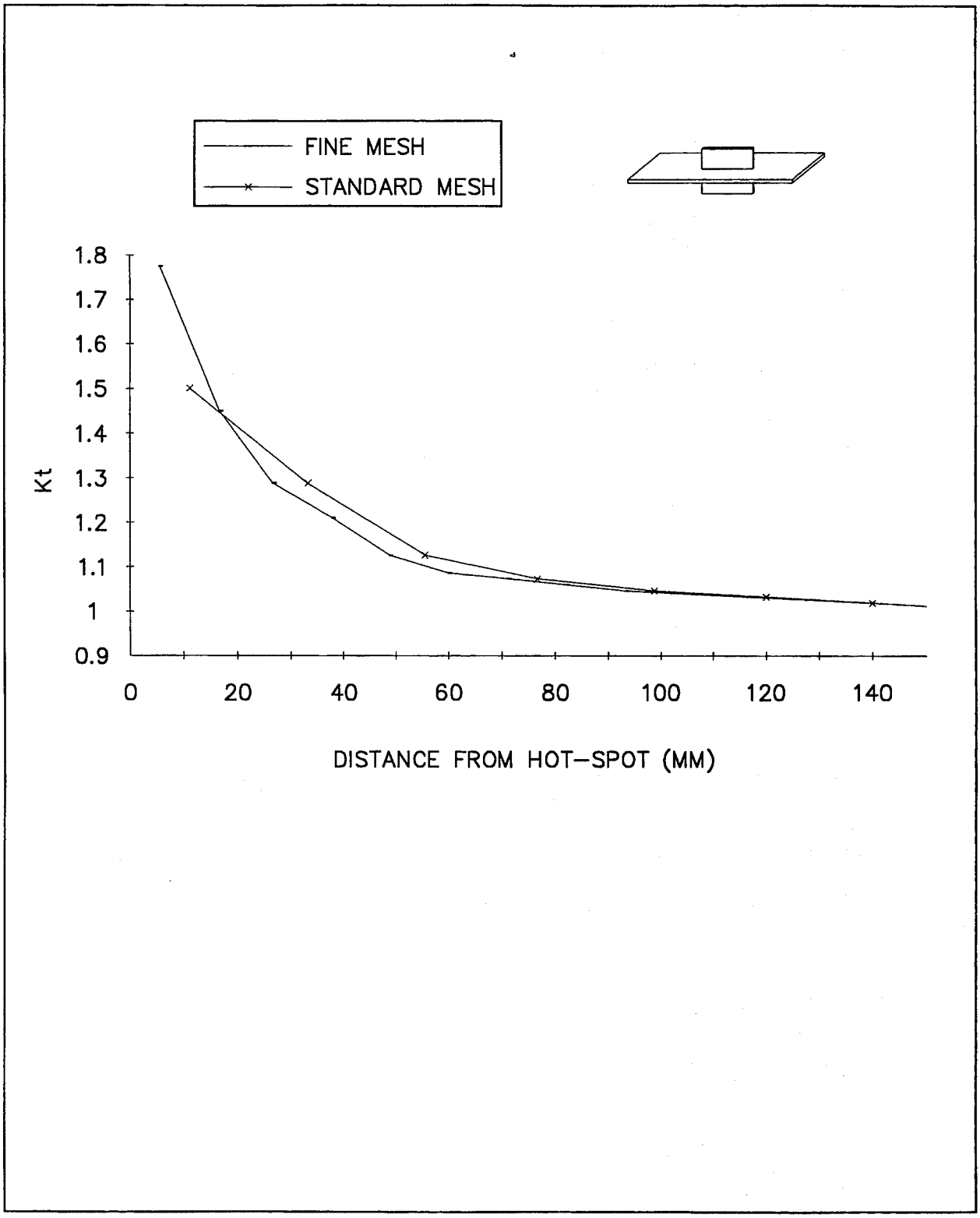

Figure B-2 FEA of attachment detail II

B-2 REFERENCES

B-1 Munse, W.H., T. W. Wilbur, M.L. Telalian, K. Nicol, and K. Wilson, 1983, "Fatigue Characterization of Fabricated Ship Details for Design," Ship Structure Committee Report SSC-318, Washington, DC.

B-2 Stambaugh, K., Lesson, D., Lawrence, R., and Banas, "Reduction of S-N Curves for Ship Structures," SSC-369, for Ship Structures Committee, 1992.

B-3 Schulte-Strathus, R. and R.G. Bea, 1993, "Fatigue Classification of Critical Structural Details in Tankers: Development of Calibrated S-N Curves and System for the Selection of S-N Curves," Report No. FACTS-1-1, University of California, Berkeley.

Appendix C

Analytical Fatigue Life Prediction

(THIS PAGE INTENTIONALLY LEFT BLANK)

C.0 INFLUENCE OF WELD PARAMETERS ON FATIGUE LIFE

The use of K_f for the weld termination and other weld configuration permits relatively easy comparisons between details and associated stress concentration factors. Thus, the K_f approach for basic weld configurations includes the effects of such important factors as weld geometry, residual stress and mean stress because it is based on test data of actual welds. This assumes good welding practice which is somewhat subjective and produces much of the unaccounted for scatter in the test data. The following analytical expressions are useful to determine the impact of controlling these parameters.

C.1 ANALYTICALLY ESTIMATING ΔS WELD

From Basquin's Law, Yung, and Lawrence (C-1) derived an expression to calculate the mean fatigue strength of weldments at long lives:

$$\Delta S_{weld} = \frac{2\,(\sigma'_f - \sigma_r)\,(2N_f)^b}{K^{eff}_{fmax}\left[1 + \frac{1+R}{1-R}(2N_f)^b\right]} \qquad \text{(C-1)}$$

where:

σ'_f = Fatigue strength coefficient
σ_r = Local (notch root) residual stress
b = Fatigue strength exponent
R = Load ratio

$$N_f = \text{Cycles to failure} \approx -\frac{1}{6}\log\left[2+\frac{689.5}{Su}\right](MPa\,,\,mm\,)$$

$$K^{eff}_{fmax} = \text{Effective fatigue notch factor} = (\,1 - X\,)\,K^{A}_{fmax} + X\;K^{B}_{fmax}$$

$$X = \frac{S_a^B}{S_a^T}$$

$$S_a^T = S_a^A + S_a^B$$

In the following section, we have assumed that the total fatigue life (N_T) is equal to the initiation fatigue life (N_I). It is expected therefore that this estimate of fatigue strength will be accurate only at long lives ($\approx 10^7$ cycles) for which the propagation portion of the fatigue life ceases to be important.

C.1.1 Ripple

The idea is that the fatigue notch provided by the ripple can be treated as an infinite array of semicircular notches. The weld metal properties determine the fatigue resistance and the residual stresses in the as-welded state.
Thus:

$$K_t = 1.6$$

$$K_{fmax} = 1 + \left[\frac{K_t - 1}{2} \right] = 1.3$$

$$\sigma_r b = f(S_{uwm})$$

$$\sigma_r = S_{yWM}$$

$$\Delta S_{weld} = \frac{2S_{uWM} - 2S_{yWM} + 689.5}{1.30} \left[\frac{2N_I^b}{1 + \left[\frac{1 + R}{1 - R} \right] 2N_I^b} \right] \quad \text{(C-2)}$$

C.1.2 Groove Welded Butt Joint

The idea is that the residual stresses at the toe of the groove weld are controlled by the yield strength of the base metal and that crack initiation occurs in the HAZ; therefore the HAZ properties control the fatigue resistance. Thus, for the as-welded state:

σ_f' , b = f(SuHAZ)

σ_r = S_{yBM}

K_{fmax}^A = $1 + 0.0015(.27) (\tan \theta)^{0.25} SuHAZ \sqrt{t}$ (MPa, mm)

K_{fmax}^B = $1 + 0.0015(0.165) (\tan \theta)^{0.167} SuHAZ \sqrt{t}$ (MPa, mm)

$$\Delta S_{weld} = \frac{2S_{uHAZ} - 2S_{yBM} + 689.5}{K_{fmax}^{eff}} \left[\frac{2NI^b}{1 + \left[\frac{1 + R}{1 - R} \right] 2N_I^b} \right] \quad \text{(C-3)}$$

C.1.3 Non-Load Carrying Fillet Weld

The idea is that the residual stresses at the toe of the fillet weld are controlled by the yield strength of the base metal and that crack initiation occurs in the HAZ and therefore the HAZ properties control the fatigue resistance, that is all is as in B.2.2 above except for differences in the models for K_f which include the effect of the LOP (2c) oriented parallel to the applied stress:

σ_f' , b = f(SuHAZ)

σ_r = S_{yBM}

Case 1 - A model for K_{fmax} which considers the effect of LOP

$$K^{A}_{fmax} = 1 + 0.0015(.35)(\tan\theta)^{0.25}\left[1 + 1.1\left[\frac{c}{l}\right]^{1.65}\right] S_{uHAZ}\sqrt{t} \qquad (MP_a, mm)$$

$$K^{B}_{fmax} = 1 + 0.0015(.21)(\tan\theta)^{0.167}\ S_{uHAZ}\ \sqrt{t} \qquad (MP_a,\ mm)$$

Case 2 - A model for K_{fmax} which considers the effect leg length

$$K^{A}_{fmax} = 1 + 0.0015(.04)\sqrt{2 - \frac{1}{t}}\ S_{uHAZ}\ \sqrt{t} \qquad (MP_a,\ mm)$$

$$\Delta S_{weld} = \frac{2S_{uHAZ} - 2S_{yBM} + 689.5}{k^{eff}_{fmax}}\left[\frac{2N_l^b}{1 + \left[\frac{1 + R}{1 - R}\right] 2N_l^b}\right] \qquad (C\text{-}4)$$

C.1.4 Load Carrying Fillet Weld

The idea is that the residual stresses at the toe of the fillet weld are controlled by the yield strength of the base metal and that crack initiation occurs in the HAZ and; therefore, the HAZ properties control the fatigue resistance, that is, all is as in C.1.3 above except for differences in the models for Kf which include the effect of the LOP (c) now oriented perpendicular to the applied stress:

$$K^{A}_{fmax} = 1 + 0.0015(.35)(\tan\theta)^{0.25}\left[1 + 1.1\left[\frac{c}{l}\right]^{1.65}\right] S_{uHAZ}\ \sqrt{t} \qquad (MP_a,\ mm)$$

$$K^{B}_{fmax} = 1 + 0.0015(.21)(\tan\theta)^{0.167}\ S_{uHAZ}\ \sqrt{t} \qquad (MP_a,\ mm)$$

Load Carrying Fillet Weld: Root Failure

$$\sigma'_{f'},\ b = f(S_{uWM})$$

$$\sigma_r = O$$

$$K\text{-}fmax^{A} = 1 + 0.0015(1.15)(\tan\theta)^{-0.2}\left[\frac{c}{l}\right]^{0.5} S_{uWM}\ \sqrt{t} \qquad (MP_a,\ mm)$$

$$K\text{-}fmax^{B} = 1 + \frac{1}{2}\left[\frac{1 + 0.0098\left[\frac{C}{l}\right]^{0.5} S_{uWM}\sqrt{t}}{\frac{w^3}{2Ct^2} - \left[2\frac{c}{t}\right]^2} - 1\right] \qquad (MPa,\ mm)$$

$$\Delta S_{weld} = \frac{2S_{uWM} + 689.5}{K^{eff}_{fmax}}\left[\frac{2N_f^b}{1 + \left[\frac{1 + R}{1 - R}\right] 2N_f^b}\right] \qquad (C\text{-}5)$$

At long lives, the likelihood of LOP failure in a weldment is increased. Increasing plate thickness (t) increases the tendency for LOP failure.

C.1.5 A Fillet-Weld Termination

For fillet weld terminations, the residual stresses at the toe at the end of the fillet weld are controlled by the yield strength of the weld metal and that crack initiation occurs in the HAZ and therefore the HAZ properties control the fatigue resistance. The models for K_f include the three dimensional effects of flow of the stress in the main plate into the weld and the attachment. This quantity is captured as a stress concentration factor of SCF which is the ratio of the stress at the location of the hypothetical strain gage a distance (t) away from the toe of the weld to the stresses

at the station of the weld toe in the absence of the weld. These results must be determined from the results of the original FEA.

σ'_f, b = f(SuHAZ)

σ_r = S_{yWM}

SCF = 1.5

$$K^A_{fmax} = SCF^*[1 + 0.0015(.35)(\tan\theta)^{0.25}\left[1 + 1.1\left[\frac{c}{l}\right]^{1.65}\right]S_{uHAZ}\sqrt{t}] \quad (MPa, mm)$$

$$K^B_{fmax} = SCF^*[1 + 0.0015(.21)(\tan\theta)^{0.167}\ S_{uHAZ}\ \sqrt{t}] \quad (MPa, mm)$$

$$\Delta S_{weld} = \frac{3.0S_{uBM} - 1.55S_{uWM} + 689.5}{K^{eff}_{fmax}}\left[\frac{2N_f^b}{1 + \left[\frac{1+R}{1-R}\right]2N_f^b}\right] \quad (C\text{-}6)$$

C.2 EFFECTS OF BENDING

Bending of attachments on plate is important because of minimal section depth. Bending of the plate causes stress gradient effects. Only one of the weld details in Table B-1 was subjected to pure bending. All others, while subjected to a nominal bending load, are of such a depth that the stress state at the fatigue initiation site is for all purposes an axial load, thus the loading is considered pseudo-axial. However, from this one example comparing SSC-318 (C-2) detail 30 with 30A shows that there can be a large difference to the fatigue response of weldment to pure axial and pure bending loading (ΔS_{design} = 99.6 MPa, axial, ΔS_{design} = 144.3 MPa, bending). This effect is captured by the analytical expressions for ΔS^1_{weld} and as well as by the experimental database; however, there are very few pure bending entries in Table B-1 probably because the data has been restricted to R = 0 loading conditions.

The analytical expressions of ΔS_{weld} can deal with various combinations of axial and bending loads directly or provide an expression for predicting the expected mean fatigue life at a given long life using the experimental results for pure axial and pure bending loading:

$$\Delta S_{weld}^{A+B} = \frac{\Delta S_{weld}^{A} * \Delta_{weld}^{B}}{\Delta S_{weld}^{B} (1 - x) + \Delta S_{weld}^{A} (x)} \qquad \text{(C-7)}$$

where:

ΔS_{weld}^{A} = Experimental fatigue strength under pure axial loading

ΔS_{weld}^{B} = Experimental fatigue strength under pure bending loading

The weld termination represents a large challenge because it cannot be dealt with adequately using a 2-D stress analysis. If the situation were axial loading, the ratio of the stress at the location of the hypothetical strain gage a distance (t) away from the toe of the weld to the nominal stresses at the station of the weld toe would be 1. However even in 2-D states of stress, local bending can cause stress gradients independent of the stress-concentrating effects of the weld toe. In situations such as the weld termination the relationship between the nominal stress at the location of the strain gage and that at the station of the weld toe is dependent upon many factors. To solve this problem the designer determines the stress at the location of the weld toe from the results of a finite element method and expressed it as an SCF. Incorporation of this SCF into the expression for K_f for the fillet weld and assuming the high level of tensile residual stresses possible because of the shrinkage of the weld metal, leading to the creation of an analytical model which predicted the behavior of the weld termination. It is believed that this process can also be used for other weld shapes having a geometry which cannot be analyzed as a simple "2-D" FEM problem.

Under pure axial loading and for normal weld toes ($0 < 45°$), fatigue is predicted always to occur at the root. Under pure bending loads, fatigue failure will always occur at the toe before the weld root. Note that most axially loaded welds have induced bending stresses at the weld toe due to the straightening of weld distortions under axial load. This effect induces secondary bending stresses which can easily cause the weld toe to become the failure site even under nominally axial loading conditions.

In Figure C-1 the ratio of ΔS_{weld}(root)/ΔS_{weld}(toe) is plotted against the ratio of bending stress amplitude to total stress amplitude (x). As seen in Figure C-1, when the value

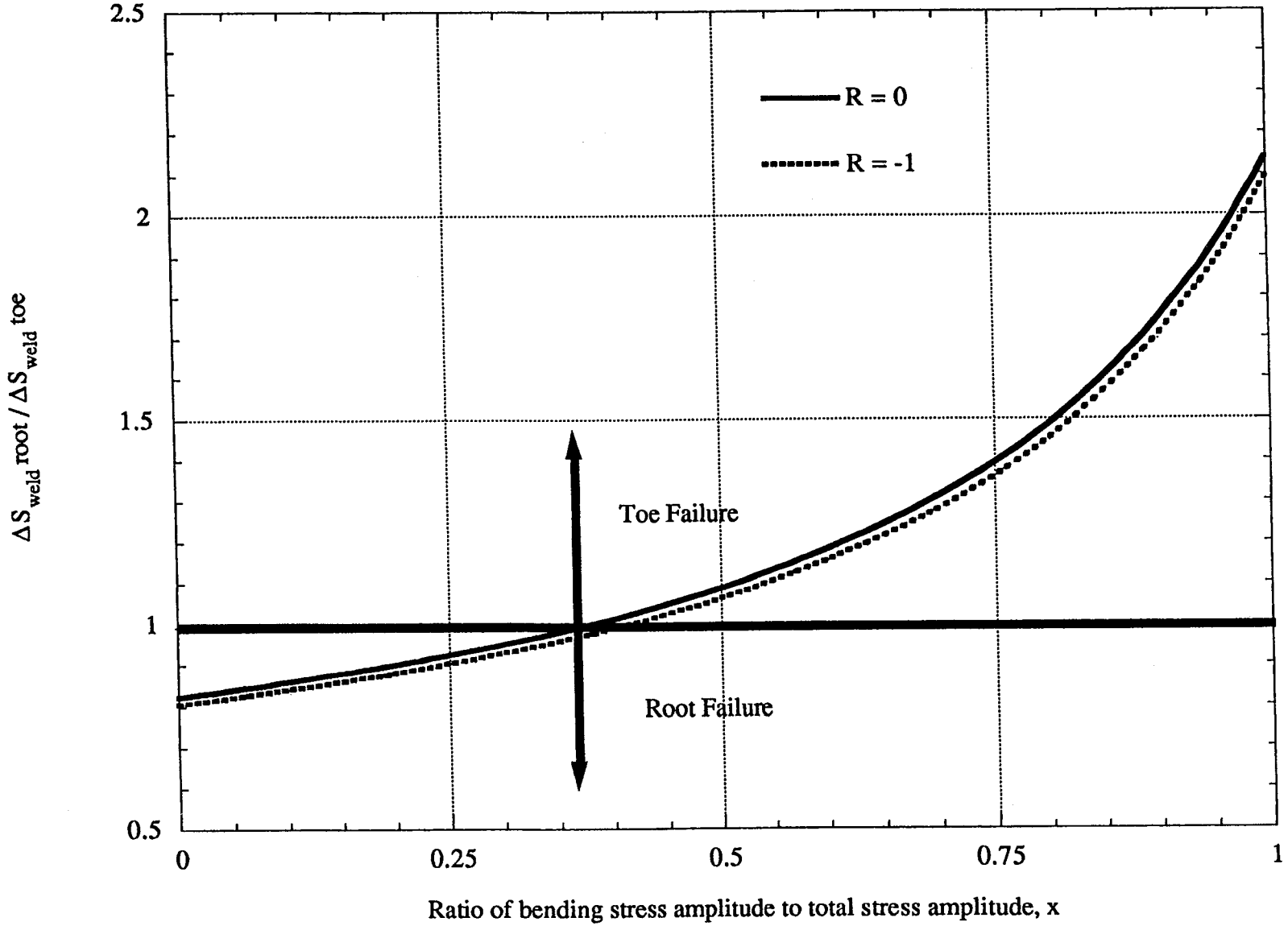

Figure C-1 The predicted effect of bending stresses on the failure location for the Primitive F' - Load Carrying Fillet Weld at 1E+07 cycles.

of (x) exceeds about 0.3 (that is, when the ratio of bending to total stresses is above 0.35, the failure location should shift to the weld toe. Unfortunately the most effective way of improving the fatigue life of the load-carrying fillet weld failing from its root is to increase the weld penetration, that is, to reduce the value of (c). This change has a large beneficial effect upon ΔS_{weld}(root), but also improves the performance at the weld toe so that shifting the failure location from the root to the toe requires large reductions in the value of (c). Note again that the above discussion assumes a zero value for the welding residual stresses at the weld root.

Calculations were made using the Initiation - Propagation Model to approximate the total fatigue life. The initiation life calculations was slightly altered to take into account the set-up cycle. The propagation life calculation was made using expressions for M_k (C-4).

C.3 CALCULATIONS MADE USING THE ANALYTICAL EXPRESSIONS

Calculations were performed for hot-rolled steel under a load ratio (R) = 0. From the work of McMahon and Lawrence (C-7), the relationships between the ultimate strength of the base metal and the ultimate strength of the heat affected zone and the yield strength of the base metal (Figures C-1 and C-2) for hot-rolled steel were found to be:

$$S_{yBM} = (5/9) * S_{uBM}$$
$$S_{uHAZ} = 1.5 * S_{uBM}$$

A reasonable (assumed) relationship between the ultimate strength of the weld metal and the yield strength of the weld metal was assumed to be:

$$S_{yWM} = (7/9) * S_{uWM}$$

In addition, the following values were assumed:

$$x = 0.0$$
$$\theta = 45^\circ$$
$$t = 19\text{mm}$$
$$S_{uBM} = 414\text{ MPa}$$
$$S_{uWM} = 483\text{ MPa}$$
$$S_{yBM} = (5/9) * S_{uBM} = 230\text{ MPa}$$
$$S_{yHAZ} = 1.5 * S_{uBM} = 621\text{ MPa}$$
$$S_{yWM} = (7/9) * S_{uWM} = 376\text{ MPa}$$

The results are plotted in Figures C-3 through C-8 together with the mean S/N data of the local fatigue details from SSC-318 (C-2). In Figure C-3, the analytical expression for the ripple primitive underestimates life but is very reasonable and a somewhat

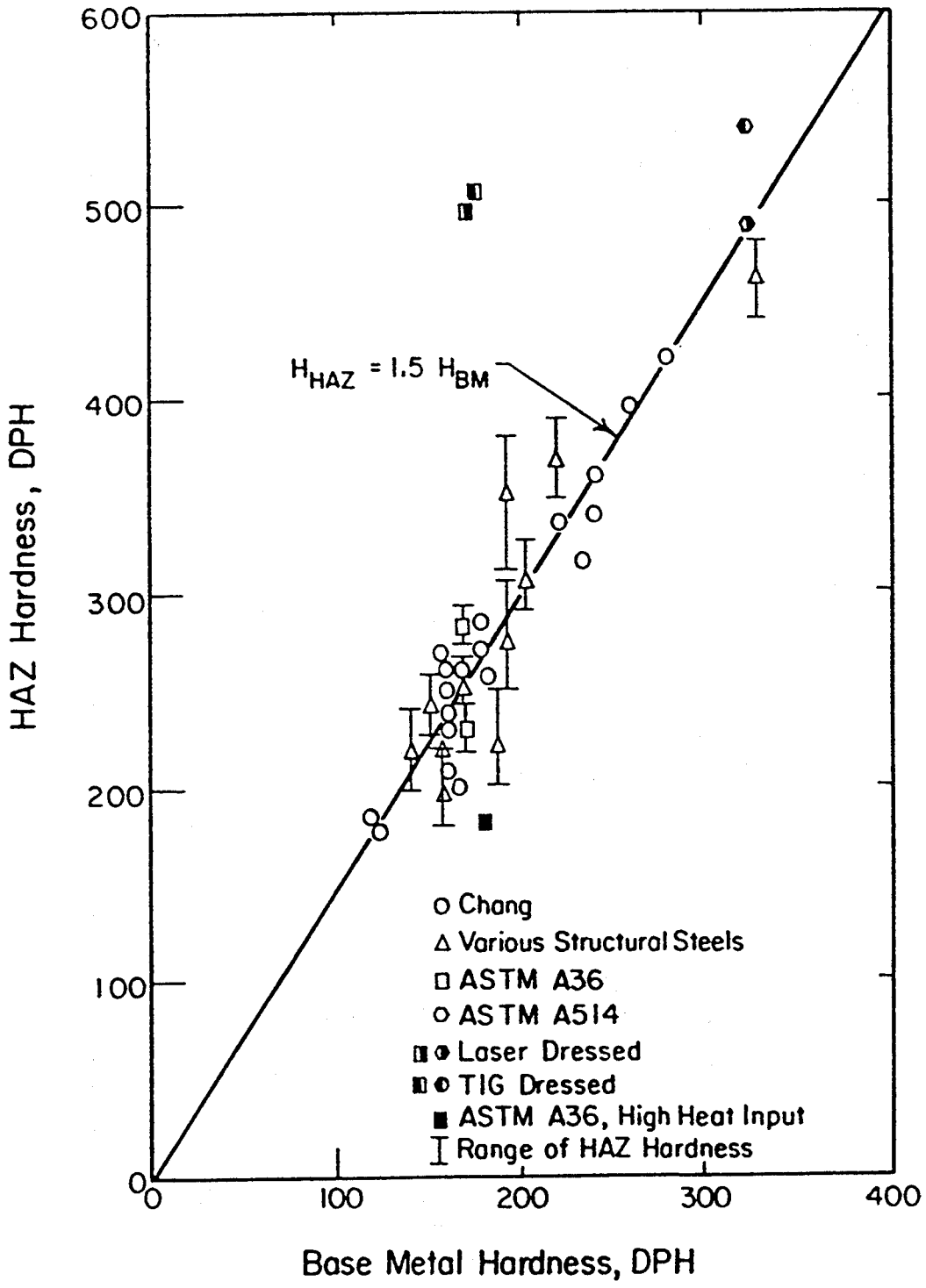

Figure C-2 Hardness of the heat affected zone as a function of base metal hardness.

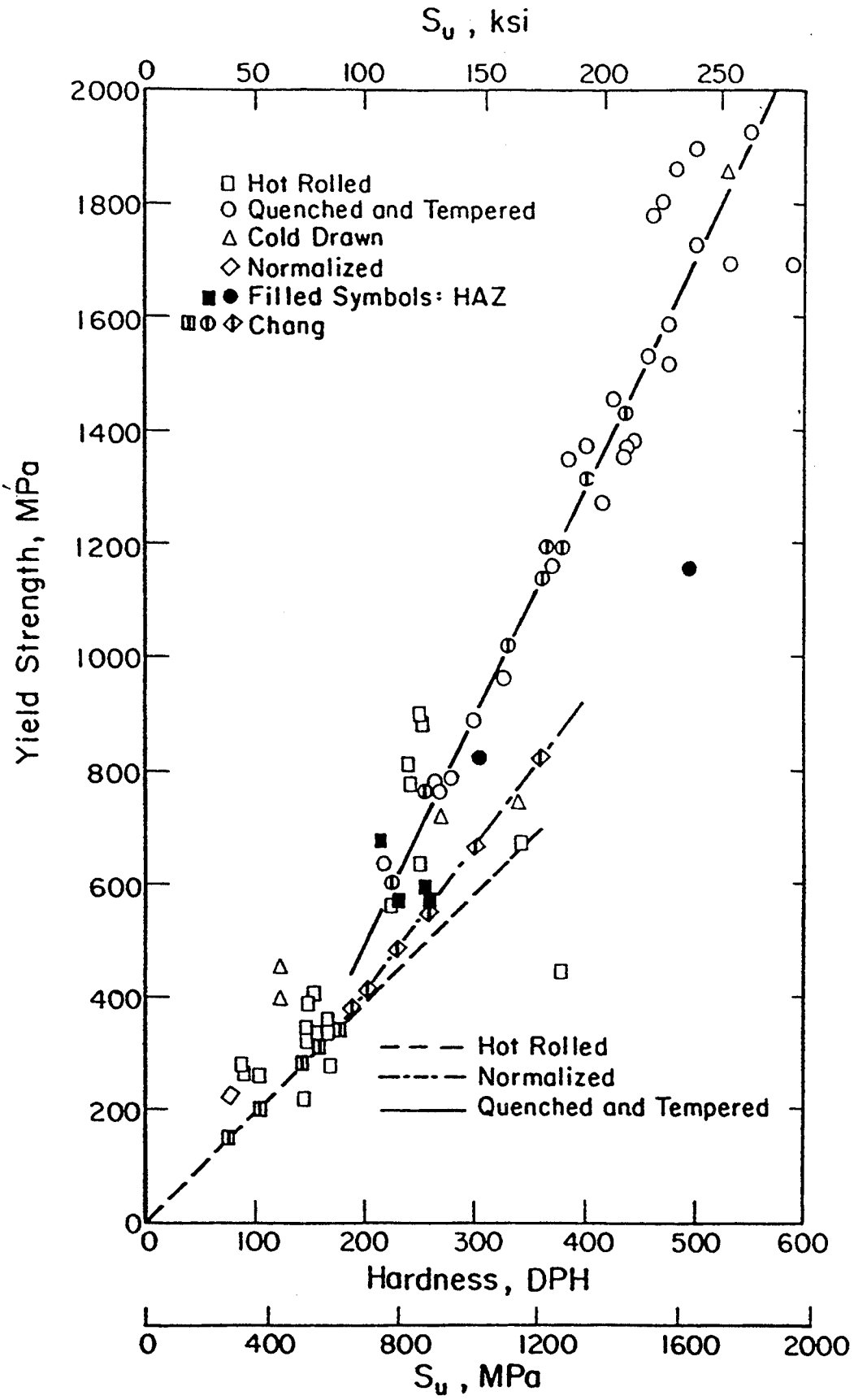

Figure C-3 Yield strength as a function of hardness

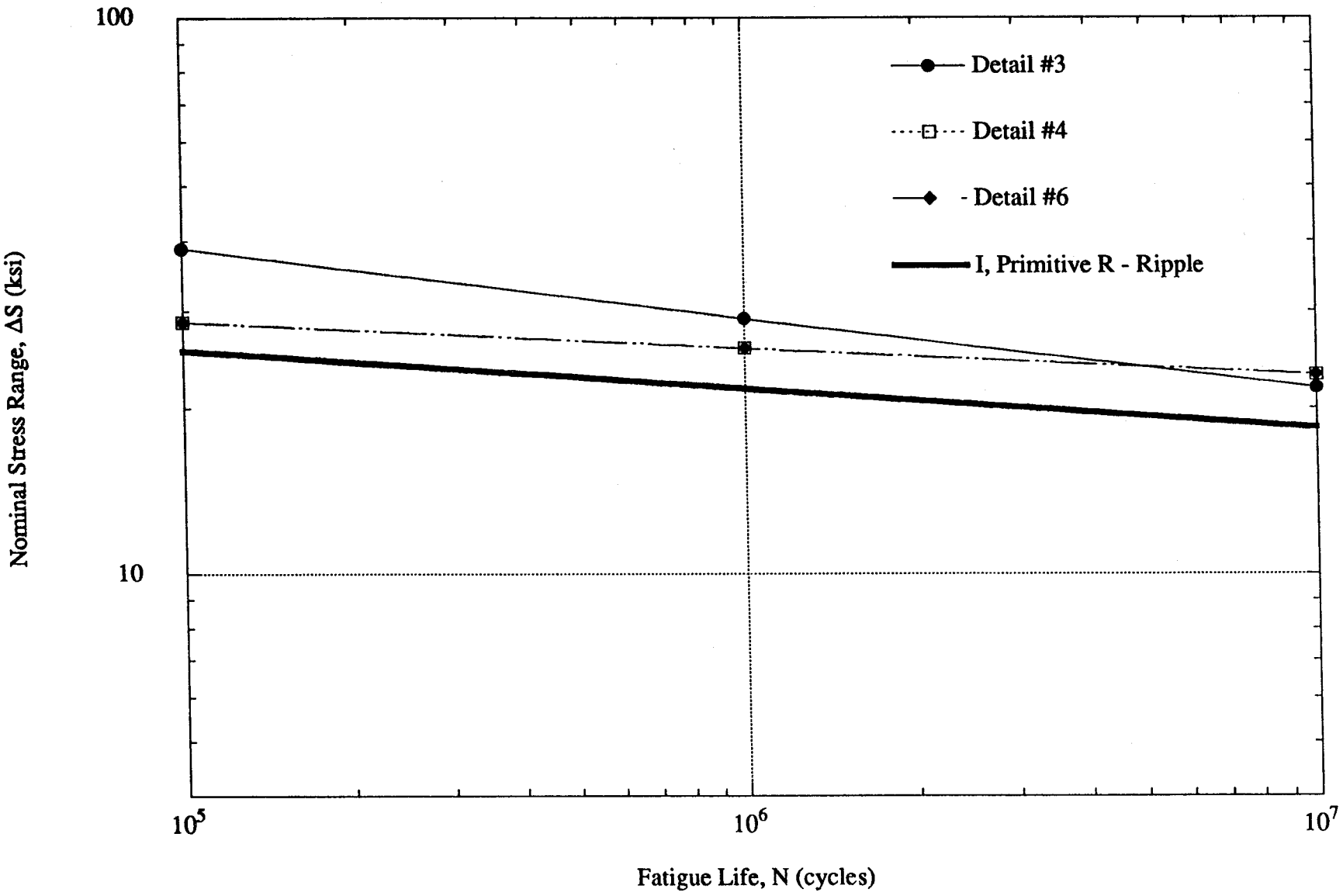

Figure C-4 Comparison of the S-N data for ship structure details and the analytical expression for the weld Primitive R-Ripple

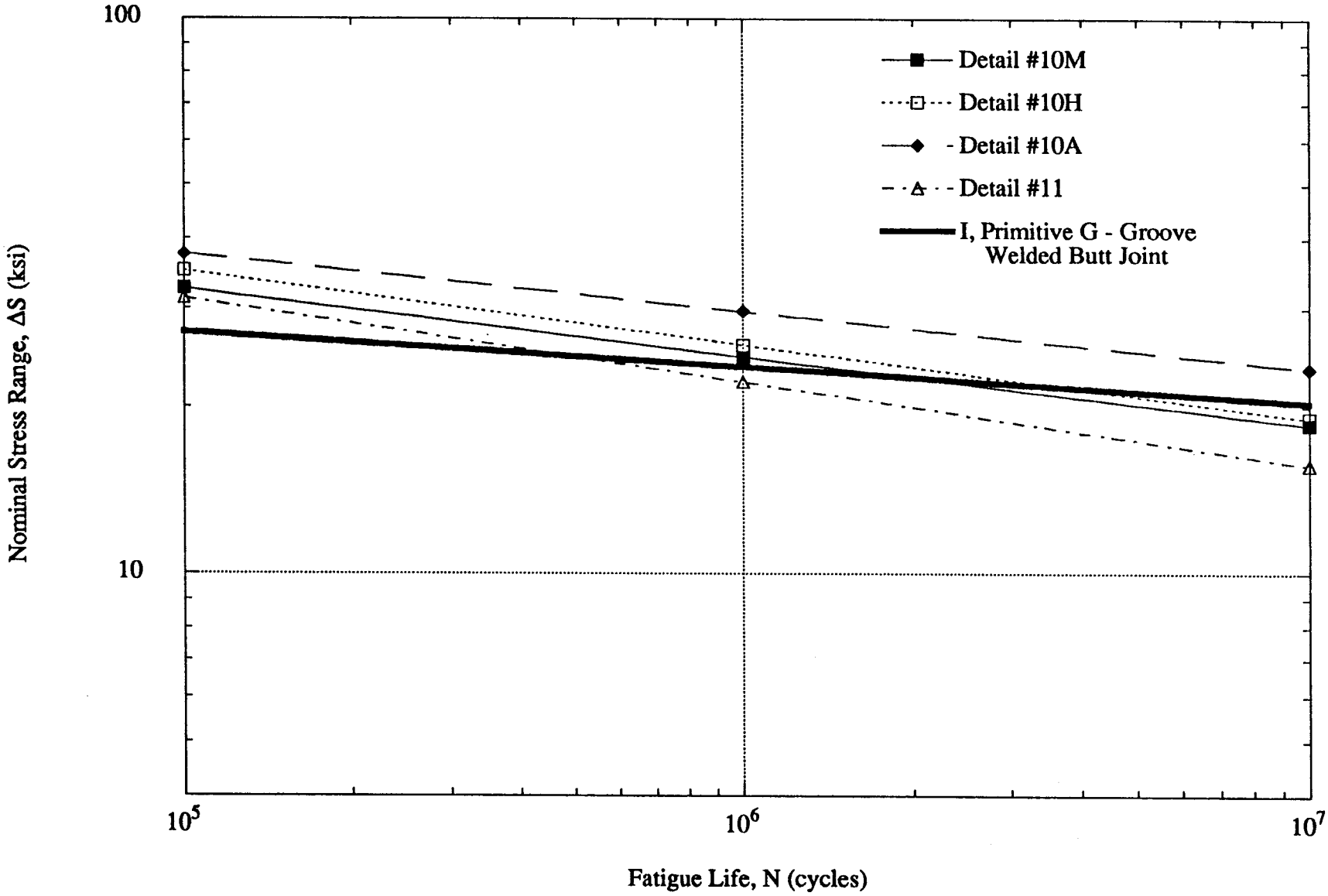

Figure C-5 Comparison of the S-N data for ship structure details and the analytical expression for the weld Primitive G - Groove Welded Butt Joint

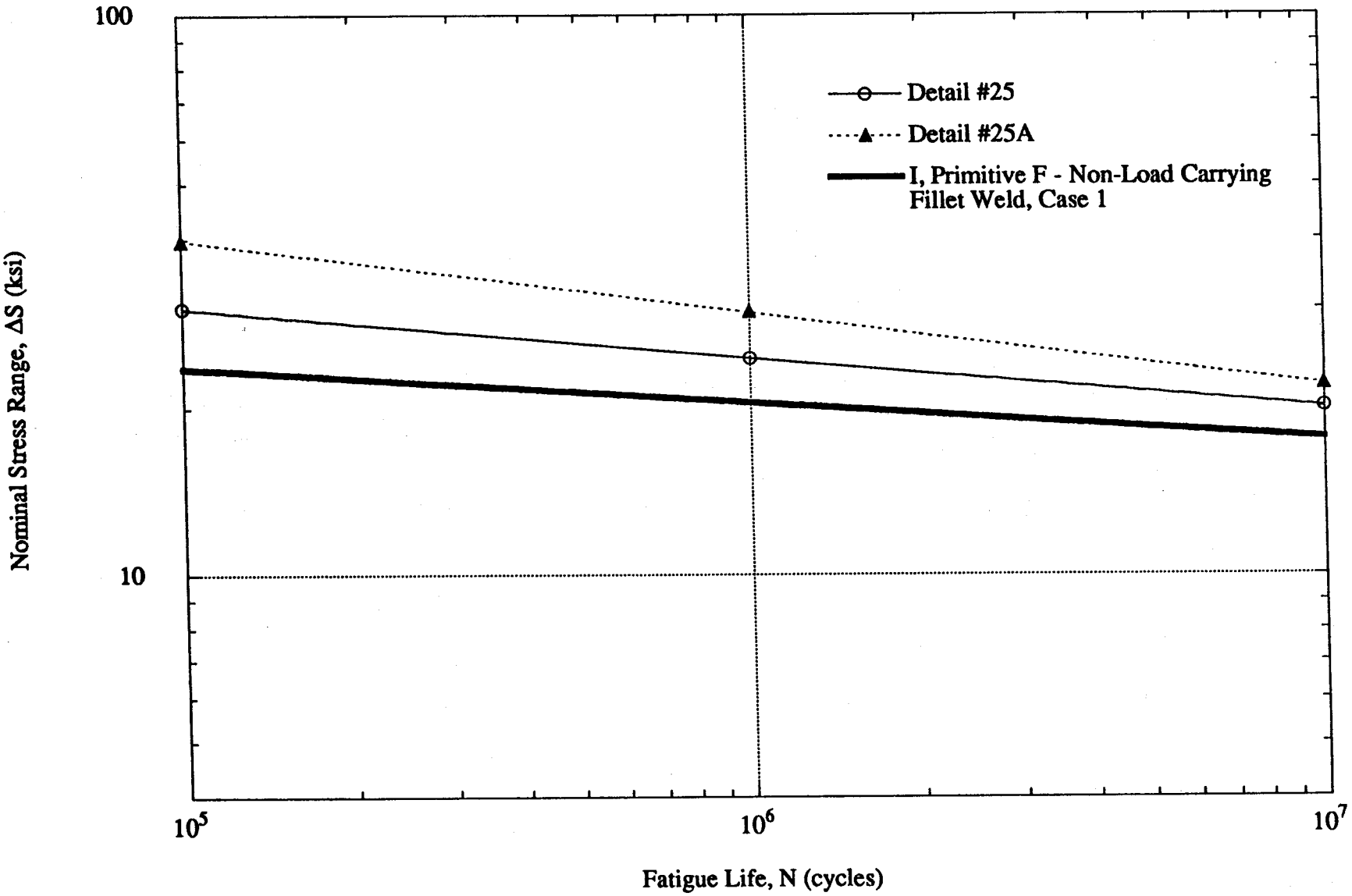

Figure C-6 Comparison of the S-N data for ship structure details and the analytical expression for the weld Primitive F - Non-Load Carrying Fillet Weld

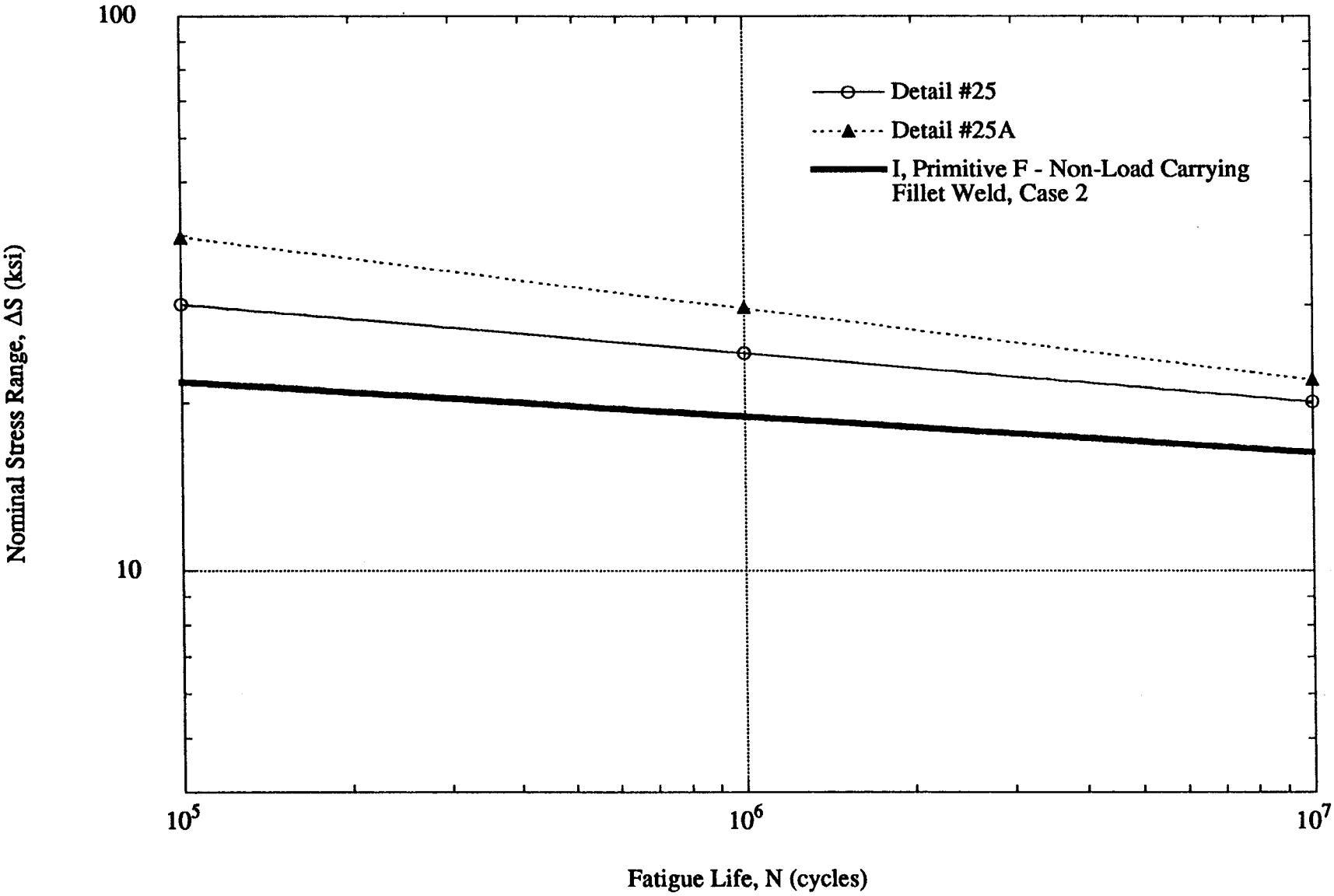

Figure C-7 Comparison of the S-N data for ship structure details and the analytical expression for the weld Primitive F - Non-Load Carrying Fillet Weld

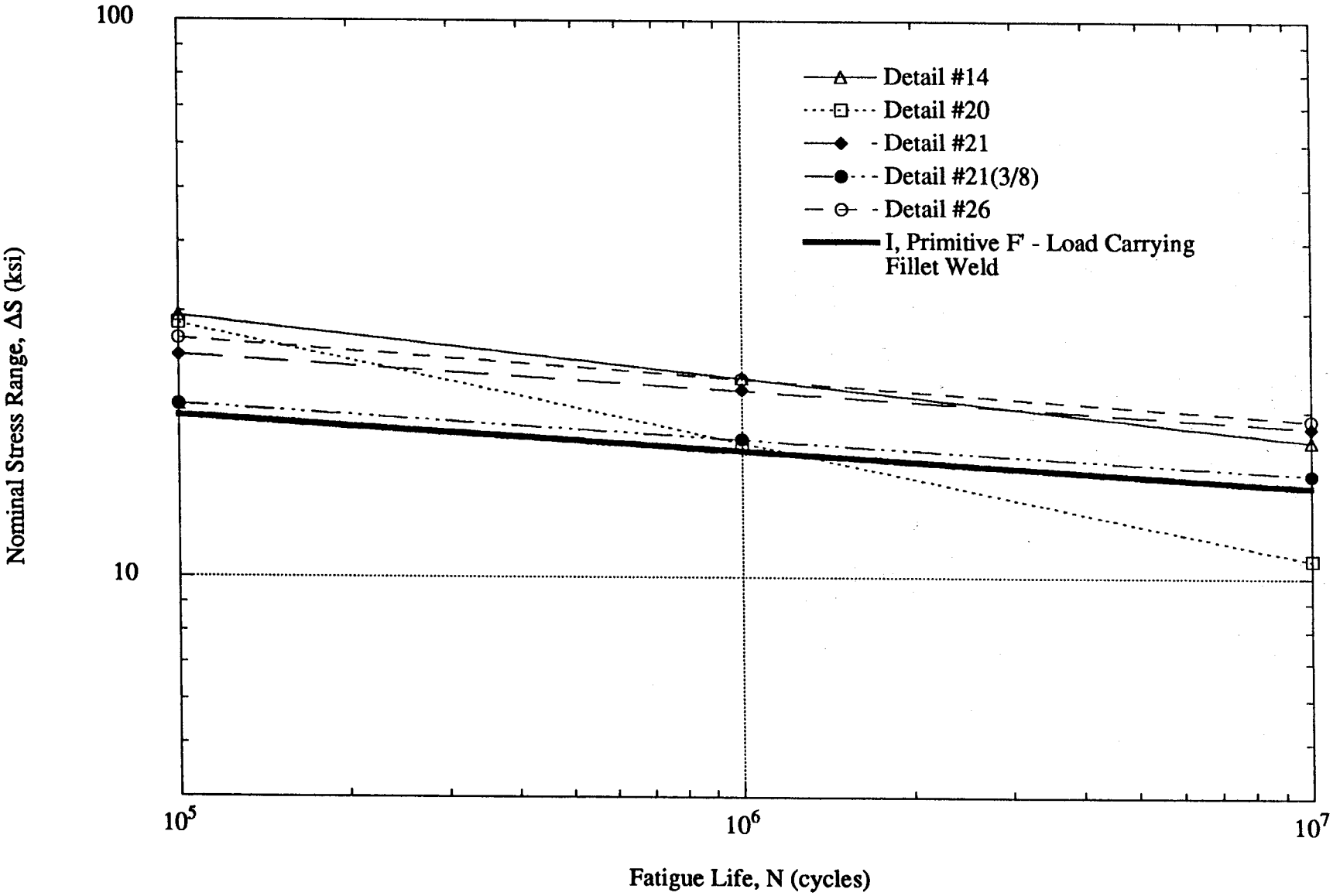

Figure C-8 Comparison of the S-N data for ship structure details and the analytical expression for the weld Primitive F' - Load Carrying Fillet Weld

conservative approximation. In Figure C-4, the analytical expression for the groove welded butt joint primitive is in very good agreement with the S-N data. It is especially good at very long lives when initiation dominates fatigue life and the absence of the propagation life does not make much of a difference. The analytical expressions for the non-load carrying fillet primitive are reasonable as shown in Figures C-5 through C-8. The analytical expressions for the termination primitive is also reasonable at long lives but is too conservative at shorter lives (N<1E+06).

The results are plotted in Figures C-9 through C-12 together with the mean S-N data of the local fatigue details from SSC-318. No calculations were made for the ripple (R) and groove weld (G) primitives because values of Mk were not available. The I-P calculations for the non-load-carrying fillet primitive are reasonable as shown in Figures C-9 and C-10. Comparing the I-P calculations with the I calculations, one can see the significant effect of propagation at shorter lives and its almost negligible effect at longer lives. In Figure C-11, the I-P calculation for the load-carrying fillet primitive is in good agreement with the S-N data. An increase in fatigue life is seen at high stresses due to the addition of the propagation life; but once again, not much of a difference is seen at long lives. The termination calculations agree with the S-N data over all the lives due to the addition of the propagation life but the estimated initiation portion of life seems to be a bit too long (un-conservative).

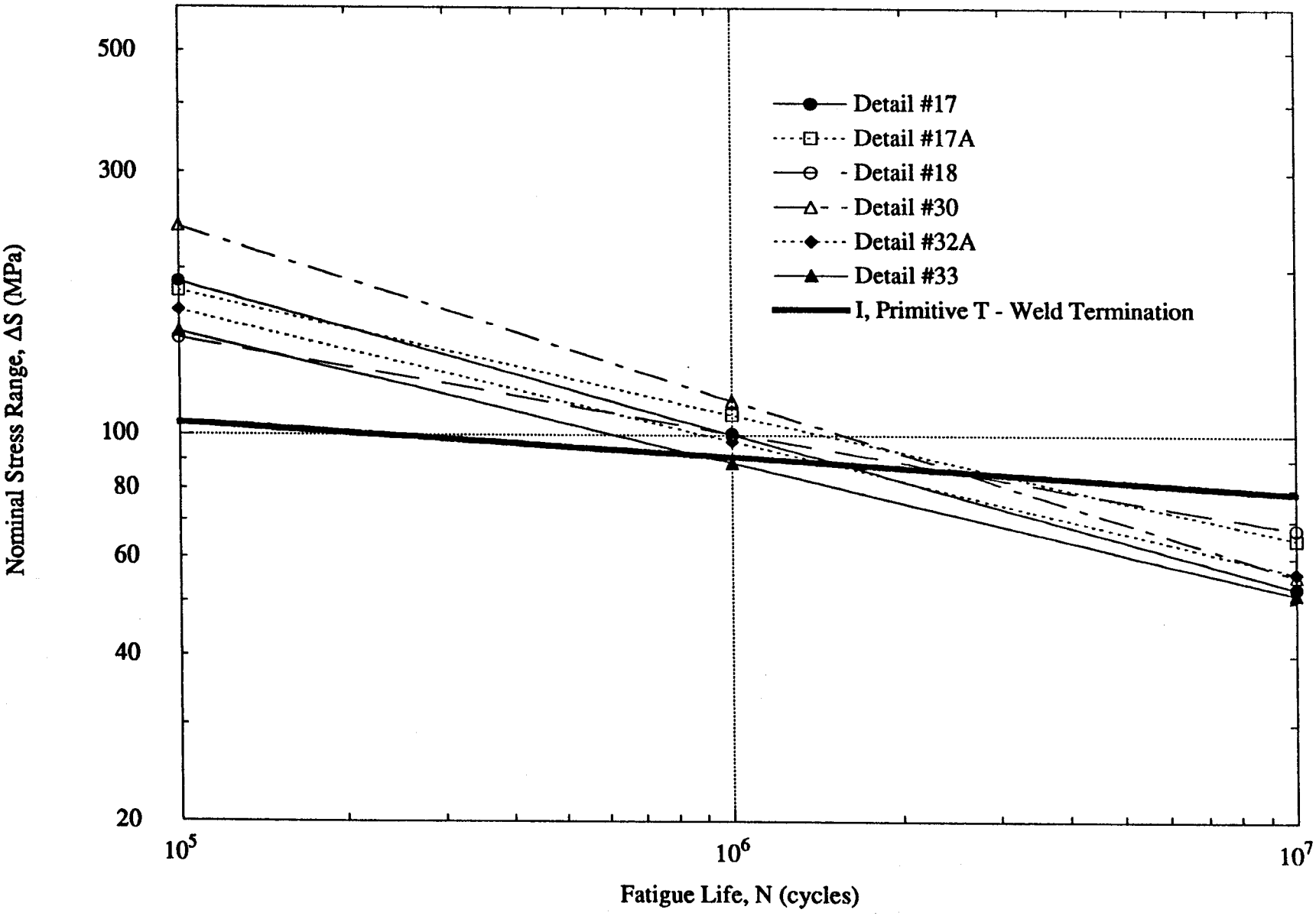

Figure C-9 Comparison of the S-N data for ship structure details and the analytical expression for the weld Primitive T - Weld Termination

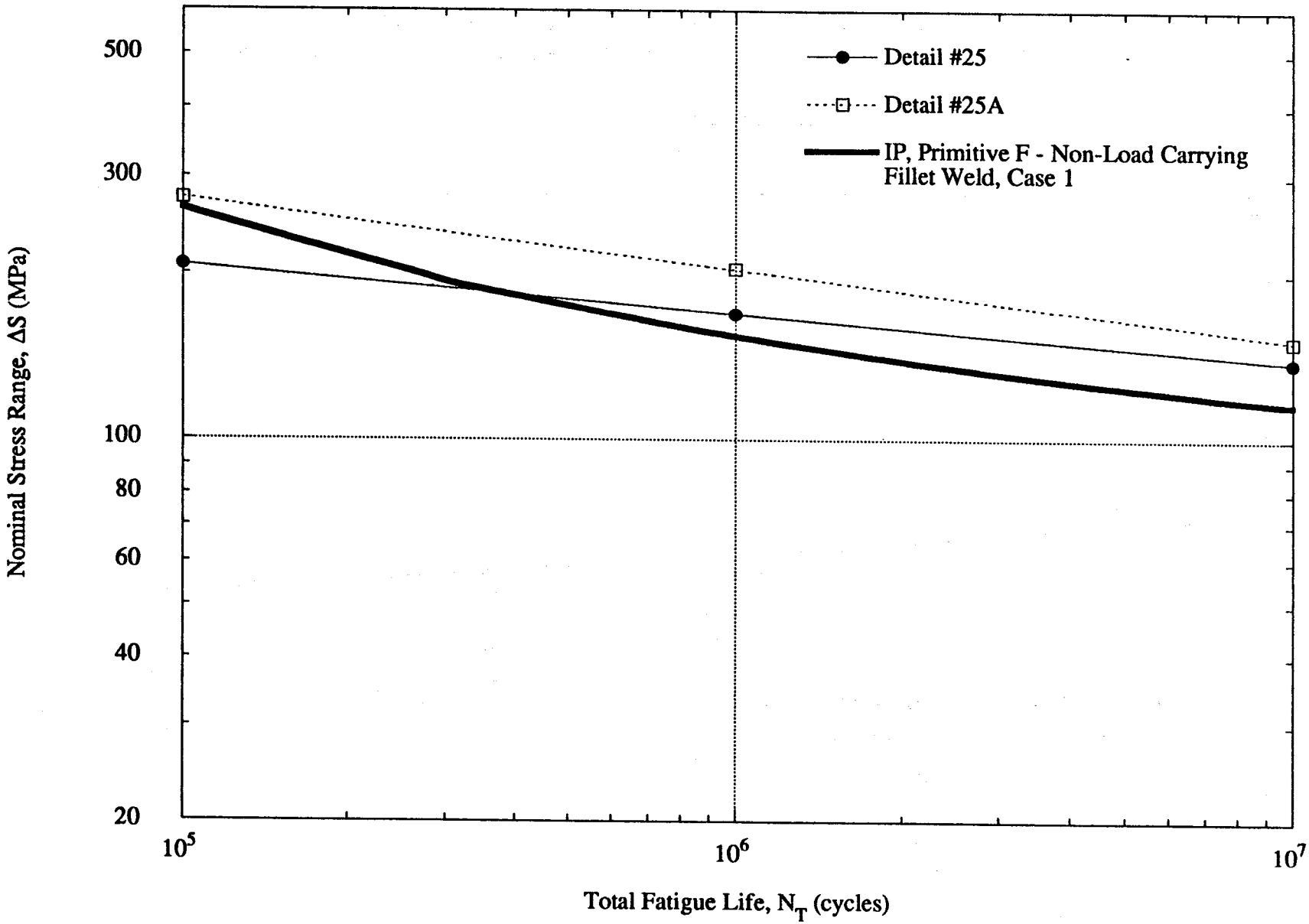

Figure C-10 Comparison of the I-P model predictions and S-N data of ship structure details for the weld Primitive F - Non-Load Carrying Fillet Weld Load Case 1.

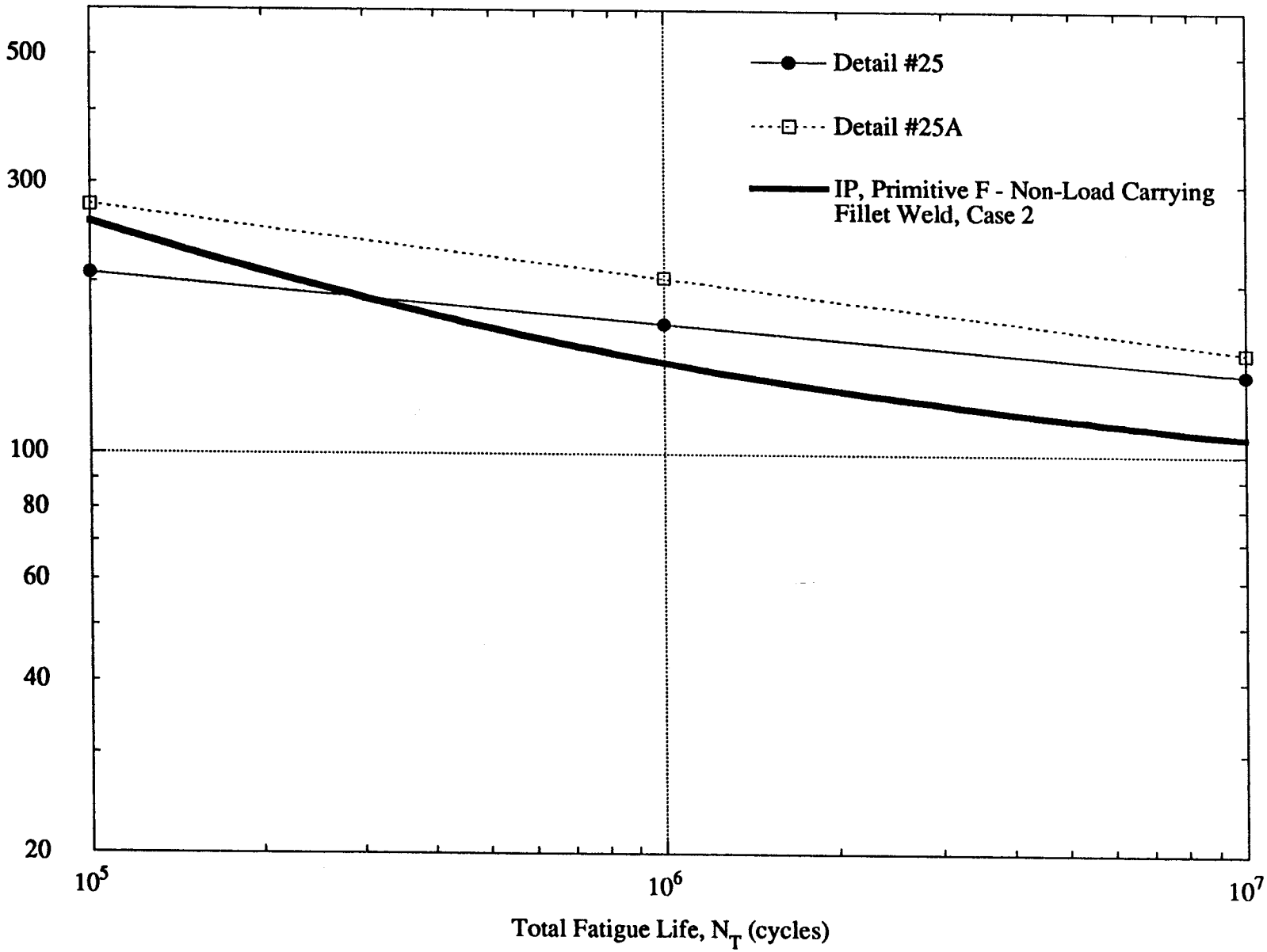

Figure C-11 Comparison of the I-P model predictions and S-N data of ship structure details for the weld Primitive F - Non-Load Carrying Fillet Weld Load Case 2.

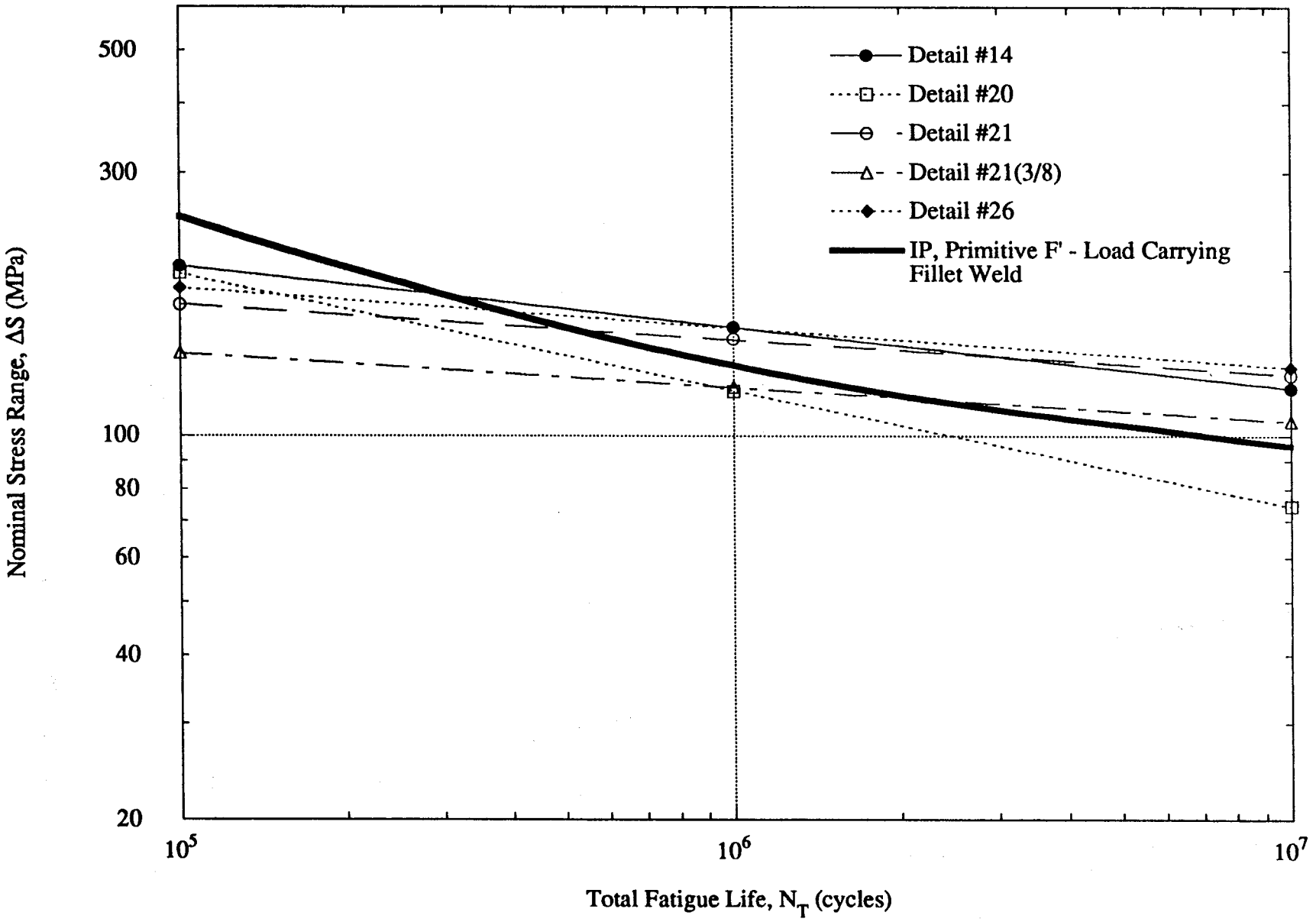

Figure C-12 Comparison of the I-P model predictions and S-N data of ship structure details for the weld Primitive F - Load Carrying Fillet Weld

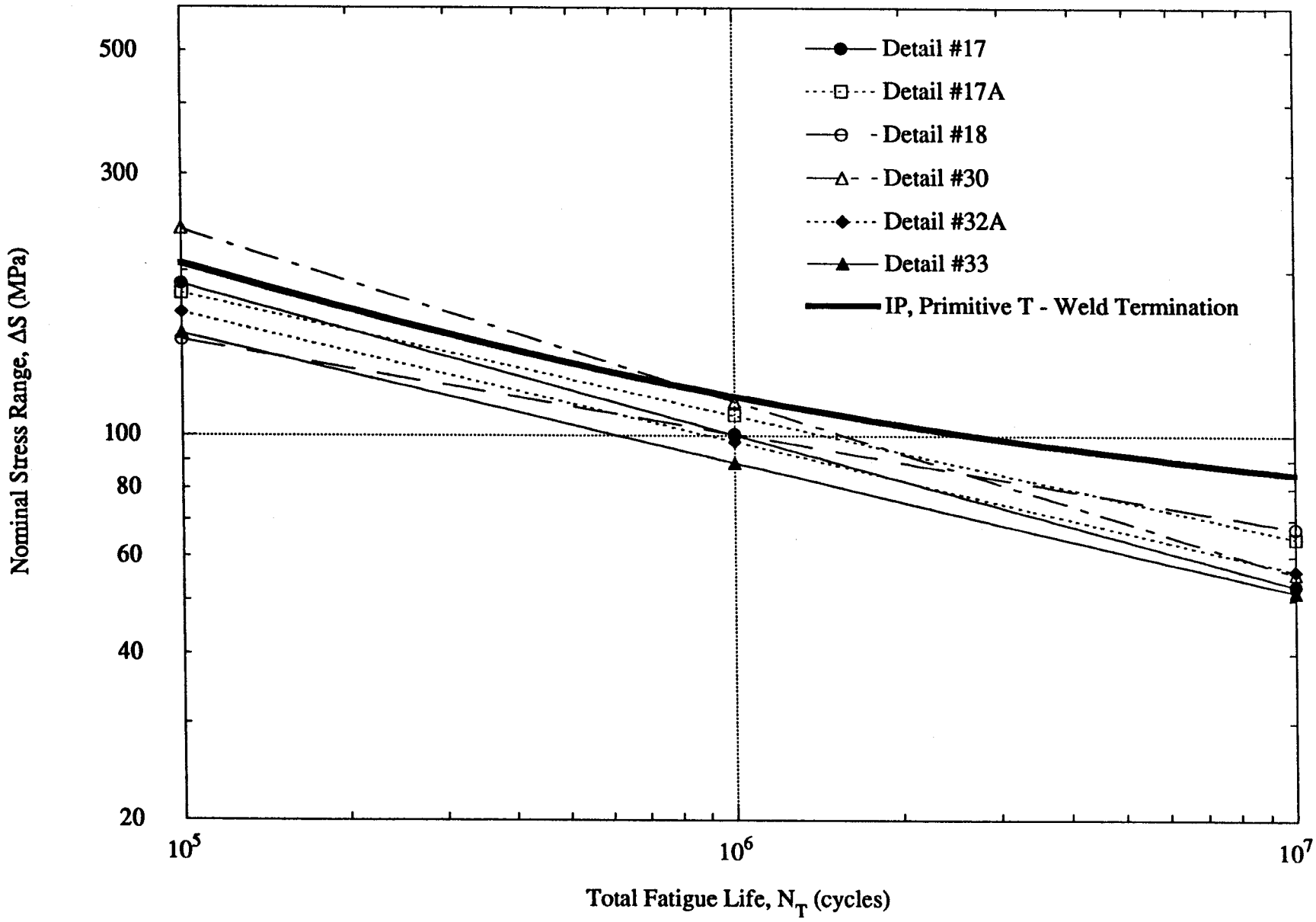

Figure C-13 Comparison of the I-P model predictions and S-N data of ship structure details for the weld Primitive T - Weld Termination

C.4 SUMMARY

The predictions of fatigue strength using the analytical expressions given for each of the primitives agree with the experimental results at long lives ($N = 10^7$). Thus, the expressions are able to predict primitive behavior through are able to predict primitive behavior through a knowledge of the weldment material properties (S_u), residual stress (σ_r), loading conditions (x), plate thickness (t), and weld geometry (θ, l, c). Finally, analytical predictions of the fatigue behavior of the primitives made using the I-P model were good at both long and short lives. Thus, it would appear that the I-P model agrees well with the experimental results but has the powerful advantage of revealing to the engineer the true importance of interconnectedness of the many fatigue variables influencing the fatigue behavior of a given primitive (weldment).

By assigning average values to the fatigue parameters reflected in the data base information for a primitive, the designer can gauge the anticipated effect on experimental S-N diagram information of substantial changes in: weldment size (t), R ratio, loading conditions (x), base metal and weld metal strength (S_u, S_y), weld geometry (θ, l, c), residual stress conditions through the use of the expression below and the provided analytical expression for the appropriate primitive.

$$\Delta S_{weld} = \frac{1.43\ \Delta S_{pp}}{SCF * K_{fweld}} \left[\frac{\Delta S_{weld}\ \textit{calculated for current conditions}}{\Delta S_{weld}\ \textit{calculated for standard conditions}} \right]$$

C-5 REFERENCES

C-1 Yung, J.Y. and F.V. Lawrence, 1985, "Analytical and Graphical Aids for the Fatigue Design of Weldments," Fatigue Fract. Engineering Mater. Struct., Vol. 8, No. 3, pp. 223-241.

C-2 Munse, W.H., T. W. Wilbur, M.L. Telalian, K. Nicol, and K. Wilson, 1983, "Fatigue Characterization of Fabricated Ship Details for Design," Ship Structure Committee Report SSC-318, Washington, DC.

C-3 McMahon, J.C. and F.V. Lawrence, 1984, "Predicting Fatigue Properties Through Hardness Measurements," Report of the Materials Engineering - Mechanical Behavior, University of Illinois at Urbana-Champaign.

APPENDIX D

Glossary

(THIS PAGE INTENTIONALLY LEFT BLANK)

Cathodic protection	A means of reducing corrosive attack on a metal by making it the cathode of an electrolytic cell. This can be done by applying an external direct current from a power source (impressed) or by coupling it with a more electro-positive metal (sacrificial).
Constant amplitude fatigue limit	The fatigue strength at $5\text{-}10^6$ cycles. When all nominal stress ranges are less than the constant amplitude fatigue limit for the particular detail, no fatigue assessment is required.
Continuous termination	Termination from continuous weld.
Cruciform or transverse load-carrying joint	Specimen made from two lengths of plate welded, via fillet or full penetration welds, to either side of a perpendicular cross piece of the same section thickness.
Cut-off limit	The fatigue strength at 10^8 cycles. This limit is calculated by assuming a slope corresponding to $m = 5$ below the constant amplitude fatigue limit. All stress cycles in the design spectrum below the cut-off limit may be ignored unless the detail is exposed to a corrosive environment.
Design life	The period during which the structure is required to perform without repair.
Detail category	The designation given to a particular structural detail to indicate which of the fatigue strength curves should be used in the fatigue assessment. The category takes into consideration the local stress concentration at the detail, the stress direction, and residual stresses.
Discontinuity	An absence of material causing a stress concen-tration. Typical discontinuities are cracks, scratches, corrosion pits, lack of penetration, slag inclusions, cold laps, porosity, and undercut.
Discontinuous termination	Termination from intermittent weld.

Fatigue	The damage of a structural part by gradual crack propagation caused by repeated stresses.
Fatigue design stress	The stress in a structural member at the location of the weld and at one plate thickness from the weld toe for weld termination typical for calculated using FEA. This stress is correlated to nominal stress range to determine fatigue life.
Fatigue limit	See "cut-off" limit.
Fatigue loading	Fatigue loading describes the relevant variable loads acting on a structure throughout the design life. The fatigue loading in ships is composed of different load cases.
Fatigue notch factor	Ratio of stress of a notched detail to stress for a plan detail at a constant fatigue life.
Fatigue strength	The stress range corresponding to a number of cycles at which failure occurs.
Geometric stress	The stress at any point around the detail inter-section necessary to maintain the compatibility of displacements. This stress excludes local stress and depends on the nominal stress and overall geometry of the intersecting members.
Hot spot stress	The stress which controls fatigue endurance in tubular nodal joints. It can be defined experi-mentally or in design by the product of the nominal stress and the design hot spot stress concentration factor. This form is used primarily for offshore structural details.
Load case	A part of the fatigue loading defined by its relative frequency of occurrence as well as its magnitude and geometrical arrangement.
Load stress	The stress due to the discontinuity at the weld and which is superimposed on the geometric stress.

Nominal stress	The detail stress remote from the intersection. This includes geometric stress at the weld toe in the absence of weld.
Nominal stress range	The algebraic difference between two extremes (reversals) of nominal stress. Usually, this difference is identified by stress cycle counting. Stress extremes may be determined by standard elastic analysis and applying forces and moments to the cross-sectional areas. Exceptions to this definition are details near cut-outs, man-holes, or other stress concentrations not shown in Table 3-1.
Ripple	Uneven weld surface.
Weld profiling	Process of mechanically altering weld surface geometry.
Weld toe	The intersection of the weld profile and parent plate.

Project Technical Committee Members

The following persons were members of the committee that represented the Ship Structure Committee to the Contractor as resident subject matter experts. As such they performed technical review of the initial proposals to select the contractor, advised the contractor in cognizant matters pertaining to the contract of which the agencies were aware, and performed technical review of the work in progress and edited the final report.

Chou Lin – Chairman	Maritime Administration
Gary North	Maritime Administration
Steve Arntson	American Bureau of Shipping
Paul Cojeen	U. S. Coast Guard
Jaideep Sirkar	U. S. Coast Guard
Mike Sieve	Naval Sea Systems Command
Dave Kihl	Naval Surface Warfare Command
Robert Clark	Clark–Cim Inc.
Mr. William Siekierka	Naval Sea Systems Command, Contracting Officer's Technical Representative
Mr. Alex Stavovy Dr. Robert Sielski	National Academy of Science, Marine Board Liaison
CDR Steve Sharpe	U.S. Coast Guard, Executive Director Ship Structure Committee

COMMITTEE ON MARINE STRUCTURES

Commission on Engineering and Technical Systems

National Academy of Sciences – National Research Council

The COMMITTEE ON MARINE STRUCTURES has technical cognizance over the interagency Ship Structure Committee's research program.

Peter M. Palermo Chairman, Alexandria, VA
Subrata K. Chakrabarti, Chicago Bridge and Iron, Plainfield, IL
John Landes, University of Tennessee, Knoxville, TN
Bruce G. Collipp, Marine Engineering Consultant, Houston, TX
Robert G. Kline, Marine Engineering Consultant, Winona, MN
Robert G. Loewy, NAE, Rensselaer Polytechnic Institute, Troy, NY
Robert Sielski, National Research Council, Washington, DC
Stephen E. Sharpe, Ship Structure Committee, Washington, DC

LOADS WORK GROUP

Subrata K. Chakrabarti Chairman, Chicago Bridge and Iron Company, Plainfield, IL
Howard M. Bunch, University of Michigan, Ann Arbor, MI
Peter A. Gale, John J. McMullen Associates, Arlington, VA
Hsien Yun Jan, Martech Incorporated, Neshanic Station, NJ
John Niedzwecki, Texas A&M University, College Station, TX
Solomon C. S. Yim, Oregon State University, Corvallis, OR
Maria Celia Ximenes, Chevron Shipping Co., San Francisco, CA

MATERIALS WORK GROUP

John Landes, Chairman, University of Tennessee, Knoxville, TN
William H Hartt, Florida Atlantic University, Boca Raton, FL
Horold S. Reemsnyder, Bethlehem Steel Corp., Bethlehem, PA
Barbara A. Shaw, Pennsylvania State University, University Park, PA
James M. Sawhill, Jr., Newport News Shipbuilding, Newport News, VA
Bruce R. Somers, Lehigh University, Bethlehem, PA
Jerry G. Williams, Conoco, Inc., Ponca City, OK

SHIP STRUCTURE COMMITTEE PUBLICATIONS

SSC-356 Fatigue Performance Under Multiaxial Load by Karl A. Stambaugh, Paul R. Van Mater, Jr., and William H. Munse 1990

SSC-357 Carbon Equivalence and Weldability of Microalloyed Steels by C. D. Lundin, T. P. S. Gill, C. Y. P. Qiao, Y. Wang, and K. K. Kang 1990

SSC-358 Structural Behavior After Fatigue by Brian N. Leis 1987

SSC-359 Hydrodynamic Hull Damping (Phase I) by V. Ankudinov 1987

SSC-360 Use of Fiber Reinforced Plastic in Marine Structures by Eric Greene 1990

SSC-361 Hull Strapping of Ships by Nedret S. Basar and Roderick B. Hulla 1990

SSC-362 Shipboard Wave Height Sensor by R. Atwater 1990

SSC-363 Uncertainties in Stress Analysis on Marine Structures by E. Nikolaidis and P. Kaplan 1991

SSC-364 Inelastic Deformation of Plate Panels by Eric Jennings, Kim Grubbs, Charles Zanis, and Louis Raymond 1991

SSC-365 Marine Structural Integrity Programs (MSIP) by Robert G. Bea 1992

SSC-366 Threshold Corrosion Fatigue of Welded Shipbuilding Steels by G. H. Reynolds and J. A. Todd 1992

SSC-367 Fatigue Technology Assessment and Strategies for Fatigue Avoidance in Marine Structures by C. C. Capanoglu 1993

SSC-368 Probability Based Ship Design Procedures: A Demonstration by A. Mansour, M. Lin, L. Hovem, A. Thayamballi 1993

SSC-369 Reduction of S-N Curves for Ship Structural Details by K. Stambaugh, D. Lesson, F. Lawrence, C-Y. Hou, and G. Banas 1993

SSC-370 Underwater Repair Procedures for Ship Hulls (Fatigue and Ductility of Underwater Wet Welds) by K. Grubbs and C. Zanis 1993

SSC-371 Establishment of a Uniform Format for Data Reporting of Structural Material Properties for Reliability Analysis by N. Pussegoda, L. Malik, and A. Dinovitzer 1993

SSC-372 Maintenance of Marine Structures: A State of the Art Summary by S. Hutchinson and R. Bea 1993

SSC-373 Loads and Load Combinations by A. Mansour and A. Thayamballi 1994

SSC-374 Effect of High Strength Steels on Strength Consdierations of Design and Construction Details of Ships by R. Heyburn and D. Riker 1994

None Ship Structure Committee Publications - A Special Bibliography